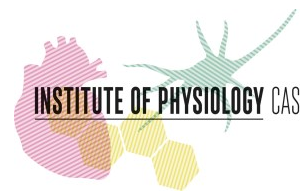Univerzita Karlova v Praze

Přírodovědecká fakulta

Charles University in Prague

Faculty of Science

Czech Academy of Sciences

Institute of Physiology, v.v.i

Úloha tukové tkáně v celotělovém energetickém metabolizmu u myší s různým genetickým pozadím

The role of adipose tissue in the whole-body energy metabolism in mice with different genetic background

Disertační práce / PhD thesis

Mgr. Jiří Funda

Školitel / Supervisor: Ing. Petra Janovská, PhD
Praha 2021

Prohlášení

Prohlašuji, že jsem závěrečnou práci zpracoval samostatně a že jsem uvedl všechny použité informační zdroje a literaturu. Tato práce ani její podstatná část nebyla předložena k získání jiného nebo stejného akademického titulu.

Statement of authorship

I certify that the thesis represents valid work elaborated under the supervision of Ing. Petra Janovská, PhD, and that neither this manuscript nor one with substantially similar content under my authorship has been submitted in support of an application for any other academical degree. My participation in the published papers is specified in the text and summarised in the list of publications on the page 90.

17.12.2021 in Prague

Mgr. Jiří Funda

Statement of co-authors

I certify that Jiří Funda substantially contributed to the formation of the papers used as a basis of this thesis, and that his participation specified in the text of the thesis is correct.

17.12.2021 in Prague

Ing. Petra Janovská, PhD

Acknowledgement

Abstract

Adipose tissue greatly contributes to the maintenance of the whole-body energy homeostasis. White adipose tissue (WAT) is the most important storage of metabolic energy in the body, while brown adipose tissue (BAT) enables the body to survive in cold environment by transforming metabolic energy to heat. Both WAT and BAT have a critical role in the control of systemic levels of fatty acids, which is necessary for the maintenance of the energy homeostasis and for the prevention of lipotoxic damage of non-adipose tissues. Abundant lipid accumulation can lead to the development of obesity, which is often accompanied by metabolic disorders such as type 2 diabetes and by the impairment of adipose tissue metabolic functions. Healthy adipose tissue prevents from the development of metabolic disorders associated with obesity by buffering the excess of nutrients. The key processes for efficient buffering of fatty acids are futile triacylglycerols/fatty acid cycling (TAG/FA cycling) and fatty acid oxidation. These processes occur in both WAT and BAT and their rates are largely affected by a set of transcriptional regulators, especially peroxisome proliferator-activated receptors (PPARs) and their coactivators. Bioactive molecules such as hormones, polyunsaturated fatty acids (PUFA) or pharmaceutics such as thiazolidinediones (TZDs) can modulate the activity of metabolic processes in adipose tissue. On the whole-body level metabolic functions of adipose tissue are controlled mostly by the nervous system through hormonal and neuronal signalling. This thesis is based on three studies demonstrating that the modulation of metabolic processes and deletion of specific genes in adipose tissue or other organs could influence the whole-body energy homeostasis.

The first study described in this thesis examined the effects of n-3 PUFA and TZDs on the modulation of WAT metabolism in mice with diet-induced obesity. The combined treatment with n-3 PUFA and TZDs exerted additive beneficial effects on metabolic functions of WAT, namely on the stimulation of TAG/FA cycling and it also improved systemic parameters of metabolic health in obese mice. The second study characterized mice with the deletion of GPR-10, which is a receptor expressed mostly in hypothalamus. GPR-10 is believed to influence energy expenditure and food intake; therefore, we examined parameters of the whole-body energy homeostasis with a special focus on adipose tissue metabolism. GPR-10 deficiency altered lipid metabolism in the liver and in WAT of both male and female mice, with a stronger effect in GPR-10 KO males. The last study examined mice with adipose tissue specific deletion of PPARγ coactivator-1β (PGC-1β) under conditions with different requirements for thermogenesis. PGC-1β deficiency in adipose tissue altered BAT morphology especially in mice housed at thermoneutral temperature and impaired BAT thermogenic and metabolic functions resulting in hypothermia upon acute cold exposure.

The studies mentioned above demonstrated that alterations of adipose tissue metabolism are reflected by changes in other metabolically relevant organs and vice versa. Better understanding of the mutual interactions between adipose tissue and other metabolically relevant organs could be potentially used for the treatment of various metabolic disorders.

Abstract (in Czech)

Tuková tkáň značně přispívá k udržování celotělové energetické homeostázy. Bílá tuková tkáň je nejdůležitějším úložištěm metabolické energie, zatímco hnědá tuková tkáň přeměňuje metabolickou energii na teplo a tím umožňuje organizmu přežít v chladném prostředí. Bílý i hnědý tuk zastávají zásadní úlohu v kontrole celotělových hladin mastných kyselin, což je nezbytné pro udržování energetické homeostázy a pro ochranu ostatních tkání před lipotoxickým poškozením. Nadbytečné ukládání lipidů může vést k rozvoji obezity, což je často spojeno s poškozením metabolických funkcí tukové tkáně a s metabolickými poruchami, jako je diabetes 2. typu. Zdravá tuková tkáň chrání před rozvojem metabolických poruch spojených s obezitou tím, že ukládá nadbytečné živiny a reguluje jejich hladiny. Klíčovými procesy pro účinnou regulaci hladin mastných kyselin jsou prázdné metabolické cyklování mezi triacylglyceroly a mastnými kyselinami (TAG/MK cyklování) a oxidace mastných kyselin. Tyto procesy probíhají v bílém i ve hnědém tuku a jejich obrat je z velké části ovlivněn transkripčními regulátory, zejména jadernými receptory PPAR a jejich koaktivátory. Bioaktivní molekuly jako jsou hormony, polynenasycené mastné kyseliny (PUFA) nebo léčiva, například thiazolidinediony (TZD) mohou ovlivňovat aktivitu metabolických procesů v tukové tkáni. Na celotělové úrovni jsou metabolické funkce tukové tkáně kontrolovány hlavně nervovým systémem prostřednictvím hormonální a neuronální signalizace. Tato disertační práce je založena na třech studiích, které demonstrují, že modulace metabolických procesů a delece specifických genů v tukové tkáni nebo v jiných metabolicky aktivních orgánech může ovlivnit celotělovou energetickou homeostázu.

První studie popsaná v této práci zkoumala efekty omega-3 PUFA a TZD na modulaci metabolizmu bílého tuku u myší s dietou indukovanou obezitou. Kombinovaná intervence obsahující omega-3 PUFA a TZD měla aditivní prospěšné účinky na metabolické funkce bílého tuku, zejména na obrat TAG/MK cyklování a zároveň zlepšila celotělové parametry metabolického zdraví u obézních myší. Druhá studie popisovala myši s delecí GPR-10, což je receptor exprimovaný především v hypotalamu. GPR-10 údajně přispívá ke kontrole energetického výdeje a příjmu potravy, proto jsme se zaměřili na výzkum parametrů celotělové energetické homeostázy a zejména na metabolizmus tukové tkáně. Delece GPR-10 ovlivnila lipidový metabolizmus v játrech a v bílém tuku u samců i u samic, s výrazně silnějším efektem u GPR-10 KO samců. Třetí studie zkoumala myši s tukově specifickou delecí PPARγ koaktivátoru 1β (PGC-1β) v podmínkách s různými požadavky na termogenezi. Delece PGC-1β v tukové tkáni změnila morfologii hnědého tuku zejména u myší v termoneutrální teplotě a narušila metabolické a termogenní funkce hnědého tuku, což u myší způsobilo hypotermii při akutní chladové expozici.

Výše zmíněné studie ukázaly, že zásahy do metabolizmu tukové tkáně jsou reflektovány změnami ve funkci ostatních metabolicky aktivních orgánů a naopak. Lepší porozumění vzájemných interakcí mezi tukovou tkání a ostatními metabolicky aktivními orgány může být potenciálně užitečné pro léčbu různých metabolických poruch.

Content

List of abbreviations

AA	arachidonic acid
ACAD	acyl-CoA dehydrogenase
ACC	acetyl-CoA carboxylase
ACS	acyl-CoA synthase
AGPAT	acylglycerolphosphate acyltransferase
AKAP	A-kinase anchoring protein
ALA	α-linolenic acid
ARC	arcuate nucleus
ATGL	adipose triglyceride lipase
BAT	brown adipose tissue
BCAA	branched chain amino acids
cAMP	cyclic AMP
CE	cold exposure
CIDEC/FSP27	fat specific protein 27
CLS	crown-like structures
CNS	central nervous system
CNS-Mcr	central melanocortin system
CPT1	carnitine palmitoyltransferase 1
CRAT	carnitine acyltransferase
DAG	diacylglycerol
DGAT	diacylglycerol acyltransferase
DHA	docosahexaenoic acid
DRP1	dynamin-related protein 1
EDTA	ethylenediaminetetraacetic acid
ELOVL	fatty acid elongase
EPA	eicosapentaenoic acid
ERRα	estrogen-related receptor alpha
eWAT	epididymal white adipose tissue
FABP	fatty acid-binding protein
FAS	fatty acid synthase
FGF21	fibroblast growth factor 21
G3P	glycerol-3-phosphate
GK	glycerol kinase
GLUT4	glucose transporter 4
GPAT	glycerol-3-phosphate acyl transferase
GPR-10	G-protein coupled receptor 10
HF diet	high-fat diet
HOMA-IR	homeostatic model assessment
HPA axis	hypothalamus-pituitary-adrenal axis
HSL	hormone sensitive lipase
ChREBP	carbohydrate response element binding protein
iAUC	incremental area under the curve

iBAT	interscapular brown adipose tissue
IGTT	intraperitoneal glucose tolerance test
IL	interleukin
INCA	indirect calorimetry
IOCB	The Institute of Organic Chemistry and Biochemistry of the Czech Academy of Science
IPHYS	The Institute of Physiology of the Czech Academy of Sciences
LCAD	long chain acyl-CoA dehydrogenase
LC–MS	chromatography–mass spectroscopy
L-OPA1	optic atrophy 1 long form
LPL	lipoprotein lipase
MAG	monoacylglycerol
MCAD	medium chain acyl-CoA dehydrogenase
MFN1/2	mitofusins 1/2
MHO	metabolically healthy obesity
MPC	mitochondrial pyruvate carrier
MTBE	methyl tert-butyl ether
mtDNA	mitochondrial DNA
Myf5	myogenic factor 5
NEFA	non-esterified fatty acids
NE-test	norepinephrine test
NMR	nuclear magnetic resonance
NPY	neuropeptide Y
NRF1/2	nuclear respiratory factors-1/2
NST	non-shivering thermogenesis
NTS	nucleus tractus solitarius
OGTT	oral glucose tolerance test
OPA1	optic atrophy 1
OXPHOS	oxidative phosphorylation
PAP	phospatidate phosphatase
PKA	protein kinase A
PC	pyruvate carboxylase
PDC	pyruvate-dehydrogenase complex
PDK	pyruvate-dehydrogenase kinase
PEPCK	phosphoenolpyruvate carboxykinase
PET	positron emission tomography
PGC-1α/β	peroxisome proliferator-activated receptor gamma coactivator-1α/β
PIO	pioglitazone
PLS-DA	partial least squares-discriminant analysis
POMC	proopiomenalocortin
PPAR	peroxisome proliferator-activated receptor
PPRE	peroxisome proliferator-activated receptor response elements
PRC	peroxisome proliferator-activated receptor gamma coactivator-related coactivator
PrRP	prolacting-releasing peptide
PUFA	polyunsaturated fatty acids

PVN	paraventricular nucleus
RQ	respiratory quotient
RT-qPCR	real-time quantitative gene expression analysis
RXR	retinoid X receptor
SAM pathway	sympathomedullary pathway
SCAD	short chain acyl-CoA dehydrogenase
SCD1	stearoyl-CoA desaturase
scWAT	subcutaneous white adipose tissue
SEM	standard error of the mean
SERCA	sarcoplasmic reticulum calcium ATPase
SNS	sympathetic nervous system
S-OPA1	optic atrophy 1 short form
SREBP	sterol response element binding protein
STD	standard laboratory chow diet
SVF	stromal vascular fraction
TAG	triacylglycerols
TAG/FA cycling	triacylglycerols/fatty acid cycling
TCA cycle	tricarboxylic acid cycle
TFAM	mitochondrial transcription factor A
TLC	thin layer chromatography
TNFα	tumor necrosis factor alpha
TZDs	thiazolidinediones
UCP1	uncoupling protein 1
VLCAD	very long chain acyl-CoA dehydrogenase
VLDL	very-low-density lipoprotein
VMN	ventromedial nucleus
WAT	white adipose tissue
αMSH	α-melanocyte-stimulating hormone
β-AR	β adrenergic receptors
ΔAUC	delta area under the curve

1   Introduction

The storage of excess metabolic energy is a key survival mechanism. The ratio between energy intake and energy expenditure determines the energy balance. When the energy balance is positive, adipose tissue is able to store metabolic energy in the form of lipids, mostly triacylglycerols (TAG). If the energy balance is negative, metabolic energy stored in adipose tissue enables the body to maintain vital functions. However, adipose tissue is much more than just an inert lipid store.

There are two types of adipose tissue in mammals, white adipose tissue (WAT) and brown adipose tissue (BAT) [1]. The primary function of WAT is the storage of energy in the form of TAG, while the main function of BAT is non-shivering thermogenesis (NST), i.e. the dissipation of energy in the form of heat. TAG are composed of glycerol and fatty acids that can be released from WAT and oxidised by other organs such as the skeletal muscle, heart or BAT. Both types of adipose tissue act as an endocrine organ. They secrete regulatory molecules known as adipokines to communicate with other organs. Adipose tissue also has a great ability to dynamically respond to environmental and dietary signals and physiological properties of adipose tissue reflect the energy balance in the whole body. If the energy balance is chronically shifted towards energy storage, excessive lipid accumulation leads to the expansion of adipose tissue and to the development of obesity.

Excessive lipid accumulation is often associated with metabolic disorders. WAT is highly expandable and it can store an enormous amount of energy. If the storage capacity of WAT is exceeded, lipids are stored in other organs, e.g. in the liver and in the skeletal muscle. The abundance of lipids causes lipotoxic damage to non-adipose tissues and decreases their insulin sensitivity [2]. The incidence of metabolic disorders is affected by the character of adipose tissue expansion and by the anatomical and physiological properties of adipose tissue. Expansion of visceral adipose tissue (abdominal or central obesity) is considered detrimental due to its effects on the function of visceral organs and connection to the portal vein [3, 4]. Abdominal obesity belongs to the metabolic syndrome: a cluster of conditions contributing to the development of cardiovascular diseases, type 2 diabetes and other disorders. On the other hand, the expansion of subcutaneous WAT (scWAT) is not directly linked to the metabolic syndrome and it is considered protective as it prevents from ectopic lipid accumulation. However, part of obese individuals with high adipose tissue storage capacity and protective adipose tissue expansion is less susceptible to the development of metabolic disorders [5]. They represent the metabolically healthy obesity (MHO).

Adipose tissue is interconnected throughout the body and it can be regarded as a single adipose organ. Moreover, adipose tissue forms various depots with different physiological and morphological properties. Different properties of adipose tissue depots are determined mostly on the cellular level [6]. Adipose tissue is mainly composed of adipocytes. The rest of the tissue is known as stromal vascular fraction (SVF) and contains pre-adipocytes, fibroblasts and immune cells. The adipocyte is the central metabolic unit of the adipose organ.
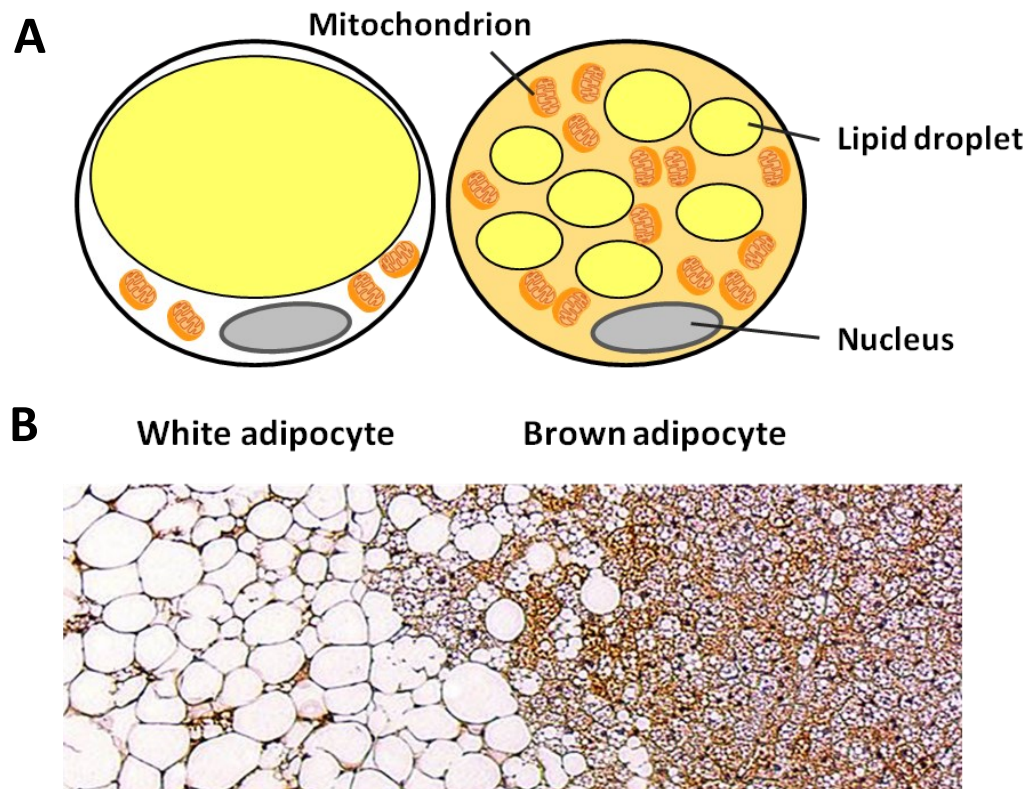
1.1 Adipocyte morphology

Adipocytes can be divided to either white or brown; white adipocytes are the main cell type in WAT, while BAT is mostly composed of brown adipocytes (Figure 1.1 A). The third type of adipocytes are brite cells (beige cells), adipocytes with cellular morphology similar to brown adipocytes. Brite cells are found in certain WAT depots, e.g. in scWAT and they develop as a result of a process called WAT browning (see 1.2.6) [7, 8]. The common feature for all types of adipocytes is the ability to store TAG.

The site of TAG storage within the adipocyte is the lipid droplet. Adipocytes are endowed either with a single lipid droplet (unilocular adipocytes) or multiple smaller lipid droplets (multilocular adipocytes). White adipocytes are mostly unilocular, while brown adipocytes are multilocular. The amount of lipids stored within the lipid droplet depends on the ratio between TAG accumulation (lipogenesis) and TAG breakdown (lipolysis).

Different metabolic properties of white and brown adipocytes are due to differences in their developmental origin and especially cellular architecture. White and brown adipocytes do not originate from the same progenitor lineage. Brown adipocytes are derived from precursor cells expressing myogenic factor 5 (Myf5), similarly as muscle cells, while the precursor cells of white adipocytes are Myf5-negative [9]. Most of the white adipocyte is filled by a single lipid droplet and all the other organelles, including nucleus, are confined to thin cytosolic rim. White adipocytes have few mitochondria; therefore, the oxidative capacity of white adipocyte is relatively low [10]. On the other hand, lipid droplets in brown adipocytes are surrounded by dense mitochondrial network. The brownish colour of brown adipocytes is due to a high mitochondrial content as mitochondria contain a lot of brown iron pigments. Cellular architecture of brown adipocytes allows abundant contact between mitochondria and the surface of lipid droplet. The oxidative capacity of brown adipocytes is considerably higher compared to white adipocytes.

Morphological properties of adipocytes in both WAT and BAT can change in response to conditions such as temperature or diet. Therefore, anatomical boundaries between WAT and BAT cannot be clearly distinguished (Figure 1.1 B) [11]. scWAT in humans forms continuous layer under the skin, while in rodents it is composed of separate depots in the upper part of the thorax and in the lower part of the abdomen. Although visceral WAT forms depots in both humans and rodents, the properties of individual depots vary between the species. Omental WAT is much more developed in humans compared to rodents. On the other hand, epididymal WAT (eWAT), frequently used for analyses in adipose tissue research is strongly developed in rodents and absent in humans [12]. The most important BAT depot in rodents is the interscapular BAT (iBAT). In humans iBAT is present in newborns, while in adult humans BAT can be found below the clavicles and in the neck area. The existence of functional BAT in adult humans was confirmed by studies using positron emission tomography (PET) [13, 14, 15].

Figure 1.1 Differences in the cellular architecture of white and brown adipocytes.
White and brown adipocytes differ in morphological and metabolic properties; however, they
can be found within the same adipose tissue depot.

1.2 Metabolism of adipocytes

White adipocytes are specialised in TAG storage, while brown adipocytes serve for the
heat production by NST. Intrinsic metabolic processes in all adipocytes involve fatty acid
uptake, fatty acid synthesis *de novo* and fatty acid oxidation, lipogenesis, lipolysis and futile
cycling between lipolysis and fatty acid re-esterification. Due to different physiological
functions of white and brown adipocytes, these processes occur for different purposes and
their enzymatic regulation might also differ. However, biochemical nature of these metabolic
processes remains the same in all adipocytes.

1.2.1   Lipogenesis

Lipogenesis is a biochemical process resulting in the formation of TAG molecule.
Lipogenesis occurs in both white and brown adipocytes and also in hepatocytes. TAG
molecule consists of glycerol backbone and three molecules of fatty acids. Fatty acids used
for lipogenesis are either taken up from the extracellular space or synthesised *de novo* from
non-lipid precursors.

Fatty acid uptake into adipocytes is critical for lipogenesis and it is also the central

mechanism how adipose tissue regulates systemic lipid homeostasis. Fatty acids are taken up into adipocytes upon their liberation from chylomicrons, very low-density lipoproteins (VLDL) and other lipoprotein particles. Chylomicrons serve for the transport of dietary lipids from the intestine, while VLDL particles originate in the liver. Lipoprotein lipase (LPL) catalyses the breakdown of all plasmatic lipoproteins which is the key step in fatty acid uptake. The activity of LPL therefore significantly affects systemic lipid levels. LPL is located on the surface of vascular endothelial cells. Fatty acids liberated by LPL are imported to the adipocyte by transport proteins such as CD36 [16]. Upon entering the cell, fatty acids bind to fatty acid-binding protein (FABP), which serves for the transport of fatty acids between cellular compartments [17].

Another way to provide fatty acids for lipogenesis is their synthesis directly in adipocytes from non-lipid precursors. *De novo* fatty acid synthesis is highly complex and energy-consuming process. Fatty acid synthesis takes place in the cytosol; however, the first precursor of fatty acid synthesis, citrate, is transported from the mitochondrion through citrate transporter [18]. In the cytosol citrate is transformed to acetyl-CoA by ATP citrate synthase [19]. The first step of fatty acid synthesis is the formation of malonyl-CoA catalysed by acetyl-CoA carboxylase (ACC). The following steps of fatty acid synthesis are catalysed by multienzymatic complex fatty acid synthase (FAS) [20]. FAS facilitates the association of malonyl-CoA with a molecule of acyl-CoA, which leads to the growth of newly formed fatty acid chain. The primary product of fatty acid synthesis is palmitic acid, a 16-carbon saturated fatty acid. Palmitic acid might be dehydrogenated to a monounsaturated fatty acid by stearoyl-CoA desaturase (SCD1). Furthermore, newly synthesised fatty acids might be elongated by enzymes from the elongase family (ELOVL1-6) [21].

In addition to fatty acids, a molecule of glycerol-3-phosphate (G3P) is necessary to form TAG. G3P is produced by glycerol phosphorylation catalysed by glycerol kinase (GK); however, GK has very low activity in WAT under normal conditions. Therefore, G3P in WAT is provided mostly by glyceroneogenesis [22]. The initial step of glyceroneogenesis is carboxylation of pyruvate to oxaloacetate catalysed by pyruvate carboxylase (PC). Oxaloacetate is further converted to phosphoenolpyruvate by phosphoenolpyruvate carboxykinase (PEPCK), which is the rate limiting enzyme of glyceroneogenesis [23]. Phosphoenolpyruvate is then converted to dihydroxyacetone phosphate, which is finally turned into G3P in the step catalysed by triosephosphate isomerase.

The final step of lipogenesis, TAG synthesis, consists of gradual esterification of G3P by activated fatty acids (Figure 1.2). Glycerol-3-phosphate acyl transferase (GPAT) catalyses the esterification of first fatty acid to form a molecule of lysophosphatidic acid. Lysophosphatidic acid is then converted to phosphatidic acid by acylglycerolphosphate acyltransferase (AGPAT) [24]. Phosphatidic acid is a precursor for the synthesis of various biomolecules, e.g. phospholipids such as phosphatidylcholine and phospatidylserine, which are critical components of membranes. Phospatidate phosphatase (PAP) is an enzyme that catalyses the conversion of phosphatidic acid to diacylglycerol (DAG). Another way to synthesise DAG is the esterification of monoacylglycerol (MAG) catalysed by monoacylglycerol acyltransferase. The esterification of DAG is mediated by diacylglycerol acyltransferase (DGAT) and it forms a TAG molecule. It was proposed that DGAT1 isoform is involved in the esterification of fatty acids taken up from the bloodstream, while DGAT2 isoform catalyses the esterification of *de*

novo synthesised fatty acids [25].
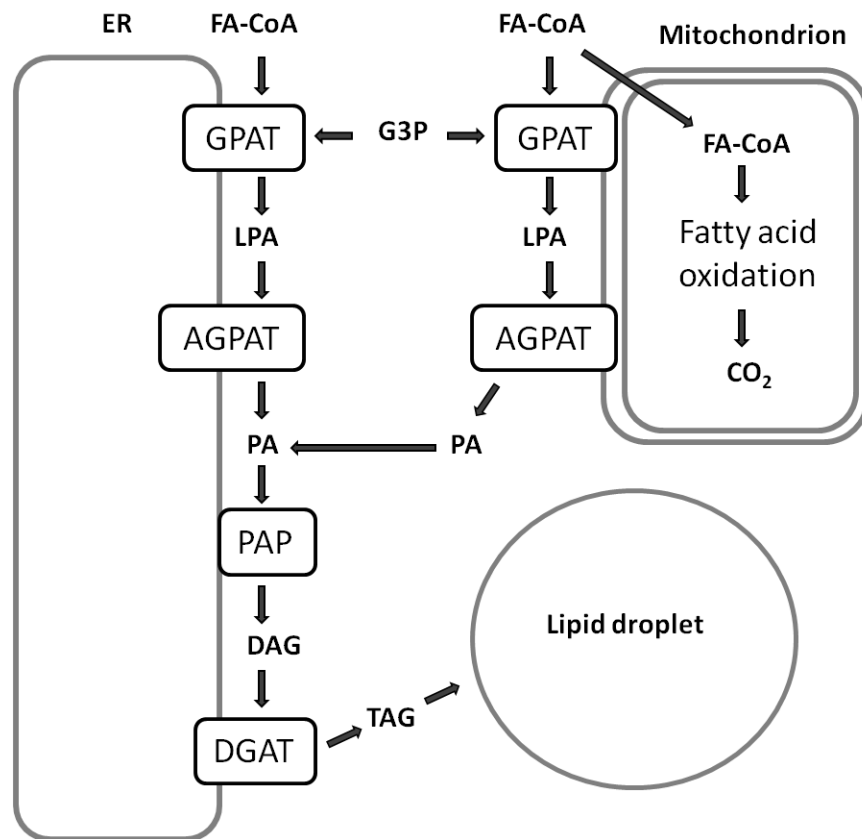
Figure 1.2 The steps of TAG synthesis. Modified from [26]. AGPAT: acylglycerolphosphate acyltransferase; DAG: diacylglycerol; DGAT: diacylglycerol acyltransferase; ER: endoplasmic reticulum; FA-CoA: fatty acyl-CoA; G3P: glycerol-3-phosphate; GPAT: glycerol-3-phosphate acyl transferase; LPA: lysophosphatidic acid; PA: phosphatidic acid; PAP: phospatidate phosphatase; TAG: triacylglycerol.

The TAG synthesis is essential for both white and brown adipocytes. In white adipocytes TAG synthesis is necessary for the storage of metabolic energy in lipid droplets. Moreover, TAG synthesis in WAT is used for the buffering of plasma lipids and their safe deposition in adipocytes, which is a critical tool for the control of lipid homeostasis. In BAT, fatty acids are taken up from plasma lipids mostly to fuel NST and they are stored only temporarily until they get combusted.

1.2.2   Lipolysis

Lipolysis is the initial phase of lipid catabolism, which is the transformation of the energy stored in TAG into the form of ATP. During lipolysis TAG molecule is hydrolysed to glycerol and non-esterified fatty acids (NEFA). Lipolysis of TAG stores in white adipocytes provides fatty acids mostly for oxidation in other tissues, while fatty acids from TAG stores in brown adipocytes are used as a substrate for NST.

The breakdown of TAG molecule within the adipocyte is catalysed by intracellular

lipases. The hydrolysis of TAG to DAG is mostly catalysed by adipose triglyceride lipase (ATGL), the rate limiting enzyme of lipolysis. Hormone sensitive lipase (HSL) is another lipase with the ability to hydrolyse TAG to DAG. However, HSL primarily hydrolyses DAG to MAG and its affinity for TAG is considerably lower. It was observed that in white adipocytes under basal conditions TAG are hydrolysed exclusively by ATGL [27]. The hydrolysis of MAG is catalysed by monoglyceride lipase. Intracellular lipases liberate fatty acids that are directed to the bloodstream or oxidised within the cell. Part of the lipolytic pathway also occurs in the extracellular space, the main lipase involved is LPL and it provides fatty acids for subsequent transport into the cell.

The rate of lipolysis is controlled by regulatory proteins. Lipolysis occurs constitutively on a low rate in all adipocytes, i.e. basal lipolysis. Basal lipolysis occurs under the basal conditions such as the thermoneutral temperature or the postprandial state. On the other hand, lipolytic rate increases in response to conditions such as cold stress or the fasted state. The rate of basal lipolysis is greatly increased in obese individuals, while the rate of stimulated lipolysis seems to be decreased [28]. The stimulation of lipolysis by stimuli such as hormones, e.g. catecholamines (see 1.4.2) triggers a signalling cascade resulting in the activation of protein kinase A (PKA) in adipocytes. Catecholamines bind to adrenergic receptors on the plasmatic membrane of adipocytes. Adrenergic receptors are coupled with G-proteins that activate an enzyme adenylyl cyclase. Adenylyl cyclase synthesises second messenger cyclic AMP (cAMP), causing its concentration in the cytosol to rise. cAMP then binds to regulatory subunits of PKA and causes their dissociation from catalytic subunits of the enzyme, which activates PKA [29]. PKA stimulates hydrolytic activity of HSL by phosphorylating the lipase. Moreover, PKA phosphorylates perilipins, proteins that play a critical role in the regulation of lipolysis.

Perilipins are located on the surface of lipid droplet. In mammals there are five known members of perilipin protein family [30]; perilipin 5 and especially perilipin 1 have the highest relevance for adipose tissue metabolism. Moreover, there are three isoforms of perilipin 1, perilipin A, B and C, with perilipin A being the predominant form in adipocytes. Perilipin layer is believed to serve as a protective barrier that prevents lipases from uncontrolled hydrolysis of TAG and by that keeping the rate of basal lipolysis low. Upon phosphorylation by PKA perilipins dissociate from the surface of lipid droplet leaving it exposed to lipases. Study with perilipin 1 ablated mice demonstrated elevated rates of basal lipolysis in white adipocytes causing a decrease in their size and the development of lean phenotype [31]. Another protein interacting with perilipin 1 is fat specific protein 27 (FSP27; also called CIDEC), which regulate lipid droplet size by controlling the rates of lipolysis and lipid accumulation [32, 33]. Isoform A of perilipin 1 also seems to have a function in mediating the translocation of phosphorylated HSL from cytosol to the surface of lipid droplet [34].

Optic atrophy 1 (OPA1) is a protein involved in the regulation of mitochondrial dynamics (see 1.3.3); however, it also seems to have an important role in the control of lipolysis. OPA1 might interact with PKA and function as A-kinase anchoring protein (AKAP). AKAPs are group of proteins that bind to regulatory subunits of PKA and facilitate the phosphorylation of PKA substrates. It was suggested that AKAPs are also associated with the surface of lipid droplet and affect PKA-stimulated lipolysis in white adipocytes [35]. Furthermore, OPA1 was

identified as AKAP that interacts with perilipin and recruits PKA to the surface of lipid droplet where perilipin is phosphorylated [36]. OPA1 is believed to be located on inner mitochondrial membrane and its involvement in mediating the interaction between proteins on the surface of lipid droplet is therefore unexpected.

Another protein involved in the regulation of lipolysis, CGI-58, binds to perilipins on the surface of lipid droplet when the protective layer is formed. Upon perilipin phosphorylation CGI-58 detach from the surface of lipid droplet and binds to ATGL in the cytosol. Binding of CGI-58 further stimulates the hydrolytic activity of ATGL [37].

Lipolysis and TAG synthesis in the adipocyte occur simultaneously in a process known as futile triacylglycerols/fatty acid cycling (TAG/FA cycling). TAG/FA cycling in WAT is crucial for the control of systemic lipid homeostasis.

1.2.3   TAG/FA cycling

A futile substrate cycle consists of opposing metabolic pathways that occur simultaneously. The term "futile cycle" is used as involved reactions consume chemical energy in the form of ATP that is due to the nature of the cycling dissipated in the form of heat. Unlike other metabolic pathways futile cycle serves as a regulatory mechanism. It amplifies the effects of changes in the activity of individual components on the resulting flux through the metabolic pathway [38]. The heat produced by futile cycles can contribute to NST such as in the futile cycle based on *de novo* FA synthesis and fatty acid oxidation in the skeletal muscle [39]. Futile Ca^{2+} cycling mediated by sarcoplasmic reticulum calcium ATPase (SERCA) in the skeletal muscle is another futile cycle contributing to NST [40].

Substantial part of fatty acids liberated by lipolysis is subsequently re-esterified, resulting in futile TAG/FA cycling. It was observed that in a basal state on average 40% of fatty acids were re-esterified in white adipocytes. After the activation of lipolysis by a stimulating agent – norepinephrine, fatty acid production increased causing the percentage of re-esterified fatty acid to decrease to approximately 7%. On the other hand, the addition of insulin suppressed fatty acid production causing the percentage of re-esterified fatty acids to increase to 55% [41]. In the basal state fatty acids that did not undergo re-esterification, only a negligible part (0.2%) was oxidised in adipocytes; therefore, the rest of fatty acids liberated from TAG was released from the cell and used as a fuel in other tissues [42].

TAG/FA cycling in adipocytes has a key role in the control of systemic lipid homeostasis, in particular, in the regulation of NEFA levels. The abundance of NEFA in the bloodstream can cause lipotoxic damage of non-adipose tissues. Therefore, NEFA levels must be tightly regulated. Moreover, NEFA provided by WAT are an important energy substrate for other tissues (Figure 1.3). TAG/FA cycling requires the enzymes of both lipolysis and TAG synthesis. Moreover, it was proposed that CD36, an enzyme regulating NEFA uptake into cells, also contributes to TAG/FA cycling in adipocytes [43]. Part of fatty acids released from white adipocytes after lipolysis are immediately taken back into the cell by CD36. In addition, CD36 seems to facilitate adrenergically stimulated lipolysis in white adipocytes. The involvement of CD36-mediated fatty acid re-uptake and regulation of lipolysis introduces an additional regulatory mechanism of TAG/FA cycling in WAT.
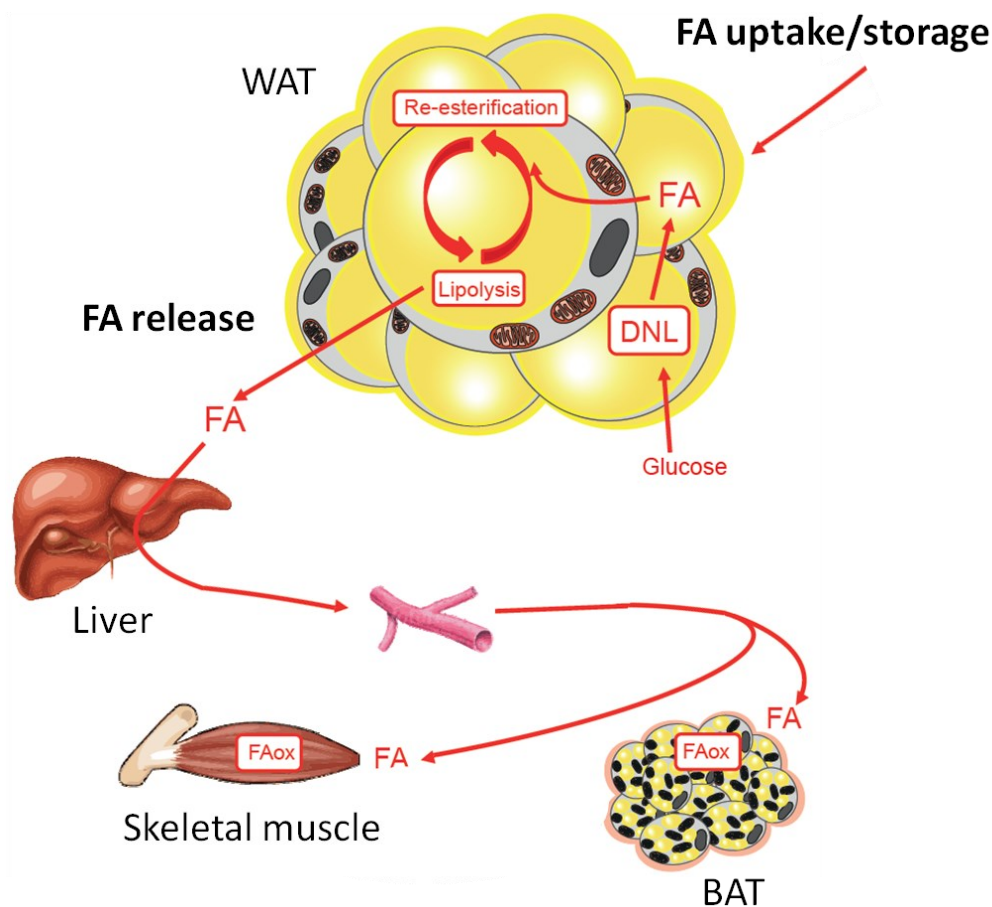
Figure 1.3 The involvement of TAG/FA cycling in WAT in the regulation of systemic lipid homeostasis. Modified from [44]. BAT: brown adipose tissue; DNL: *De novo* lipogenesis; FA: fatty acids; FAox: fatty acid oxidation; WAT: white adipose tissue.

TAG/FA cycling modulates the properties of lipid droplets in adipocytes. It was reported that in white adipocytes fatty acid re-esterification results in the formation of micro-lipid droplets [45]. The formation of micro-lipid droplets changes the morphology of unilocular white adipocyte to multilocular. The total surface of lipid droplets within the adipocyte increases, resulting in increased efficiency of lipid catabolism.

TAG/FA cycling consumes metabolic energy. The relevance of TAG/FA cycling to whole-body energy balance has been discussed already five decades ago [46]. The release and re-esterification of 3 fatty acid molecules was estimated to consume 8 ATP molecules. The activation of TAG/FA cycling in brown adipocytes was connected with higher fatty acid utilization and increased energy expenditure [47]. However, the sum of hepatic and peripheral re-esterification, i.e. re-esterification in adipose tissue and other lipogenic tissues was calculated only as 1.5% of basal metabolic rate in human [48]. TAG/FA cycling in adipocytes therefore does not seem to have a major impact on the whole-body energy balance [49].

TAG/FA cycling is one of the central metabolic processes in the adipocyte. In WAT, the role of TAG/FA cycling in the buffering of NEFA is important for the prevention of lipotoxic damage to non-adipose tissues. TAG/FA cycling regulates lipid metabolism in adipocytes as well as on

the systemic level.

1.2.4   Fatty acid oxidation

Fatty acids are crucial energy substrate. Complete oxidation of a single molecule of palmitic acid generates 129 ATP molecules. Fatty acid oxidation is called β-oxidation, as the beta-carbon of the fatty acid chain is being oxidised to form a carbonyl group.

β-oxidation is preceded by the activation and transport of fatty acid from cytosol to the mitochondrion. Fatty acid activation occurs in cytosol and it is catalysed by acyl-CoA synthase (ACS), which produces fatty acyl-CoA. Major site of β-oxidation within the cell is the mitochondrion. Fatty acyl-CoA is transported to the mitochondrion by carnitine palmitoyltransferase 1 (CPT1). CPT1 is believed to be the rate limiting enzyme of β-oxidation [50]. The activity of CPT1 is inhibited by malonyl-CoA, the first intermediate of fatty acid synthesis [51]. Therefore, the rate of β-oxidation is inhibited by fatty acid synthesis.

β-oxidation consists of repeating cycles of four reactions. The process of β-oxidation is similar to the fatty acid synthesis; it only occurs in the opposite order. In β-oxidation, the first reaction in each cycle is catalysed by substrate-specific acyl-CoA dehydrogenases (ACAD), i.e. short chain ACAD (SCAD), medium chain ACAD (MCAD), long chain ACAD (LCAD) and very long chain ACAD (VLCAD). Each cycle shortens the fatty acid chain by 2 carbons and produces a molecule of acetyl-CoA together with the reduced forms of coenzymes $FADH_2$ and $NADH^+$. Acetyl-CoA can be oxidised in tricarboxylic acid cycle (TCA cycle) and reduced coenzymes are used by respiratory chain to build a proton gradient in mitochondrial intermembrane space.

Fatty acids released from TAG stores during lipolysis are oxidised either directly in adipocytes or transported to other tissues. NEFA in plasma are mostly transported with albumin, which is the main fatty acid binding protein in the extracellular space [52]. Metabolic partitioning of fatty acids is affected by factors such as physical activity, fasting or environmental temperature. Only a minor fraction of fatty acids is oxidised in WAT under normal conditions [42]. On the other hand, fatty acids from TAG stores in activated BAT are oxidised exclusively in brown adipocytes and used as a fuel for NST.

1.2.5   TCA cycle and mitochondrial fuel selection

TCA cycle is a central metabolic pathway that interconnects metabolism of carbohydrates, proteins and lipids. A common intermediate in the catabolism of all three macronutrients, acetyl-CoA, is oxidised in the cycle to carbon dioxide and water. In addition to carbohydrate catabolism, major source of acetyl-CoA for TCA cycle is β-oxidation. Alternatively, acetyl-CoA can be made up from ketogenic amino acids, which can be degraded either to acetyl-CoA or acetoacetyl-CoA. Amino acids that are degraded to intermediates of glucose catabolism are termed glucogenic amino acids. Most of amino acids are both glucogenic and ketogenic; only leucine and lysine are solely ketogenic. When carbohydrates are used as a primary energy source, acetyl-CoA is being produced mostly from pyruvate, the final product of glycolysis. As glycolysis occurs in the cytosol, pyruvate needs to be transported into mitochondrion (see

below), the site of TCA cycle. Once inside the mitochondrion, pyruvate is decarboxylated to acetyl-CoA by pyruvate-dehydrogenase complex (PDC) and subsequently enters TCA cycle [53].

PDC plays a crucial role in controlling the balance between the oxidation of glucose and fatty acids. In the fed state with glucose abundance, PDC is highly active to utilize pyruvate from glycolysis. In the starved state, PDC activity is decreased to conserve pyruvate as a potential substrate for gluconeogenesis [54]. The activity of PDC is inhibited by pyruvate-dehydrogenase kinases (PDK), with PDK4 being the most relevant PDK isoform for the adipose tissue metabolism. High PDK4 activity therefore favours fatty acid oxidation. Another enzyme that affects PDC activity is carnitine acyltransferase (CRAT), which converts acetyl-CoA to its carnitine ester in order to enable its transport through mitochondrial membranes [55]. CRAT thus regulates mitochondrial substrate utilization, which impacts glucose homeostasis and insulin sensitivity [56].

Mitochondrial pyruvate availability also determines the fuel selection for TCA cycle. Mitochondrial pyruvate carrier (MPC) is a protein complex responsible for the transport of pyruvate into mitochondrial matrix. MPC affects various mitochondrial oxidative processes and it is critical for the mitochondrial substrate selection [57]. MPC inhibition results in an increased utilization of non-carbohydrate fuels, which was reported to activate lipolysis and increase the rate of TAG/FA cycling in adipocytes [47]. In addition, MPC inhibition in brown adipocytes stimulated β-oxidation and increased energy expenditure. These effects are dependent on the activity of malate-aspartate shuttle, which is a set of enzymes responsible for the transport of reducing equivalents (e.g. NADH) into mitochondrial matrix. MPC inhibition is one of the mechanisms how insulin-sensitizing drugs thiazolidinediones (TZDs) exert their beneficial effects (see 1.5.3) [58].

Each turn of TCA cycle produces one molecule of GTP together with reduced forms of coenzymes $FADH_2$ and $NADH^+$. Reduced coenzymes are further used by respiratory chain to build a proton gradient on the inner mitochondrial membrane. The proton gradient is then used to create ATP by ATP synthase in the process of oxidative phosphorylation (OXPHOS). OXPHOS is coupled to respiratory chain in most of the mitochondria in order to provide ATP to sustain cellular functions. However, in brown and brite adipocytes ATP production can be uncoupled from respiratory chain by uncoupling protein 1 (UCP1), which is a key protein responsible for NST in BAT (see 1.2.6).

1.2.6   UCP1-mediated thermogenesis

Thermogenesis is necessary for survival. Enzymes that catalyse reactions in metabolic pathways require specific range of temperature to stay active. Therefore, stable body temperature is essential for the maintenance of vital functions. All mammals have a range of ambient temperatures within which the heat sufficient to maintain stable body temperature is produced as a by-product of metabolic processes. This range of temperatures is known as the thermoneutral zone [59]. Additional heat must be produced by thermogenesis in any environment colder than the thermoneutral zone. Thermoneutral zone for mouse is around 30 °C, while in human, due to a great difference in the body size and in the ratio of body volume

to body surface, thermoneutral zone is around 21 °C [60].

The major thermogenic organs in mammals are the skeletal muscle and BAT. The skeletal muscle produces heat mostly by shivering thermogenesis. Shivering thermogenesis in skeletal muscles is based on muscle contractions, which consume ATP and dissipate heat. BAT is the main site of NST mediated by UCP1. Unlike in WAT, TAG storage per se is not the primary function of BAT and TAG stored in BAT are used to fuel UCP1-mediated NST.

UCP1-mediated NST occurs in the mitochondrion. UCP1 is an integral protein of the inner mitochondrial membrane; it was proposed that UCP1 operate as H^+ uniport [61, 62]. UCP1 facilitates proton leak through the inner mitochondrial membrane and depletes the proton gradient. Thus, the energy of the proton gradient is dissipated in the form of heat and the respiratory chain is uncoupled from OXPHOS (Figure 1.4). Mitochondrial respiration decreases in response to high proton gradient; therefore, by depleting the proton gradient UCP1 increases mitochondrial respiration [63].
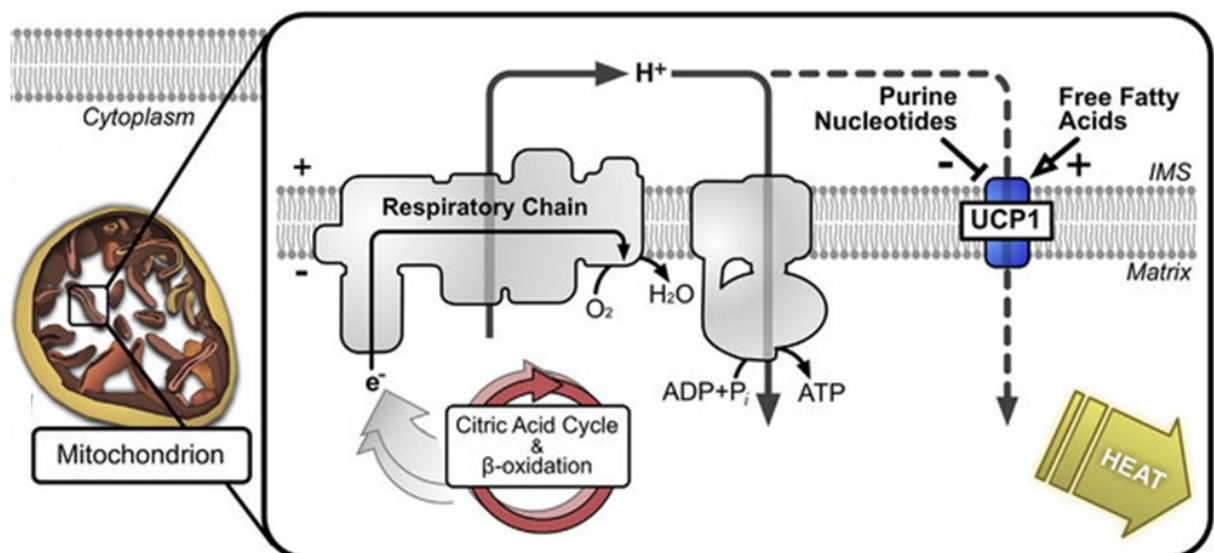
Figure 1.4 The mechanism of UCP1-mediated thermogenesis. Adapted from [64]. IMS: intermembrane space; UCP1: uncoupling protein 1.

Increased mitochondrial respiration requires increased supply of both oxygen and energy substrates. The activation of NST in BAT is associated with increased glucose uptake into brown adipocytes. High glucose uptake is used to determine the metabolically active BAT using [18]fluorodeoxyglucose PET [13]. However, fatty acids represent the major energy source to fuel UCP1-mediated NST. Activation of UCP1 in adipocytes stimulates lipolysis of the intracellular TAG stores in order to provide fatty acids for β-oxidation. In addition, the activity of LPL is stimulated, resulting in increased fatty acid uptake from the bloodstream [1]. UCP1-mediated NST significantly affects plasmatic levels of both glucose and lipids.

Different models of UCP1 activation were suggested and supported by experimental evidence; therefore, the exact mechanism remains unclear. One of the models proposed that coenzyme Q (ubiquinone) is necessary for UCP1 activation [65]. In non-active state UCP1 is

believed to be inhibited by purine nucleotides and its function as an ion transporter is supposed to be induced by fatty acids [66, 67]. However, UCP1 activation by fatty acids remains controversial as there is no agreement on what fatty acid concentration is sufficient for the induction of uncoupling function. It was also proposed that increased fatty acid concentration due to adrenergic stimulation of lipolysis in brown adipocytes further stimulate already activated UCP1 [68].

UCP1 gene is expressed in adipocytes in both BAT and WAT. In certain WAT depots UCP1 gene expression and also protein activity can be induced by adrenergic stimulation mediated pharmacologically or by stimuli such as cold exposure (CE). Active UCP1 protein in WAT is a marker of WAT browning [7, 8]. There are two distinct theories describing the nature of WAT browning. The first theory suggests that brite adipocytes are derived from different progenitor cells than white adipocytes, while the other one proposes that white adipocytes are converted to brite cells upon proper stimulation, e.g. adrenergic stimulation during chronic CE [69, 70]. Besides the activation of UCP1, WAT browning also involves mitochondrial biogenesis, which results in an increased oxidative capacity of the cell. Browning temporarily changes the morphology of WAT depot to BAT-like phenotype.

1.2.7   Healthy white adipocyte in obesity

Substantial part of obese adult humans (up to 25%) is not susceptible to the development of the metabolic syndrome and they possess the MHO phenotype [71]. MHO is characterized by protective WAT expansion along with preserved healthy metabolic functions in white adipocytes. WAT expansion in response to caloric overload is necessary for the prevention of disorders such as lipid storage in non-adipose tissues or dyslipidemia and it is accompanied by WAT remodelling. WAT remodelling changes the properties of white adipocytes including their metabolic functions.

Different types of WAT remodelling accompany WAT expansion. Pathological WAT remodelling causes the development of metabolic disorders in WAT that subsequently manifest on the level of whole-body. Adipocyte hypertrophy is the enlargement of the adipocyte due to increased lipid accumulation in the lipid droplet, while adipocyte hyperplasia is the formation of new adipocytes. As the number of adipocytes is relatively fixed in adulthood, adipocyte hypertrophy is believed to be the prevailing mechanism of WAT expansion. However, it was reported that in human certain WAT depots, e.g. scWAT expand by hyperplasia rather than by adipocyte hypertrophy [72, 73]. WAT from individuals with the metabolic syndrome is characterized by high degree of adipocyte hypertrophy and tissue hypoxia due to insufficient blood supply. WAT from individuals with MHO exhibits high ratio of smaller adipocytes and dense network of blood vessels [74]. High angiogenic capacity and a low degree of adipocyte hypertrophy therefore seem to be critical for the maintenance of metabolically healthy WAT.

The adipocyte secretion profile represents another parameter of healthy WAT. A high degree of adipocyte hypertrophy is associated with a low-grade WAT inflammation. Hypertrophic adipocytes secrete pro-inflammatory cytokines that activate immune response, namely the infiltration of macrophages into WAT (see 1.4.4) [75]. The amount of

macrophages accumulated in WAT correlates with the degree of adipocyte hypertrophy. In addition, macrophages infiltrated into WAT further secrete pro-inflammatory cytokines and supress the process of inflammation resolution. On the other hand, healthy white adipocytes secrete molecules that stimulate lipid metabolism and support the inflammation resolution. One of the markers of healthy WAT is a high secretion of adipokine adiponectin (see 1.4.3), which has anti-inflammatory properties and increases fatty acid oxidation and insulin sensitivity of WAT and other tissues [76].

The maintenance of high metabolic rate in WAT is another marker of healthy white adipocytes. WAT of obese individuals exhibits reduced oxygen consumption and decreased rate of TAG/FA cycling [77, 78]. It was also reported that the incidence of type 2 diabetes correlates with impaired mitochondrial function in WAT [79]. On the other hand, individuals with MHO displayed high expression of mitochondrial metabolic genes, suggesting preserved normal mitochondrial functions [80].

In conclusion, healthy white adipocyte is characterized by a low degree of hypertrophy, low pro-inflammatory secretion profile and high rates of TAG/FA cycling and mitochondrial oxidation (Figure 1.5). The presence of healthy white adipocytes in WAT of obese individuals contributes to the protection against metabolic disorders.
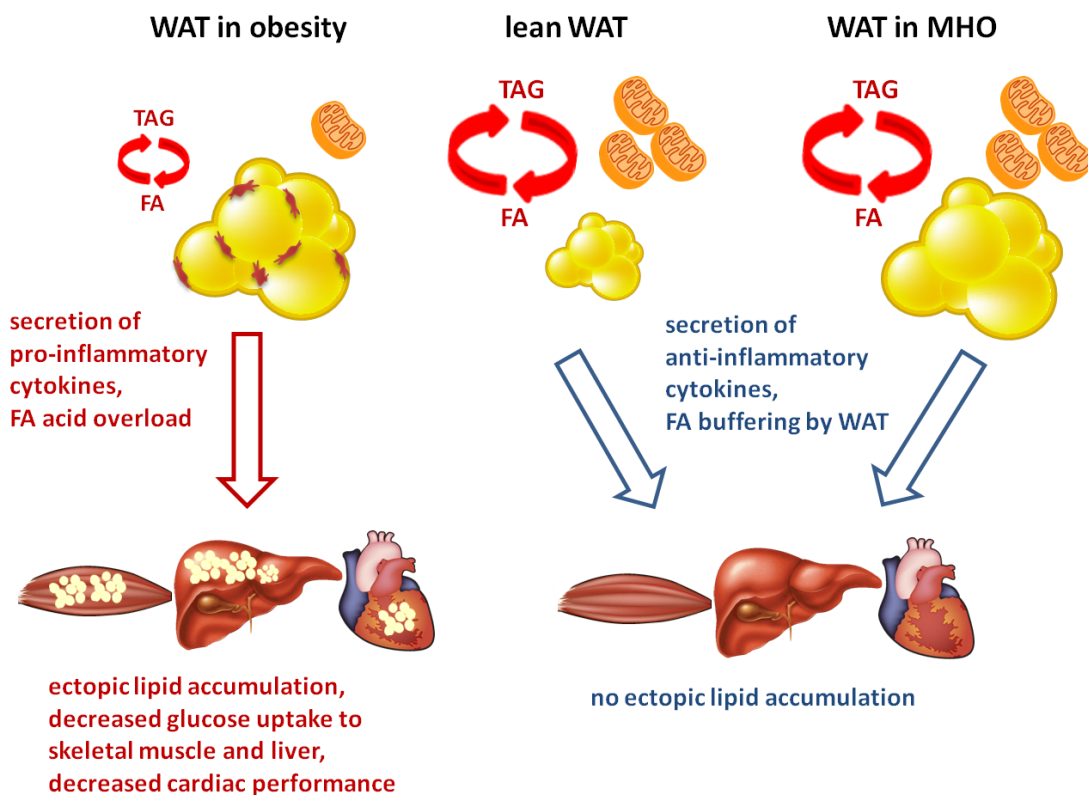
Figure 1.5 The summary of characteristic features of metabolically healthy WAT in obesity. Healthy WAT in obesity maintains healthy secretory profile, high rate of mitochondrial oxidation and high mitochondrial content. The rate of TAG/FA cycling stays high in healthy obese WAT, which is necessary for fatty acid buffering and prevention from ectopic lipid accumulation. FA: fatty acids; MHO: metabolically healthy obesity; TAG: triacylglycerols; WAT: white adipose tissue.

1.3 Transcriptional control of adipocyte metabolism

A group of transcriptional regulators contribute to the control of adipocyte metabolism. They act through the regulation of gene expression, which modulates metabolic pathways as well as the properties of mitochondria and lipid droplets within the adipocyte (see Figure 1.7 for summary). The family of peroxisome proliferator-activated receptors (PPARs) plays a critical role in the control of adipocyte energy metabolism. PPARs control lipogenesis and lipid catabolism as well as mitochondrial functions and they affect wide-range of cellular processes due to interactions with other transcriptional regulators, namely PPARγ coactivators-1α/β (PGC-1α/β). Carbohydrate and sterol response element binding proteins (ChREBP and SREBP) are transcription factors involved in the control of lipogenic genes. Transcriptional control of adipocyte metabolism represents an important tool for the maintenance of lipid homeostasis.

1.3.1 PPAR Family

The highest relevance for the control of lipid metabolism is attributed to the family of PPAR nuclear receptors. PPARs modulate activities of numerous metabolic pathways; most importantly, all PPARs are important regulators of lipid catabolism.

PPARs require activation and binding with other transcription factors in order to regulate the expression of target genes. PPARs can be activated by variety of endogenous ligands, e.g. unsaturated fatty acids and eicosanoids. A number of drugs also work as PPAR-agonists and they can be used for the treatment of various health disorders ranging from metabolic, neurological and autoimmune diseases to chronic inflammatory diseases and cancer [81]. PPARs dimerize with another nuclear receptor: retinoid X receptor (RXR), regardless of the presence of a ligand [82]. Upon activation the PPAR-RXR heterodimer interacts with the promoter of target genes by binding to DNA sequences known as PPAR response elements (PPRE). PPRE sequences were found in promoter regions of central metabolic genes including UCP1 [83]. Numerous coregulatory proteins interact with PPAR-RXR heterodimer in the process of transcriptional regulation [84]. Interaction with PPAR coactivators further expands the set of processes affected by PPARs (see 1.3.2).

PPARα is critical for the control of lipid catabolism. Although PPARα is known as the master regulator of hepatic lipid metabolism, it also regulates lipid metabolism in adipocytes. Various fatty acids and compounds with structural resemblance to fatty acids such as acyl-CoAs act as natural PPARα ligands. PPARα therefore serves as a sensor for the fatty acid cellular concentration. Target genes of PPARα (e.g. ACS, CPT1, SCAD, MCAD and VLCAD) are involved in different phases of fatty acid oxidation process [85]. Studies with PPARα deficient mice revealed a key role of PPARα for hepatic lipid metabolism during fasting as PPARα controls the expression of fasting-activated genes involved in fatty acid oxidation in the liver [86]. PPARα gene expression in the liver and in BAT follows circadian rhythm and increases in fasting period when the tissues oxidise fatty acids from WAT. PPARα expression in WAT is not rhythmical and substantially lower compared to BAT, possibly due to lower β-oxidation rate in WAT [87].

PPARβ/δ, another member of PPAR family, influences systemic lipid homeostasis due to its ubiquitous expression. However, its importance for adipocyte metabolism is minor compared to other PPARs. PPARβ/δ affects fatty acid oxidation by regulating the expression of genes such as CPT1 [88]. It was also reported that PPARβ/δ contributes to the suppression of inflammatory processes [89].

PPARγ, the third member of PPAR family, is responsible for the differentiation of mature adipocytes due to its role in the control of lipogenesis and lipid droplet formation. PPARγ controls the gene expression of PEPCK, the key enzyme of glyceroneogenesis in adipocytes, which is tightly linked to TAG/FA cycling [23, 90]. Other PPARγ target genes are involved in fatty acid oxidation (ACS) or in fatty acid uptake (LPL, CD36) [91, 92, 93]. It was also proposed that PPARγ has a role in the regulation of angiogenesis [94]. High angiogenic capacity is required for adipose tissue development as well as for the protective adipose tissue expansion in order to prevent hypoxia. PPARγ therefore greatly influences lipid metabolism in adipocytes. Due to its effects on TAG/FA cycling and lipid catabolism, PPARγ activation contributes to the maintenance of the healthy adipose tissue phenotype.

Due to its key role in the control of lipogenesis in adipocytes, PPARγ is an important target for the treatment of metabolic disorders associated with obesity. The most studied group of drugs that act as PPARγ agonists are TZDs (see 1.5.3). Endogenous PPARγ ligands are polyunsaturated fatty acids (PUFA), namely *n*-3 PUFA such as α-linolenic acid (ALA), eicosapentaenoic acid (EPA) and docosahexaenoic acid (DHA) [95]. PUFA exert variety of beneficial effects such as the suppression of inflammation and improvement of insulin sensitivity in obesity [96, 97]. These effects seem to be partly mediated through the stimulation of lipid metabolism by PPARγ target genes (see 1.5.2). In conclusion, PPARs represent a powerful tool for the regulation of various cellular processes and they greatly contribute to the control of systemic lipid homeostasis.

1.3.2 Transcriptional coactivators PGC-1α/β

PGC-1α/β coactivators are known as the major players in the control of mitochondrial metabolic functions. Although PGC-1α/β are named after PPARγ, they interact with all members of PPAR family [98, 99]. PGC-1α is the first identified and the most studied PPAR coactivator [100]. PGC-1β has a high degree of sequence and functional similarity with PGC-1α. Another transcriptional coactivator, PGC-related coactivator (PRC), displays sequence similarity with PGC-1α/β. PRC also contributes to the regulation of PPAR target genes [101].

PGC-1α affects lipid homeostasis on both cellular and systemic levels due to its central role in the regulation of mitochondrial functions. In adipocytes, PGC-1α interacts with PPARα and they are responsible for the induction of adaptive thermogenic program [102]. Upon cold stimulation, PGC-1α stimulates the uptake of glucose and fatty acids into brown adipocytes as well as the increase in β-oxidation and mitochondrial biogenesis in both brown and white adipocytes. PGC-1α also activates the expression of the gene for UCP1 in brown and brite adipocytes. Mice with PGC-1α deficiency are highly cold-sensitive [103]. PGC-1α stimulates mitochondrial respiration by activating the transcription of nuclear respiratory factors-1/2 (NRF1/2) [104], estrogen-related receptor alpha (ERRα) [105] and other metabolic genes. In

addition, activated NRF1 regulates the expression of mitochondrial transcription factor A (TFAM) [104]. TFAM controls the replication and transcription of mitochondrial DNA (mtDNA). PGC-1α is a key regulator of mitochondrial oxidation and mitochondrial biogenesis, moreover, it affects mitochondrial dynamics (see 1.3.3).

PGC-1α and PGC-1β share the majority of target genes. However, both coactivators seem to have certain exclusive functions. It was proposed that PGC-1β controls hepatic lipogenesis through interactions with both ChREBP and SREBP (see 1.3.4 and 1.3.5), while PGC-1α is important in the regulation of hepatic gluconeogenesis [105, 106, 107]. In BAT acute CE resulted in the upregulation of the gene for PGC-1α but not PGC-1β, suggesting major contribution of PGC-1α to adaptive thermogenesis [108]. PGC-1β seems to be important mostly for the control of basal mitochondrial functions. In addition, mice with whole-body PGC-1β deletion displayed decreased norepinephrine-stimulated energy expenditure, hypothermia and also altered expression of mitochondrial genes in BAT. This phenotype was more pronounced in mice exposed to cold despite the compensatory upregulation of PGC-1α [109]. PGC-1β therefore seems to have a role in the control of BAT metabolism that cannot be fully compensated by PGC-1α.

PGC-1α/β exert the majority of their effects through the regulation of mitochondrial oxidative functions. Both coactivators are abundantly expressed in tissues with high oxidative capacity, e.g. BAT, heart and skeletal muscle, while in WAT PGC-1α/β expression is rather low. Mitochondrial oxidation, lipolytic rate and also mitochondrial dynamics affect the amount of TAG stored in adipocytes [110].

1.3.3   Mitochondrial dynamics

In the cell, mitochondria form a network, which continuously changes its morphology. Such changes are known as mitochondrial dynamics and they consist of fission and fusion events. Changes in the morphology of mitochondrial network are accompanied by changes in mitochondrial metabolic functions. Mitochondrial dynamics is critical for cells with abundancy of mitochondria, e.g. brown adipocytes and muscle cells. Mitochondrial dynamics is affected by stimuli that change energy requirements or the availability of metabolic energy [111]. Conditions that require high mitochondrial ATP synthesis, e.g. fasting, favour mitochondrial elongation, while conditions with excess energy supply are associated with mitochondrial fragmentation [111, 112]. By changing their architecture mitochondria regulate energy expenditure and metabolic efficiency and dysregulation of mitochondrial dynamics is therefore linked with metabolic disorders [113].

Mitochondrial dynamics is mediated by a group of proteins with GTPase activities (Figure 1.6). Dynamin-related protein 1 (DRP1) is the key mediator of mitochondrial fission. Mitofusins 1 and 2 (MFN1/2) are responsible for the fusion of the outer mitochondrial membrane while another protein, OPA1, mediates the fusion of the inner mitochondrial membrane [114]. Two distinct forms of OPA1 were identified: the long form (L-OPA1) and the short form (S-OPA1). It was proposed that L-OPA1 is more involved in mitochondrial fusion, while S-OPA1 organises the structure of mitochondrial cristae [115]. Thus, S-OPA1 maintains the activity of the respiratory chain in changing mitochondrial network. However,

both forms of OPA1 are needed for the optimal mitochondrial fusion. In addition to mitochondrial fusion, OPA1 seems to directly regulate metabolism in adipocytes. It was reported that OPA1 interacts with both PKA and perilipin on the surface of lipid droplet and it promotes lipolysis by facilitating the phosphorylation of perilipin by PKA (see 1.2.2) [36].

MFN2 is believed to affect mitochondrial energy metabolism through mechanism independent of mitochondrial fusion. MFN2 overexpression in myoblasts and HeLA cells resulted in increased activity of respiratory chain [116]. Mice with adipose tissue specific MFN2 deletion displayed impaired BAT thermogenesis and decreased oxidative capacity of brown adipocytes [110]. The study further proposed that MFN2 mediates the interaction between mitochondrion and lipid droplet by docking the outer mitochondrial membrane to perilipins on the surface of lipid droplet.
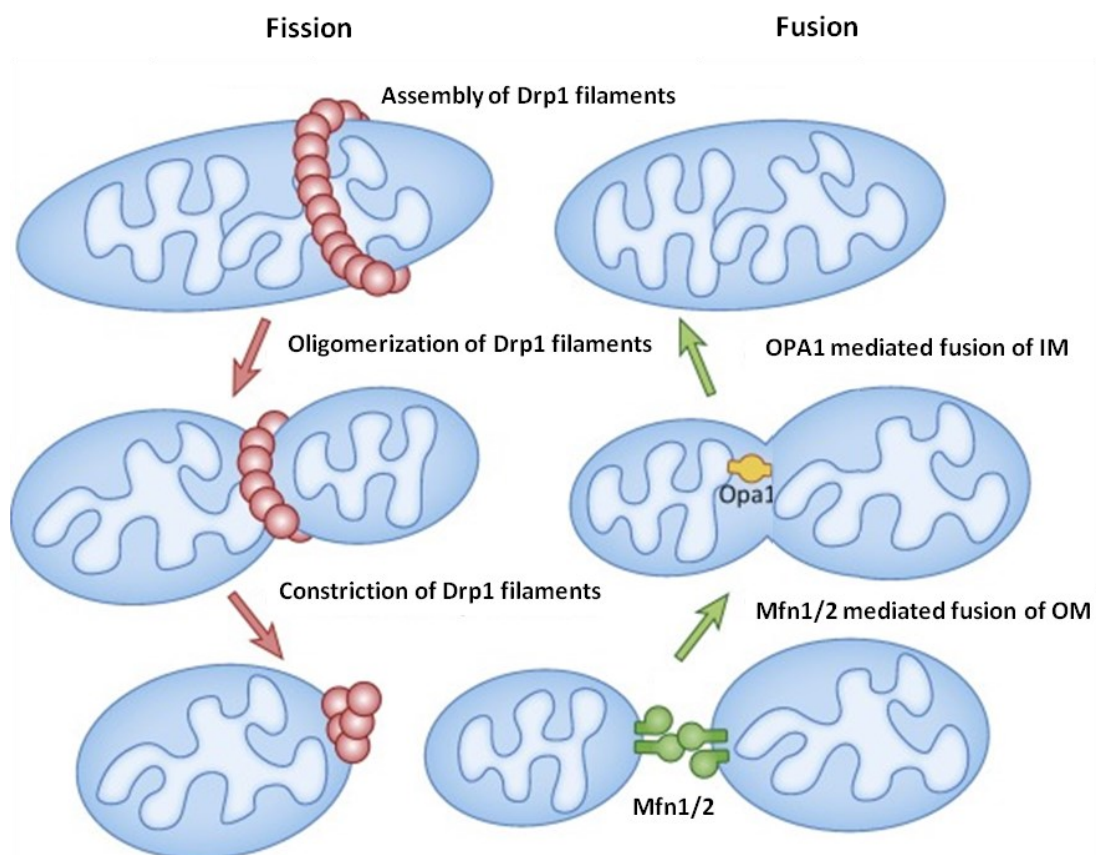
Figure 1.6 Molecular mechanisms of mitochondrial fission and fusion. Modified from [117]. Drp1: dynamin-related protein 1; IM: inner membrane; Mfn1/2: mitofusin 1/2; OM: outer membrane; Opa1: Optic atrophy 1.

PGC-1 coactivators seem to contribute to the control of proteins that mediate mitochondrial dynamics. PGC-1β overexpression in muscle cells increased the protein levels of DRP1, OPA1 and MFN1/2. Interestingly, whole-body PGC-1β-ablated mice displayed decreased protein levels of MFN2 in the skeletal muscle, while the protein levels of MFN1, DRP1 and OPA1 remained unchanged. It was observed that the control of MFN2 by PGC-1β requires binding of ERRα to MFN2 promoter [118]. PGC-1β seems to regulate MFN2 only in

basal conditions. On the other hand, PGC-1α induced MFN2 in muscle cells under the conditions of increased energy expenditure such as CE and adrenergic stimulation. In addition, PGC-1α and MFN2 shared the same expression profile in the skeletal muscle and BAT of rats treated by adrenergic agonist. The control of MFN2 expression by PGC-1α is also mediated through ERRα [119]. Moreover, the function of PGC-1α-ERRα-MFN2 pathway seems to be impaired in the skeletal muscle of diabetic patients [120].

Mitochondrial dynamics is a physiological mechanism that adjusts cellular metabolism to changing energy demands. Mitochondrial dynamics in adipocytes affects lipid metabolism by changing the shape of mitochondria and thus modifying the interactions between mitochondria and lipid droplets. Proteins involved in mitochondrial dynamics also directly affect mitochondrial oxidation as well as the rate of lipolysis. PGC-1α/β-ERRα-MFN2 regulatory pathway is an example of transcriptional control of energy metabolism in adipocytes.

1.3.4   ChREBP

Transcription factor ChREBP links glucose metabolism with the metabolism of lipids. ChREBP induces lipogenesis in response to increased intracellular glucose concentration. It was observed that glucose induces ChREBP activation and its subsequent binding to FAS promoter [121]. The activity of ChREBP is regulated by glucose transporter 4 (GLUT4) [122]. GLUT4 is the major insulin-sensitive glucose transporter in adipose tissue and it is largely responsible for glucose uptake into the adipocyte [123]. ChREBP is abundantly expressed in both BAT and WAT; however, ChREBP levels are higher in BAT, reflecting higher rate of *de novo* lipogenesis. Two ChREBP isoforms were identified: ChREBPα and ChREBPβ. The gene expression levels of ChREBPβ but not ChREBPα correlate with ChREBP activity, suggesting that ChREBPβ represent the transcriptionally active form [124]. The coupling of adipocyte glucose uptake with lipogenesis is a unique function of ChREBP.

1.3.5   SREBP

SREBP is involved in the regulation of cholesterol metabolism and fatty acid synthesis. SREBP is highly expressed in both BAT and WAT as well as in the liver. Three distinct SREBP protein isoforms were identified: SREBP-1a, SREBP-1c and SREBP-2. SREBP-1a and SREBP-1c are encoded by a different gene than SREBP-2 [125]. All three SREBP isoforms activate the transcription of target lipogenic genes, e.g. ACC and FAS. Study with the overexpression of SREBP-1a/c reported increased fatty acid biosynthesis and unchanged cholesterol synthesis. Oppositely, overexpression of SREBP-2 in mice resulted in increased cholesterol/fatty acid ratio in the liver and adipose tissue due to increased cholesterol synthesis [126]. SREBP-1a/c and SREBP-2 therefore seem to favour the activation of different lipogenic pathways.

Figure 1.7 The summary of transcriptional regulators involved in the control of adipocyte energy metabolism and their targets. ATGL: adipose triglyceride lipase; ChREBP: carbohydrate response element binding protein; CPT-1: carnitine palmitoyltransferase 1; ERRα: estrogen-related receptor alpha; FA: fatty acids; FAS: fatty acid synthase; G3P: glycerol-3-phosphate; HSL: hormone sensitive lipase; NRF1/2: nuclear respiratory factors-1/2; PKA: protein kinase A; PEPCK: phosphoenolpyruvate carboxykinase; PGC-1α/β: peroxisome proliferator-activated receptor gamma coactivator-1α/β; PPARα: peroxisome proliferator-activated receptor alpha; PPARγ: peroxisome proliferator-activated receptor gamma; SREBP: sterol response element binding protein; TAG: triacylglycerols; TFAM: mitochondrial transcription factor A; UCP1: uncoupling protein 1.

1.4   Adipose tissue in the inter-organ crosstalk

Adipose tissue plays a central role in the crosstalk of metabolically active organs. As a key storage of energy substrates, adipose tissue has to respond to various regulatory signals. These signals can be neuronal, hormonal (endocrine) or paracrine. Neuronal and hormonal signals originate mostly in hypothalamus, which is a part of the central nervous system (CNS). Neuronal signals are transferred to adipose tissue mostly through the sympathetic nervous system (SNS). Hormonal signals are delivered to adipose tissue through endocrine glands such as pancreas or adrenal glands. Adipose tissue itself is an endocrine organ. It secretes a variety of bioactive factors, i.e. adipokines. Adipokines act in many sites in the body including CNS. Immune system also greatly affects the metabolism of adipose tissue. Immune cells mostly interact with adipose tissue by paracrine signalling. The metabolic crosstalk between adipose tissue and other organs is critical for the control of systemic

energy homeostasis.

1.4.1 Neuronal control of adipose tissue

CNS controls adipose tissue through hormonal and neuronal signalling. Hormonal signalling involves hypothalamus and endocrine glands that secrete hormones into the bloodstream (see 1.4.2). Endocrine glands are often co-regulated by SNS. In addition, SNS directly innervates both WAT and BAT. Therefore, SNS has a critical role in the neuronal control of adipose tissue. CNS regulates the activity of SNS and it also controls the metabolism of adipose tissue by regulating the energy balance and food intake [127].

CNS controls energy balance through regulatory circuits that involve orexigenic and anorexigenic brain centres. These centres receive signals from periphery, integrate the signals and respond to them. The main centre for the control of food intake is hypothalamic paraventricular nucleus (PVN). PVN integrates peripheral signals such as gut hormones, e.g. cholecystokinin and also interacts with limbic system and other brain areas to mediate the reward aspects of feeding [128]. Neuropeptides in hypothalamic neurons mediate the perception of hunger or satiety. Neuropeptide Y (NPY) is an orexigenic neuropeptide, while α-melanocyte-stimulating hormone (αMSH) is an example of anorexigenic neuropeptide [129].

Prolacting-releasing peptide (PrRP) is another peptide with the ability to regulate energy balance. PrRP administration to CNS resulted in the activation of hypothalamus-pituitary-adrenal axis (HPA axis) [130]. Another study reported that PrRP administration to CNS in rats reduced food intake [131]. G-protein coupled receptor 10 (GPR-10) was identified as a receptor for PrRP. In both human and rodents GPR-10 was detected in the hypothalamus and in the brainstem [132]. The deletion of GPR-10 in mice resulted in increased food intake, increased adiposity and decreased glucose tolerance [133]. In another study GPR-10 deficient mice displayed increased bodyweight and adiposity possibly due to lower energy expenditure [134].

The key brain centres for the regulation of adipose tissue metabolism are the arcuate nucleus (ARC) and the ventromedial nucleus (VMN) in the hypothalamus together with nucleus tractus solitarius (NTS) in the brainstem [135]. The central melanocortin system (CNS-Mcr) also contributes to the control of adipose tissue metabolism. CNS-Mcr includes NPY-expressing neurons from ARC and also neurons from both ARC and NTS that express proopiomenalocortin (POMC), which is a precursor of αMSH. It was reported that decreased activity of CNS-Mcr results in increased glucose and lipid uptake into WAT and increased TAG synthesis in WAT and in the liver [136]. Electrical stimulation of VMN resulted in lipolytic response in WAT, which was blunted by β-adrenergic blockers. Therefore, the VMN-WAT connection seems to be dependent on SNS and β-adrenergic receptors within WAT [137].

VMN and ARC are involved in the control of BAT metabolism. VMN was the first brain centre to be identified as a regulator of BAT thermogenesis. Electrical stimulation of VMN increased temperature of iBAT in rats [138]. It was reported that ARC controls the sympathetic outflow to BAT through NPY-expressing neurons [139]. The effects of SNS on

the metabolism of both BAT and WAT are mediated by adrenergic receptors with norepinephrine being the main neurotransmitter. In addition, adrenergic receptors in adipose tissue are stimulated by norepinephrine and epinephrine that are released to the bloodstream from adrenal glands (through HPA axis).

1.4.2   Hormonal control of adipose tissue

The most important hormones for the control of metabolism in both WAT and BAT are catecholamines (norepinephrine/noradrenaline and epinephrine/adrenaline). Catecholamines stimulate catabolic processes in adipose tissue, especially lipolysis. Insulin is another hormone with great importance mostly for the control of WAT metabolism. Insulin inhibits lipolysis and stimulates lipogenesis in adipocytes. Effects of other hormones on the metabolism of adipose tissue are less considerable or they act indirectly, e.g. through the regulation of food intake [140].

Catecholamines are necessary for the acute stress response. They are produced by adrenal medulla upon stimulation by SNS in the sympathomedullary pathway (SAM pathway). SAM pathway and HPA axis are the main neuro-hormonal regulatory tools for the response to acute and chronic stress (Figure 1.8). Both norepinephrine and epinephrine stimulate β adrenergic receptors (β-AR) in adipocytes [141]. The stimulation of β-AR activates PKA, which stimulates the lipolytic activity of HSL and it also phosphorylates perilipins on the surface of lipid droplet (see 1.2.2). As a part of the acute stress response catecholamines suppress food intake and food absorption; this attenuates anabolic processes in adipose tissue [140]. In addition, catecholamines inhibit insulin-stimulated glucose uptake into adipocytes [142].

The primary function of insulin is to facilitate the transport of glucose from the bloodstream into cells in the postprandial state. Insulin is secreted from pancreatic β-cells in response to the increase in plasmatic levels of glucose and other nutrients such as amino acids [143]. The effects of insulin on adipose tissue metabolism are anti-catabolic and pro-lipogenic. The main anti-catabolic effect of insulin in adipocytes is mediated by the inhibition of HSL. In addition, insulin stimulates the activity of LPL, which increases fatty acid uptake into adipocytes [144]. Beside the inhibition of lipolysis and stimulation of fatty acid uptake in adipose tissue, insulin also stimulates preferential use of carbohydrates as an energy substrate in the skeletal muscle [145]. Insulin therefore has a strong fat-sparring effect on the whole-body level.

Insulin is necessary for glucose buffering by adipose tissue and other organs. Insulin binds to insulin receptor on the cellular surface and activates signalling cascade that results in the translocation of GLUT4 to the plasmatic membrane [146]. The activation of cellular processes leading to insulin-mediated glucose uptake depends on insulin sensitivity. Cells with decreased insulin sensitivity require more insulin to take up glucose; such condition is known as insulin resistance. Individuals with insulin resistance have to increase insulin secretion in order to maintain glucose uptake into cells. If pancreatic β-cells cannot produce more insulin, insulin resistance eventually develops to type 2 diabetes. One of the main causes of insulin resistance is high plasmatic concentration of NEFA, which impairs insulin signalling [147]. Insulin resistance and the onset of type 2 diabetes are therefore often associated with

hyperlipidemia and obesity.

Other substrates associated with insulin resistance are branched chain amino acids (BCAA), i.e. valine, leucine and isoleucine. BCAA acutely stimulate insulin secretion from pancreatic β-cells and it was demonstrated that high BCAA intake in obese mice further decreased insulin sensitivity [148, 149]. Adipose tissue seems to have the ability to buffer plasmatic BCAA levels [150]. However, BCAA metabolism in adipose tissue is blunted in obesity, which results in further increase in plasmatic BCAA levels.

HPA axis regulates adipose tissue metabolism through hormone cortisol. Cortisol has only a minor effect on lipid metabolism; however, cortisol greatly affects glucose metabolism. It stimulates gluconeogenesis and increases plasmatic glucose levels. Cortisol therefore indirectly stimulates lipogenesis in adipose tissue. On the other hand, cortisol seems to directly stimulate lipolysis [151]. Hormonal control of adipose tissue is a complex process and the hormones that are involved can act both antagonistic as well as synergistic [142, 152].
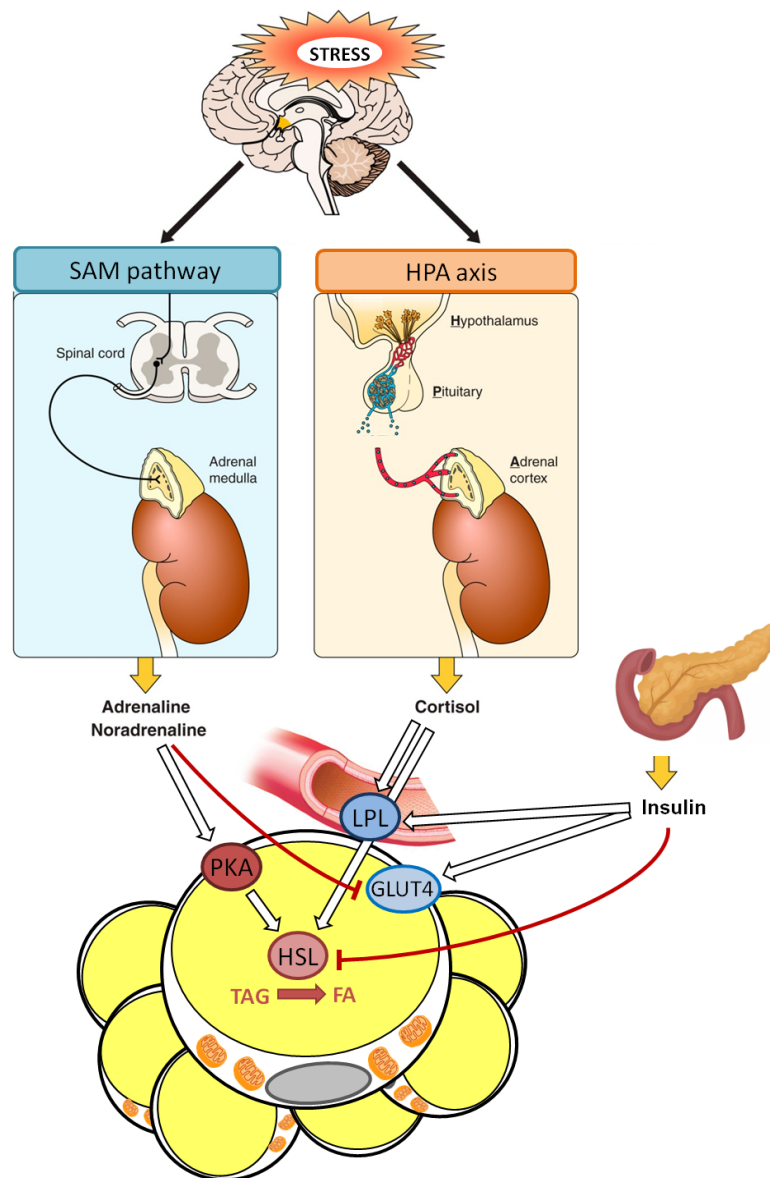
Figure 1.8 The summary of hormonal control of WAT metabolism. Modified from [153].

FA: fatty acids; GLUT4: glucose transporter 4; HPA axis: hypothalamus-pituitary-adrenal axis; HSL: hormone sensitive lipase; LPL: lipoprotein lipase; PKA: protein kinase A; SAM pathway: sympathomedullary pathway; TAG: triacylglycerols.

1.4.3   Adipose tissue as an endocrine organ

One of the fundamental features of adipose tissue is the ability to secrete adipokines. Adipokines are small proteins that regulate variety of processes including the metabolism of lipids and glucose, immune response and inflammation [154]. Adipokines exert their effects on adipose tissue as well as on other tissues and organs including CNS (Figure 1.9). Adipokines are secreted from adipose tissue, predominantly by adipocytes but also by immune cells and other cell types. Leptin and adiponectin are adipokines with the highest importance for the regulation of whole-body energy metabolism. Leptin and adiponectin are expressed in both WAT and BAT; however, their expression in BAT is considerably lower and it decreases upon BAT adrenergic stimulation [1]. Fibroblast growth factor 21 (FGF21) is another adipokine that acts as a potent metabolic regulator. Tumor necrosis factor α (TNFα), another protein secreted from adipose tissue, is associated with inflammation and the alteration in adipose tissue functions in obesity and other metabolic disorders. FGF21 as well as TNFα are secreted by both WAT and BAT.

Leptin has a great ability to influence systemic energy homeostasis through its effects on CNS. Leptin binds to leptin receptor primarily in hypothalamus. Leptin receptor (also known as OB-R) is a protein encoded by Ob gene and it is located on the plasmatic membrane of neurons and several other cell types [155]. Effects of leptin on the regulation of food intake in hypothalamic neurons are mediated through transcription factor STAT3 [156]. The phosphorylation of STAT3 can be therefore used as a marker of leptin binding in hypothalamic neurons. Activation of leptin receptor in POMC-expressing neurons in ARC increases POMC mRNA levels and the activity of these neurons, which has an anorexigenic effect. On the other hand, leptin seems to inhibit the activity of orexigenic NPY-expressing neurons in ARC [157]. Therefore, leptin signalling in hypothalamus leads to suppression of food intake. By modulating the activity of neurons in ARC and other hypothalamic nuclei leptin also affects the activity of SNS [158]. By increasing the activity of SNS leptin indirectly influences metabolic processes in BAT. Leptin increases energy expenditure and thermogenesis in BAT. Obese mice with high plasmatic leptin levels displayed higher iBAT temperature, while leptin-deficient mice had decreased iBAT temperature [159]. The link between leptin and the activity of SNS represents another mechanism how leptin regulates energy metabolism as increased BAT activity strongly affects the homeostasis of lipids and glucose.

Plasmatic leptin levels positively correlate with the amount of adipose tissue. Leptin seems to signalize the size of adipose tissue energy stores to the brain [160]. Similarly as in the case of insulin, sensitivity to leptin can decrease in leptin-responsive cells, leading to the development of leptin resistance. Obesity is associated with an impairment of intracellular leptin signalling and reduced leptin transport into the brain [161]. Therefore, appetite-supressing effects of leptin are blunted in obese individuals in spite of high plasmatic leptin

levels.

Adiponectin exerts various beneficial effects on metabolically active tissues. Adiponectin stimulates lipid metabolism in the liver and in skeletal muscle through the activation of PPARα. Stimulation of PPARα-target genes increases the rate of β-oxidation and fatty acid uptake [162]. Stimulation of lipid combustion in these tissues could be one of the mechanisms how adiponectin increases insulin sensitivity. Insulin-sensitising effects of adiponectin were demonstrated both in rodents and humans [162, 163]. In contrast to leptin, plasmatic levels of adiponectin negatively correlate with the amount of adipose tissue [164]. Adiponectin receptor was detected in human brain and pituitary gland, suggesting potential role of adiponectin in the regulation of CNS-endocrine axes [165].

FGF21 influences several metabolic processes in adipose tissue. The gene for FGF21 is expressed in the liver, skeletal and cardiac muscle and in both WAT and BAT. FGF21 is secreted mainly from the liver; secretion from adipose tissue does not seem to contribute to plasmatic FGF21 levels [166]. FGF21 from adipose tissue therefore acts as an autocrine or paracrine factor. It was reported that treatment with exogenous FGF21 improved metabolic health in obese mice [167]. FGF21 administration induced the gene expression of TAG/FA cycling regulators such as PEPCK and DGAT1 in WAT as well as the expression of the gene for UCP1 in both BAT and WAT [168]. This represents potential mechanism how FGF21 exerts its beneficial effects.

Obesity is associated with increased TNFα production in adipose tissue. Major producers of TNFα are macrophages, which are infiltrated into WAT in obesity due to chronic low-grade inflammation [75]. TNFα impairs insulin signalling in insulin responsive tissues and therefore decreases insulin sensitivity. Chronic administration of TNFα to rats increased their plasmatic lipid levels suggesting that TNFα is involved in the regulation of lipid metabolism [169].
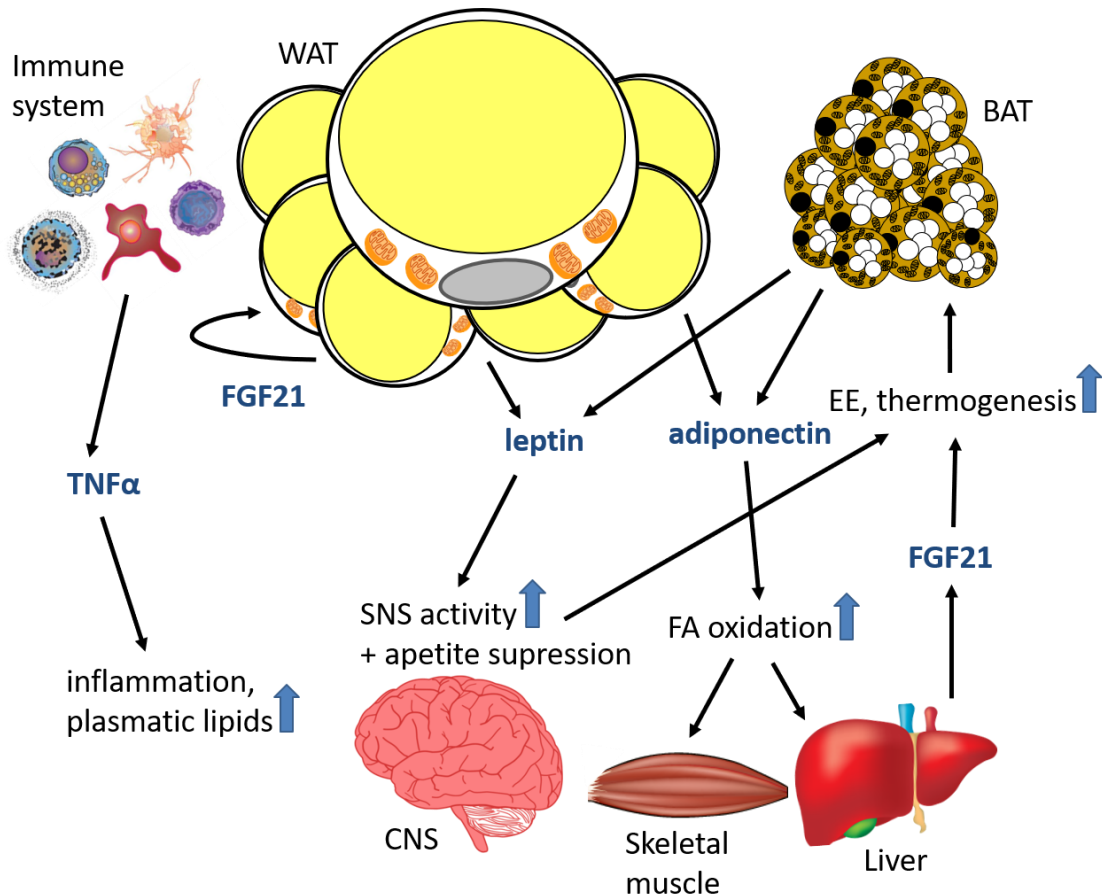
Figure 1.9 The summary of the most important adipokines and their effects on other metabolically active organs. BAT: brown adipose tissue; CNS: central nervous system; EE: energy expenditure; FA: fatty acids; FGF21: fibroblast growth factor 21; SNS: sympathetic nervous system; TNFα: tumor necrosis factor alpha; WAT: white adipose tissue.

1.4.4   Adipose tissue and the immune system

Interactions between adipose tissue and the cells of the immune system have a great importance for the regulation of adipose tissue metabolism. Certain adipose tissue depots (e.g. subcutaneous depot) contain lymphoid tissue, particularly lymph nodes. Immune cells residing in the lymph nodes interact with adipocytes in their proximity. Another population of immune cells resides directly in adipose tissue and it represents an important part of SVF. Immune cells secrete paracrine and autocrine signalling molecules that affect metabolism of adipocytes.

Adipocytes from lymph node-containing depots exhibit different properties compared to adipocytes from depots without lymphoid tissue. It was observed that dendritic cells from lymph nodes use various cytokines to stimulate lipolysis in adipocytes in order to acquire fatty acids for fuelling the immune response [170]. In addition, adipocytes surrounding the lymph nodes seem to be less responsive to general lipolytic signals such as norepinephrine [171]. The size of the node-containing depots remains relatively constant during seasonal fluctuations in fat mass of wild animals, which suggests lower contribution of node-

containing depots in lipid catabolism and lipid accumulation in response to environmental stimuli [172].

The amount of adipose tissue-resident immune cells as well as their secretion profile depends on the physiological state of adipose tissue. Abundant lipid accumulation in adipose tissue during obesity is associated with increased production of pro-inflammatory cytokines by both adipocytes and immune cells [173]. Pro-inflammatory cytokines such as interleukin 6 (IL-6) and TNFα (see 1.4.3) further stimulate the infiltration of macrophages and other immune cells into adipose tissue resulting in a vicious circle.

There are two main types of macrophages, pro-inflammatory M1 and anti-inflammatory M2 macrophages. M1 macrophages are characterized by the expression of integrin CD11c, inducible nitric oxide synthase and the secretion of pro-inflammatory TNFα. On the other hand, markers of M2 macrophages are the expression of an enzyme arginase and anti-inflammatory interleukin 10 (IL-10) [174]. A part of macrophage population also displays markers of both M1 and M2 types [175]. However, in a healthy lean state with a low degree of inflammation majority of macrophages are M2 type. Obesity is associated with a great increase in the amount of M1 macrophages resulting in more than a half of total macrophage population being M1 type. Although switching between macrophage types is a reversible process, massive increase in pro-inflammatory M1 type strongly contributes to the low-grade systemic inflammation that accompanies obesity [176].

Abundant adipocyte hypertrophy might result in cell necrosis. Macrophages removing the remnants of dead adipocytes form crown-like structures (CLS), one of the markers of WAT inflammation. It was reported that CLS comprise over 90% of macrophages in WAT of obese individuals [177]. Galectin-3 (Mac-2) is a protein expressed on the surface of both M1 and M2 macrophages and it has a role in the process of cellular adhesion [178]. Mac-2 is frequently used as a marker for the detection of macrophages in CLS.

The activation of immune response generally promotes catabolic processes in adipose tissue. Inflammation inhibits TAG storage and stimulates the release of fatty acids from adipocytes [179]. Increased plasmatic fatty acid levels then contribute to the development of additional metabolic disorders such as insulin resistance. Immune system has a great ability to influence the whole-body energy balance.

1.5 Environmental and dietary modulation of adipose tissue metabolism

Metabolic processes in adipocytes are affected by signals that are released in response to stimuli such as changes in environmental temperature or diet. Hormonal, neuronal and paracrine signals from CNS or the immune system activate signalling cascades that modulate rates of metabolic pathways and the expression of transcriptional regulators and other genes. Transcriptional regulators directly affect the expression of genes for metabolic enzymes, which regulate fluxes through metabolic pathways. Three treatments that are discussed in publications included in this thesis are CE, dietary supplementation by *n*-3 PUFA and pharmacological treatment with insulin-sensitizing dugs TZDs. Cold stress is a potent activator of SNS, in particular it stimulates β-AR in adipose tissue. The stimulation of β-AR results in the mobilization of TAG stores in adipocytes. *n*-3 PUFA directly activate

transcriptional regulators involved in the control of adipose tissue metabolism (namely PPARα and PPARγ) and also serve as precursors for variety of bioactive substances [180]. In WAT TZDs were reported to stimulate lipid metabolism, in particular lipogenesis, both in *vivo* and *in vitro* [181, 182]. TZDs also act through the nuclear receptor PPARγ; however, due to adverse effects associated with PPARγ activation second generation TZDs were developed and they are examined in one of the studies in this thesis.

1.5.1 Effects of cold exposure

Cold stress activates variety of physiological mechanisms. In the initial stage of CE, acute mechanisms for the heat preservation such as vasoconstriction of skin vessels are activated. Subsequently, heat is produced by muscle contractions in the process of shivering thermogenesis. The endurance of muscle shivering is limited and muscle fatigue accompanied by cramping and glycogen depletion eventually results in decreased heat production by this mechanism [183]. Some mammals such as mice and other rodents as well as human infants therefore employ additional thermogenic mechanism, i.e. BAT NST mediated by UCP1 (see 1.2.6). Both muscle shivering as well as UCP1-mediated NST are highly energy-consuming processes and they cause massive increase in energy expenditure. The early stage of CE is therefore characteristic by depletion of energy stores. Cold stress significantly affects systemic energy homeostasis.

The predominant usage of lipids as a more abundant energy substrate is one of the critical advantages of NST. Carbohydrates seem to be the major energy substrate fuelling the process of shivering thermogenesis, while thermogenesis in BAT is primarily fuelled by fatty acids from TAG stores in brown adipocytes [184, 185]. It was calculated that NST in BAT is fuelled by glucose only from approximately 10 % with the rest being dependent on fatty acid combustion [186]. The rate of fatty acid turnover increases in CE and fatty acids liberated from WAT are taken up by brown adipocytes to be esterified to TAG. The utilization of fatty acids in brown adipocytes in response to cold is stimulated by several mechanisms (see 1.2.6). In addition, the release of fatty acids from WAT is also increased due to stimulation of lipolysis by the activation of β-AR [187]. The weight of WAT and BAT depots in mice decreased after 2 days of CE; however, only BAT regained its original weight after 7 days of CE due to elevated rate of lipogenesis [44]. Cold stress increases the rate of TAG/FA cycling and lipid metabolism in general in both WAT and BAT.

1.5.2 Effects of n-3 PUFA

n-3 PUFA influence adipose tissue energy metabolism on the cellular level by stimulating lipid catabolism and TAG/FA cycling. Dietary sources of ALA are seeds such as flaxseed and rapeseed. ALA is a precursor of EPA and DHA; however, the conversion of ALA to EPA and DHA occurs at insufficiently low rates. EPA and DHA therefore have to be gained from diet. EPA and DHA are abundant in dietary sources such as marine fish, krill and marine plankton. An important target of EPA and DHA are PPAR nuclear receptors and their activation mediates the effects on the rate of lipid metabolism in adipocytes [180]. It was demonstrated

that *n*-3 PUFA stimulate both lipolysis and fatty acid re-esterification and therefore increase the rate of TAG/FA cycling in adipocyte and other cell types [188, 189]. *n*-3 PUFA also stimulated mitochondrial biogenesis, mitochondrial fatty acid oxidation and overall rate of lipid catabolism in adipocytes [190]. Effects on TAG/FA cycling seem to be mediated through PEPCK and DGAT1, which are the key enzymes catalysing fatty acid re-esterification. Effects on the stimulation of lipid catabolism are probably mediated through transcriptional coactivator PGC-1α.

n-3 PUFA are necessary for the synthesis of various lipid mediators. Lipid mediators are made from membrane phospholipids upon cleavage of fatty acid from the phospholipid molecule. Fatty acid cleavage is catalysed by phospholipase A2 while the further processing is catalysed by cytochrome P450 epoxygenases, lipoxygenases or cyclooxygenases. *n*-3 PUFA are substrates giving rise to lipid mediators known as protectins and resolvins [191]. Protectins and resolvins can influence metabolic processes in the cell by interacting with various transcriptional regulators including PPARγ. On the tissue level these lipid mediators have anti-inflammatory effects. Resolvins interact with immune cells and decrease the production of pro-inflammatory cytokines such as IL-6 and TNFα [192]. Other group of PUFA are known as *n*-6 PUFA and they involve molecules such as linoleic acid or arachidonic acid (AA). AA gives rise to lipid mediators with pro-inflammatory properties, namely prostaglandins, thromboxanes and leukotrienes [193]. These lipid mediators promote the inflammation by modulating vascular permeability and smooth muscle contractility in the inflamed area and stimulate immune cells to further produce pro-inflammatory cytokines. Balanced intake of *n*-3 and *n*-6 PUFA is therefore necessary in order to limit inflammatory processes in the adipose tissue as well as on the systemic level [194].

1.5.3   Effects of TZDs

TZDs are insulin-sensitizing drugs used for the treatment of type 2 diabetes. TZDs promote lipogenesis in WAT through the activation of PPARγ [195]. Besides acting as a high affinity PPARγ ligand, TZDs are supposed to inhibit obesity-associated phosphorylation of PPARγ mediated by protein kinase Cdk5 [196, 197]. TZDs were also shown to acutely inhibit MPC resulting in the stimulation of mitochondrial fatty acid oxidation and increased overall rate of lipid and amino acid catabolism in various cell types [58]. In addition, MPC inhibition possibly stimulates the rate of TAG/FA cycling in adipocytes [47]. Treatment with TZDs is accompanied by adverse effects such as weight gain and fluid retention [198]. Such effects seem to be the result of PPARγ activation in non-adipose tissues, e.g. the brain and kidneys. Due to detrimental effects of rosiglitazone on the cardiovascular system, pioglitazone (PIO) is the only TZD remaining in clinical use. Therefore, second generation PPARγ-sparing TZDs were developed. Second generation TZDs exert their effects through the inhibition of MPC with minimal direct activation of PPARγ [199, 200]. An example of PPARγ-sparing TZDs is MSDC-0602K (MSDC), which was used in recent clinical trial [201]. In this study MSDC was shown to generally improve markers of liver health and decreased fasting glucose and insulin levels without dose limiting side effects. MSDC therefore seems to have a great potential as a treatment for obesity-associated metabolic disorders. One of the studies in this

thesis examined combined effects of TZDs and *n*-3 PUFA and compared the effects of PIO and MSDC on metabolic health of obese mice.

2 Aims of the thesis

The general aim of this thesis was to study effects of the modulation of adipose tissue metabolism on whole body energy homeostasis. The main focus was on mutual interactions between adipose tissue and other metabolically active organs.

The specific aims were following:

1) To characterize the effect of *n*-3 PUFA and anti-diabetic drugs TZDs on WAT metabolism, in particular on the activity of TAG/FA cycling in eWAT and to study the effects of *n*-3 PUFA and TZDs on the maintenance of healthy metabolic phenotype in obese mice.

2) To examine the effects of GPR-10 deletion in the CNS on the whole-body energy homeostasis with a focus on adipose tissue metabolism in mice.

3) To characterize the role of transcriptional regulator PGC-1β in adipose tissue under conditions with different energy demands on thermogenesis.

3 Methods

3.1 General description of conducted experiments

All the presented studies were performed using mice on C57BL/6 genetic background. During the experiments mice were single-caged (publications A and B) or three per cage (publication C) and their body weight and food consumption were monitored daily (publication C) or weekly (publication A, B). With the exception of high-fat (HF) diet-fed groups in publications A and B, all mice were fed standard laboratory chow diet (STD; energy density 13.0 kJ.g-1, ~3.4% wt/wt as lipids, rat/mouse-maintenance extrudate; Ssniff Spezialdiäten GmbH, Soest, Germany). Mice were maintained on 12-h light-dark cycle (light from 6.00 a.m.) with free access to water and diet. Experiments were terminated by sacrificing the mice in randomly fed state under diethyl ether anaesthesia (between 8.00 and 10.00 a.m.). Tissue samples were collected, flash frozen in liquid nitrogen immediately upon dissection (if not specified otherwise) and stored at -80 °C for further analyses. Plasma samples treated with ethylenediaminetetraacetic acid (EDTA) were collected and stored at -80 °C for further analyses. All animal procedures were conducted according to all appropriate regulatory standards under protocols 172/2009 or 81/2016 approved by the Animal Care and Use Committee of the Czech Academy of Sciences and followed the guidelines for the use and care of laboratory animals of the Institute of Physiology (IPHYS).

3.1.1   Publication A

In publication A, male C57BL/6N mice (Charles River Laboratories, Sulzfeld, Germany) were used. Mice were maintained at 22 °C and fed standard chow diet. At the age of 3 months, mice were randomly assigned to (i) HF diet (~35% wt/wt as lipids, mainly corn oil) or to (ii) the same HF diet, in which 15% wt/wt of dietary lipids was replaced with n-3 PUFA concentrate EPAX 1050TG (Epax AS, Aalesund, Norway) so the total EPA and DHA concentrations were 30 mg/g diet [202]. Four other interventions were based on these two HF diets (either with or without n-3) further supplemented with (iii-iv) 50 mg pioglitazone/kg diet (PIO; Actos, Takeda, Japan) or with (v-vi) 330 mg MSDC-0602K/kg diet (MSDC; Cirius Therapeutics, USA; see Table 3.1 for further details). Mice fed STD were used to serve as lean controls. Mice were fed respective diets for 8 weeks and food consumption and body weight were recorded weekly. 21 days prior to dissection, i.e. during the 5th week of interventions, drinking water of all the mice (excluding 2 mice per group that served as negative controls) was replaced by 10% concentrated ^2H_2O in order to incorporate ^2H into TAG (see 3.10).

Table 3.1 Macronutrient composition and energy content of diets. cHF diet was prepared as in [203], except that Ssniff rat/mouse-maintenance extrudate and corn oil were used instead of chow ST-1 diet and sunflower oil. All the cHF-based diets contained 210 mg α-tocopherol/kg diet. [a]—Percentage of dietary lipids replaced by EPAX 1050TG concentrate (containing 46% DHA and 14% EPA in a form of TAG, Epax AS, Aalesund, Norway), [b]—Pioglitazone (Actos, Takeda, Japan),[c]—MSDC-0602K (Cirius Therapeutics, USA). DHA: docosahexaenoic acid; EPA: eicosapentaenoic acid; cHF: high-fat diet; F: *n*-3 PUFA; MSDC: MSDC-0602K.

	cHF	cHF+F	cHF+PIO	cHF+F+PIO	cHF+MSDC	cHF+F+MSDC	Chow
Macronutrient composition							
Lipid (% diet, wt/wt)	35.2	35.2	35.2	35.2	35.2	35.2	3.4
Carbohydrate (% diet, wt/wt)	35.4	35.4	35.4	35.4	35.4	35.4	55.3
Protein (% diet, wt/wt)	20.5	20.5	20.5	20.5	20.5	20.5	19.3
Energy density (kJ/g)	22.8	22.8	22.8	22.8	22.8	22.8	16.3
Supplement							
DHA/EPA concentrate (%)[a]	0	15	0	15	0	15	0
Pioglitazone (mg/kg diet)[b]	0	0	50	50	0	0	0
MSDC-0602K (mg/kg diet)[c]	0	0	0	0	330	330	0

3.1.2   Publication B

In publication B, frozen heterozygous Gpr10$^{+/-}$ mouse embryos were purchased from AstraZeneca (AstraZeneca R&D, Mölndal, Sweden) by the Institute of Organic Chemistry and Biochemistry (IOCB). Gpr10$^{-/-}$ homozygous mice were subsequently crossed with C57BL/6J mice (Jackson Laboratory, ME, USA) at IOCB. GPR-10 deficient mice on C57BL/6J background were then transported to the IPHYS where experimental procedures were performed. Mice were maintained at 22 °C and both genders were used in experiments. In experiment 1, mice were fed STD. In experiment 2, mice were fed STD until the age of 12 weeks and some of them were subsequently assigned to lard-based HF diet (~35% wt/wt as lipids, Research Diets Inc., NJ, USA) for the period of 28 weeks. Other mice in experiment 2 were maintained on STD to serve as lean controls. Mice were sacrificed at the age of 24 weeks (experiment 1) or 40 weeks (experiment 2).

3.1.3   Publication C

In publication C, mice with adipose tissue-specific PGC-1β deletion and their wild type littermates on C57BL/6J genetic background were used. The site-specific Cre/loxP recombination system was used for the generation of mice with PGC-1β floxed alleles, similarly as described in [204], except that Cre recombinase was expressed under AdipoQ

promoter instead of aP2 promoter. Mice with PGC-1β floxed alleles were subsequently crossed with C57BL/6J mice (Jackson Laboratory, ME, USA) to produce adipose tissue-specific PGC-1β deficient animals. Mice were produced in Vall d'Hebron-Institut in Barcelona and delivered at IPHYS in collaboration with the group of Dr. Villena. Only male mice were used in the experiments. Mice were born and maintained at 22 °C until the age of 8 weeks and then transferred to 30 °C for the period of 10 days. After 10 days at 30 °C, mice were exposed to 6 °C for either 2 or 7 days and then sacrificed. Mice in control group were not exposed to cold and stayed at 30 °C until they were sacrificed.

3.2 Analysis of plasma parameters and tissue TAG content

Plasma parameters, i.e. levels of NEFA, TAG, cholesterol and insulin were measured in EDTA-plasma samples. NEFA levels were assessed by the NEFA kit (Wako Chemicals, Neuss, Germany). Plasmatic TAG and cholesterol levels were evaluated by enzymatic assays (ErbaLachema, Brno, Czech Republic). Insulin levels were determined by the Sensitive Rat Insulin RIA Kit (MilliporeSigma, MA, USA). Measurements were performed according to instructions from the kits. Levels of blood glucose were measured by OneTouch Ultra glucometers (LifeScan, CA, USA) in arterial blood immediately after sacrifice. TAG content in liver and skeletal muscle samples was estimated in ethanolic KOH tissue solubilisates in the same way as TAG in plasma. *The determination of insulin levels was performed by Dr. Petra Janovská.*

3.3 RNA isolation

Frozen tissue samples were homogenized in 1 ml of TRI Reagent (Sigma, USA) using a mixer mill MM40 (Retsch, Germany, 30 s-1, 3 minutes). Homogenates were centrifuged (4 °C, 12000g, 10 minutes), the interphase was collected and incubated for 5 minutes at room temperature. 200 μl of chloroform were added after incubation then mixed well and incubated for 10 more minutes at room temperature. The interphase-chloroform mixture was again centrifuged (4 °C, 14000g, 15 minutes). The aqueous phase was removed, mixed with 0.5 ml of isopropanol and incubated 10 minutes at room temperature to precipitate RNA. After centrifugation (4 °C, 12000g, 10 minutes) pellets were washed with 1 ml of 70% ethanol and centrifuged again (4 °C, 12000g, 5 minutes). Subsequently, ethanol was removed and pellets were dried in vacuum at 40 °C and then dissolved in redistilled water. RNA concentration and purity was analysed by NanoDrop Instrument (Thermo Scientific, USA)**.** *RNA isolation was performed mostly by Dana Šálková.*

3.4 Gene expression analysis

Isolated RNA was transcribed to cDNA using oligoT primers (GeneriBiotech, Czech Republic) and M-MLV reverse transcriptase (Invitrogen, USA). Reverse transcriptase was

added into master-mix containing 5x concentrated First Strand buffer, Dithiothreitol and dNTP mix (Invitrogen, USA). cDNA was 20-times diluted and used for the real-time quantitative gene expression analysis (RT-qPCR) by LightCycler480 Instrument (Roche, Germany). Primer sequences were designed using the NCBI database and Lasergene software (DNASTAR, USA); see primer sequences in Table 3.2. Designed primers (GeneriBiotech, Czech Republic) were added as 10-times diluted to the master-mix together with SybrGreen I Master 2x concentrated buffer (Roche, Germany). In publication A, the levels of gene expression were normalized to the geometric mean signal of four reference genes (β-actin - *Actb*; eukaryotic translation elongation factor 1 alpha 1 - *Eef1a1*; eukaryotic translation elongation factor 2 - *Eef2* and peptidylprolyl isomerase B - *Ppib*). In publication B, the geometric mean signal of three reference genes (beta 2 microglobulin - *B2m*; glyceraldehyde-3-phosphate dehydrogenase - *Gapdh* and peptidylprolyl isomerase B - *Ppib*) was used. In publication C, the geometric mean signal of three reference genes (18s ribosomal RNA - *Rna18s*; beta 2 microglobulin - *B2m* and hypoxantine phosphoribosyl transferase - *Hprt*) was used.

Table 3.2 Sequences of used primers.

Gene Name	Gene ID	Forward primer	Reverse primer
18SRna	19791	GCCCGAGCCGCCTGGATAC	CCGGCGGGTCATGGGAATAAC
Acaca	107476	AGCAGATCCGCAGCTTGGTCC	AGATGGGAGAGGCAGCCCGA
Acadm	11364	TCGCCCCGGAATATGACAAAA	GCCAAGGCCACCGCAACT
Acadsb	66885	GCATCTGAGGTCGCTGGGCTAAC	CGATGTGCTTGGCGATGGTGT
Acadvl	11370	CAGGGGTGGAGCGTGTGC	CATTGCCCAGCCCAGTGAGTTCC
Acot1	26897	AGCGCTGGCATGCACCTCCTG	TTCCCCAACCTCCAAACCATCATA
Acot2	171210	TGGGAACACCATCTCCTACAA	CCACGACATCCAAGAGACCA
Acsl1	14081	GAAGCCGTGGCCCAGGTGTTTGTC	TTCGCCTTCAGTGTTGGAGTCAGA
Actb	11461	GAACCCTAAGGCCAACCGTGAAAAGAT	ACCGCTCGTTGCCAATAGTGATG
B2m	12010	AATTGAAGTCTGTCACTGTGCCCAA	ACAAAAGCAGAAGTAGCCACAGGGT
Bckdha	12039	ACGGCGGGCTGTGGCTGAGAA	GAGATTGGGTGGTCCTGCTTGTCC
Cart	27220	TATGGGAACCGAAGGTGGCGG	CCCCATGTGTGACGCTGGAGA
Cd36	12491	TGATACTATGCCCGCCTCTCC	TTCCCACACTCCTTTCTCCTCTAC
Cidec	14311	GACAAGCCCTTCTCCCTGGTG	TCTCTTCTTGCGCTGTTCTGATGG
Cox5a	12858	AGGTTGTTAAGGACAAAGCAGGACC	TCAAGGCCCAGCTCCTCTGGA
Cpt1	12894	GCAGCTCGCACATTACAAGGACAT	AGCCCCCGCCACAGGACACATAGT
Crat	12908	ACATGGTGGTGGTAGCAAGTTCAA	GGCAAGGGCACCATAGGAGA
Cyc1	66445	ATTTCAACCCTTACTTTCCCG	CCACTTATGCCGCTTCATGGC
Dgat1	13350	TGGCCAGGACAGGAGTATTTTTGA	CTCGGGCATCGTAGTTGAGCA
Dgat2	67800	CCAGCCCCCAGGTGTCAGAGGAG	GGGGCCGACGGGTCCAGAAGAAG
Eef1a1	13627	TGACAGCAAAAACGACCCACCAAT	GGGCCATCTTCCAGCTTCTTACCA
Eef2	13629	GAAACGCGCAGATGTCCAAAAGTC	GCCGGGCTGCAAGTCTAAGG
Elovl5	68801	CCTCTCGGGTGGCTGTTCTTCC	AGGCTTCGGCTCGGCTTGTC
Esrra	26379	CAGGATCTGCCCAGCATAGG	GCTTCTGACAATCCCCCACA
Fabp4	11770	CCAGGCCTCTTCCTTTGGCTCA	TGGTGACAAGCTGGTGGTGGAAT
Fasn	14104	TGGGTGTGGAAGTTCGTCAG	GTCGTGTCAGTAGCCGAGTC

46

G6pc	14377	CATGGGCGCAGCAGGTGTAT	TGGGGAAAGTGAGCAGCAAGGTA
Gapdh	14433	CCCGGCATCGAAGGTGGAAGAGT	CTGACGTGCCGCCTGGAGAAAC
Gk	14933	TCGTTCCAGCATTTTCAGGGTTAT	TCAGGCATGGAGGGTTTCACTACT
Gpr10	226278	CGAACACCCAGCCCGAGGT	TTGGCAACCTGGCCTTGTCCG
Gsk3β	56637	TGGCGTGTGATGTCAGGTAT	TAAGCTGGCATCTGCAACAC
Hprt	15452	GCTGAGGCGGCGAGGGAGAG	GCTAATCACGACGCTGGGACTGC
Hsl/Lipe	16890	TGCGCCCCACGGAGTCTATGC	CTCGGGGCTGTCTGAAGGCTCTGA
Lpl	16956	AGCCCCCAGTCGCCTTTCTCCT	TGCTTTGCTGGGGTTTTCTTCATTCA
Mfn1	67414	TGGGTGCTGGGTTGCAGTATTCA	CGGGAGCAAACCCAGAGAACCA
Mfn2	170731	GGTCAAAGCAGGGAGGATGCCA	AGACTGAGGGGCGAGTGAGCA
Mlxipl	58805	ATCTTGGTCTTAGGGTCTTCAGG	CACTCAGGGAATACAGCGCTAC
Mpc1	55951	TCATTCAGGGAGGACGACTTATC	TGTTTTCCCTTCAGCACGACTAC
Mpc2	70456	CTCCCACCCTGCTGCTGTCG	GGCCTGCCGGGTGGTTGTA
Npff	54615	AGAACTGTCTGGCCTGCGGAT	TTCAGCCCCAGAGGTTTGGCAG
Npff-r2	104443	AGGGAATAGGCTTCCTGGGGCT	CACTGGCTCGCCTTCTGCAAC
Nrf1	18181	TGGCGCAGCACCTTTGGAGA	CCCCCGACCTGTGGAATACTTGA
Opa1	74143	GTGCAGCATGAACCACAGGAAGC	AACGGGGCCCGATGAGGAGAG
Pc	18563	CCCCTGGATAGCCTTAATACTCGT	TGGCCCTTCACATCCTTCAAA
Pck1	18534	GGCAGCATGGGGTGTTTGTAGGA	TTTGCCGAAGTTGTAGCCGAAGAAG
Pck2	74551	GGCAGCATGGGGTGTTTGTAGGA	TTTGCCGAAGTTGTAGCCGAAGAAG
Pdk4	27273	GGCTTGCCAATTTCTCGTCTCTA	TTCGCCAGGTTCTTCGGTTCC
Pnpla2	66853	GGCAATCAGCAGGCAGGGTCTTA	GCCAACGCCACTCACATCTACG
Pomc	18976	CTGCTGTTCCTGGGGCCGAA	GTGCCAGGACCTCACCACGG
Pparα	19013	TGCGCAGCTCGTACAGGTCATCAA	CCCCCATTTCGGTAGCAGGTAGTCTTA
Pparγ	19016	GCCTTGCTGTGGGGATGTCTC	CTCGCCTTGGCTTTGGTCAG
Pparγc1a	19017	CCCAAAGGATGCGCTCTCGTT	TGCGGTGTCTGTAGTGGCTTGATT
Pparγc1b	170826	AGTGGGTGCGGAGACACAGATG	GTATGGAGGTGTGGTGGGTGGC
Ppib	19035	ACTACGGGCCTGGCTGGGTGAC	TGCCGGAGTCGACAATGATGA
Prrp	623503	CCAGGTCCGGTGACATCCCT	CTGCCTGGTACACGGGTCGT
Scd1	20249	GCTCCAGCCAAGGTGCCTCTTA	CAGAGTGTCCTCCTGAGCTGATGC
Slc2a4	20528	CAGTATGTTGCGGATGCTATGG	TTCTCATCTGGCCCTAAGTATTCA
Srebf1	20787	TACCCGTCCGTGTCCCCTTTTC	TGCGCTTCTCACCACGGCTCTG
Tfam	21780	AGGAGCTGAAGGCATGCGGTGAAG	GTCCAGTGCGTGCGGGTGAAC
Ucp1	22227	CACGGGGACCTACAATGCTTACAG	GGCCGTCGGTCCTTCCTT

3.5 Indirect calorimetry

In publication B, the indirect calorimetry (INCA) system (Somedic, Horby, Sweden) was used for the evaluation of the respiratory quotient (RQ) and the energy expenditure. Single-caged mice were placed into sealed measuring chambers in cages where they are normally maintained and concentrations of O_2 and CO_2 were measured every 2 minutes under constant airflow in each chamber. O_2 consumption (VO_2) and CO_2 production (VCO_2) were used for the calculation of RQ (RQ = VO_2/VCO_2) and the energy expenditure (cal) was calculated as $3.9 \times VO_2$ (ml)+$1.1 \times VCO_2$ (ml). The measurements were performed at an ambient temperature of 22 °C under a 12/12 h light–dark cycle, started at 9:00 a.m. and lasted until 9:00 a.m. the

following day.

In publication C, INCA was used for cold tolerance test and norepinephrine test (NE-test) [205]. No food or water was provided during the tests. 5 weeks old mice were intraperitoneally implanted with E-mitters in order to detect body core temperature during the cold tolerance test. After one week of recovery at 22 °C mice were housed at 30 °C for 10 more days. The cold tolerance test was performed at ambient temperature of 5 °C and any mouse showing hypothermia, i.e. core body temperature < 28 °C, was rescued from INCA. The test was ended after 2 hours.

NE-test was performed at 33 °C on pentobarbital anaesthetized (100 mg/kg of body weight) mice that were housed at 30 °C or exposed to 6 °C for 7 days. The concentration of O_2 was measured every 2 minutes and used for the calculation of O_2 consumption in response to intraperitoneal injection of norepinephrine (1mg/kg of body weight) or saline solution (0.9 % NaCl; used as a control). Data were evaluated from the oxygen consumption curves, areas under the curves were calculated, normalised to the baseline values (oxygen consumption 30 minutes before injection) and expressed as a delta area under the curve (ΔAUC). *Indirect calorimetry measurements were performed mostly by Dr. Kristina Bardová.*

3.6 Western blotting

In publication C, protein levels were quantified in iBAT homogenates. Frozen iBAT samples were homogenised in STE medium (250 mM sucrose; 50 mM TRIS; 5 mM Na2EDTA; 1 mg/ml aprotonin; 1 mg/ml pepstatin; 1mg/ml leupeptin; 1 mM phenylmethylsulfonylfluoride; pH 7,5) using a mixer mill MM40 (Retsch, Germany; 30 s-1, 3 minutes). Total protein concentration was determined using bicinchoninic acid assay. Homogenate samples were diluted with 2x concentrated Laemli buffer (Bio-Rad, USA) with 5% mercaptoethanol, heat-denaturated (85 °C, 12 minutes) and applied into 10% polyacrylamide gel together with PageRuler Protein Ladder (Thermo Scientific, USA), which was used as a size standard. Proteins separated by tris-glycine SDS-PAGE were transferred to PVDF membrane and blocked by Odyssey blocker (Li-cor Biosciences, USA) diluted with Tris-buffered saline (0.15 M NaCl, 10 mMTris–HCl, pH 7.4). Membranes were subsequently incubated overnight at 6 °C with primary murine monoclonal antibodies against UCP1 (MAB 6158, R&D systems), OPA1 (612606, BD Biosciences) and Mfn2 (ab56889, Abcam). Infrared dye-labeled antibodies were used as secondary antibodies and signals were quantified using the Odyssey IR Imaging Systems (Li-Cor Biosciences, USA). Band intensities were related to protein standard prepared from iBAT homogenate of mice exposed to cold for 7 days. Data were expressed in arbitrary units. *Western blotting analyses were performed with the help of Dr. Petra Janovská.*

3.7 Immunohistochemical analyses and light microscopy

Samples were fixed for 24 hours in 10% neutral buffered formalin (Sigma-Aldrich, USA) and subsequently stored in 70% ethanol until tissue processing. 5 μm-thick tissue sections

were stained by hematoxylin and eosin (VWR Chemicals, France) and used for adipocyte morphometry and for the detection of hepatic steatosis. In publication A, specific antibodies against macrophage marker Mac-2 (CL8942AP, Cedarlane) were used in order to assess a relative density of CLS. In publication C, the antibody against sodium potassium ATPase (ab76020, Abcam,) was used to determine the size of adipocytes and anti-perilipin 1 antibody (ab61682, Abcam) was used to assess the size of lipid droplets. All analyses were performed using NIS-Elements imaging software (Laboratory Imaging, Prague, Czech Republic). Digital images were captured by Olympus AX70 light microscope and DP 70 digital camera (Olympus, Tokyo, Japan). *Immunohistology analyses were performed by Dr. Kristina Bardová and MSc. Ilaria Irodenko.*

3.8 Electron microscopy

In publication C, samples of brown adipose tissue were fixed with 2% glutaraldehyde and 2% formaldehyde in Sörensen's buffer (SB; 0.1 M Na/K phosphate buffer, pH 7.2 – 7.4). After an initial fixation (4 °C, 1.5 hours) samples were cut to smaller pieces, put back to the same fixative and kept overnight at 4 °C. Samples were subsequently incubated with 0.02 M glycine in SB for 30 minutes and then fixed with 1% OsO_4 in SB in dark (4 °C, 1.5 hours). Samples were then dehydrated by ethanol and propylene oxide and embedded in Quetol-NSA resin. After polymerization for 72 hours at 60 °C, resin blocks were cut into 85 nm ultrathin sections and collected on 200 mesh size copper grids. Sections were examined by JEOL JEM-1400Flash transmission electron microscope operated at 80 kV equipped with Matataki Flash sCMOS camera (JEOL Ltd., Tokyo, Japan). The evaluation of images was performed using NIS-Elements imaging software (Laboratory Imaging, Prague, Czech Republic). Twenty images per sample were used with magnification 3000x for the evaluation of both mitochondrial length and the contact between mitochondria and lipid droplets, while magnification 1200x was used for the assessment of lipid droplets size. Ten randomly chosen mitochondria per image were used for the calculation of mean mitochondrial length. Mitochondria/lipid droplets contact was expressed as a percentage of contact length between mitochondria to total surface of lipid droplets per image. The size of 10 lipid droplets per image was measured and due to a high magnification and a large size of lipid droplets in samples from mice at 30 °C, only samples from 7-day-CE group could be evaluated. *The samples for electron microscopy were prepared by MSc. Erik Vlčák and the electron microscopy was performed by Dr. Vlada Filimonenko at the Institute of Molecular Genetics. The evaluation of images was performed by MSc. Ilaria Irodenko at IPHYS.*

3.9 Glucose tolerance test

In publication A, an intraperitoneal glucose tolerance test (IGTT) was performed using 1 mg of glucose/g body weight after an overnight fasting. In publication B, an oral glucose tolerance test (OGTT) was performed using 4 mg of glucose/g body weight with glucose being administered by gavage after 6 hours of fasting. In both studies, blood was collected

from tail vessels and levels of blood glucose were measured by OneTouch Ultra glucometers (LifeScan, CA, USA) before glucose administration (0 min time point) and at 15, 30, 60, 120 and 180 minutes after glucose administration. The rate of glucose clearance was expressed as an incremental AUC (iAUC) of a blood glucose response curve. In addition, levels of insulin and NEFA were determined in blood samples collected at 0 and 30 minutes (see 3.2). Homeostatic model assessment for insulin resistance (HOMA-IR) was calculated from glucose and insulin levels at 0 min. *Glucose tolerance tests were performed with the help of MSc. Karolína Seďová and Dana Šálková.*

3.10 Determination of TAG synthesis *in vivo*

In publication A, ^{2}H was incorporated to TAG of mice *in vivo* by administrating 10% concentrated ^{2}H$_2$O as a drinking water 21 days before the mice were sacrificed. TAG were isolated from eWAT samples and ^{2}H enrichment was determined in fatty acids as well as in glycerol moiety. Analyses were performed using nuclear magnetic resonance (NMR) spectroscopy and liquid chromatography–mass spectroscopy (LC–MS).

3.10.1 TAG isolation

Frozen adipose tissue samples were homogenized in a mixture of citric acid and ethylacetate using a mixer mill MM40 (Retsch, Germany; 30 s-1, 3 minutes). The organic phase was collected and dried in a Speed-vac Savant SPD121P (Thermo Scientific, USA). Dried organic phase was subsequently resuspended in hexane with methyl tert-butyl ether (MTBE) and applied on SPE tubes Discovery DSC-Si (52 μm, 72 Å; MERCK, Darmstadt, Germany). TAG were eluted from the tubes with a mixture of hexane and MTBE and concentrated in a Speed-vac. Thin layer chromatography (TLC) was used to control the presence of lipid species other than TAG. Samples were applied on the TLC plate (TLC Silica gel 60 F254; MERCK, Darmstadt, Germany) and the mixture of petroleum ether, diethylether and acetic acid in the ratio 70:10:1 was used as a mobile phase.

3.10.2 NMR Spectroscopy

The ^{1}H and ^{2}H NMR spectroscopy was performed using AVANCE III HD 500 MHz system (Bruker Corporation). The spectra were evaluated in Mnova software (Mestrelab, Spain) and the amount of ^{1}H and ^{2}H in both glycerol and fatty acyl moieties of TAG were calculated using ^{1}H/^{2}H pyrazine standard. TAG synthesis was determined from ^{2}H enrichment of glycerol and *de novo* lipogenesis was determined from the enrichment of fatty acid methyl groups. *NMR Spectroscopy analyses were performed by Dr. Radek Pohl at IOCB.*

3.10.3   LC–MS analysis

LC–MS was used for lipidomic analysis, in particular the analysis of TAG species and the composition of their fatty acids. Adipose tissue samples were homogenized in methanol using a mixer mill MM40 (Retsch, Germany; 30 s-1, 3 minutes). After that, 1 ml of MTBE was added to the homogenates. Homogenates were then shaken for 1 minute and centrifuged (16 000g, 5 minutes). For TAG profiling, 10 μL of the upper organic phase was collected and diluted with 990 μL of methanol containing internal standard (CUDA). Thereafter the mixture was shaken for 30 s, centrifuged (16 000g, 2 minutes) and used for the lipidomic analysis. For the profiling of fatty acids, 50 μL of the upper organic phase was collected, evaporated, dissolved in 500 μL of 0.3 M KOH in a methanol:water mixture (9:1) and shaken at 55 °C for 1 hour. 3 M HCl in methanol, 500 μL of water and 500 μL of hexane were subsequently added to the mixture, shaken for 30 s and centrifuged (16 000g, 5 minutes). 200 μL of the upper phase was then dissolved in 200 μL of a dichloromethane:methanol:isopropanol mixture (1:2:4), shaken for 30 s, centrifuged (16 000g, 5 minutes) and diluted with methanol containing internal standard. The LC–MS system consisted of a Vanquish UHPLC System, which is coupled to a Q Exactive Plus mass spectrometer (Thermo Fisher Scientific, Bremen, Germany). LC–MS data from lipidomic profiling were processed through MS-DIAL v.4.24 software. *LC-MS analyses were performed by a group of Assoc. Prof. Tomáš Čajka at IPHYS.*

3.11 Statistical analysis

In publications A and B, GraphPad Prism 8 software (GraphPad Software, Inc., CA, USA) was used for the statistical evaluation. Data were analysed either by analysis of variance (one-way or two-way ANOVA) followed by the Tukey's multiple comparison test or by unpaired t-test. Significant outliers as determined by Grubb's test were excluded from further analyses. If necessary logarithmic transformation was used to stabilize variance or normality of samples in order to pass the equal variance and normality tests. Comparisons were judged to be significant at $p < 0.05$. All values are presented as means ± standard error of the mean (SEM). Partial least squares-discriminant analysis (PLS-DA) was performed using MetaboAnalyst 4.0 [206]. In publication C, SigmaStat 3.5 software (Systat Software, CA, USA) was used for the statistical evaluation. Data were analysed by analysis of variance (one-way or two-way ANOVA) and logarithmic or square root transformations were used to stabilize variance or normality of samples if necessary. All values are presented as means ± SEM and comparisons were judged to be significant at $p < 0.05$.

3.12 My contribution

I was mainly involved in scheduling and supervising animal experiments as well as taking care of animals. I performed glucose tolerance tests, the implantation surgeries prior to INCA experiments, statistical analyses, measuring of plasma parameters and tissue TAG content as well as the gene expression analyses. In addition, I performed the western blotting analyses

including the preparation of samples and protein content quantification. I was also responsible for the preparation of samples for the *in vivo* determination of TAG synthesis and *de novo* lipogenesis, namely the isolation of TAG for NMR Spectroscopy.

4 Results

4.1 Publication A: Effects of n-3 PUFA and TZDs on the rate of TAG/FA cycling in WAT of obese mice

Results published in this study cover the first aim of this thesis. We focused on the examination of beneficial effects of *n*-3 PUFA and anti-diabetic drugs TZDs on the improvement of metabolic health in obese mice. TZDs act as insulin-sensitizing drugs and *n*-3 PUFA exert beneficial effects on metabolic health including a decrease of adiposity (see 1.5.2 and 1.5.3). It is expected that the combination of both these treatments multiply the beneficial effects. We have previously observed additive effects of *n*-3 PUFA and TZDs on the improvement of metabolic health in obese mice [202, 207, 208]. In this study we examined effects of a new type of TZD – MSDC alone or in combination with *n*-3 PUFA on the metabolism of eWAT, a typical WAT depot that does not undergo browning and has an important role in the buffering of NEFA and glucose. The effect of MSDC was compared with already known TZD – PIO, with a special focus on TAG/FA cycling. The study aimed to investigate possible involvement of TAG/FA cycling in eWAT in the beneficial effects of *n*-3 PUFA and TZDs and its influence on metabolic health on the systemic level.

4.1.1 Characterization of general metabolic parameters in mice fed different diets

Male C57BL/6N mice were fed either STD or obesogenic HF diet supplemented or not by *n*-3 PUFA or/and two different TZDs. Mice were assigned to HF diet at the age of 3 months and they were fed respective diets for a period of 8 weeks. Body weight was significantly increased by HF diet feeding in all groups compared to the group fed STD only with the exception of the group with combined *n*-3 PUFA and MSDC treatment (HF+MSDC+F, Figure 4.1.1, Table 4.1.1). Treatments with MSDC (HF+MSDC) and combined treatment with *n*-3 PUFA and PIO (HF+F+PIO) reduced the obesogenic effect of HF diet. Treatment with *n*-3 PUFA (HF+F) and with PIO (HF+PIO) tended to reduce body weight gain but did not significantly differ from the group on HF diet without intervention (Figure 4.1.1, Table 4.1.1).
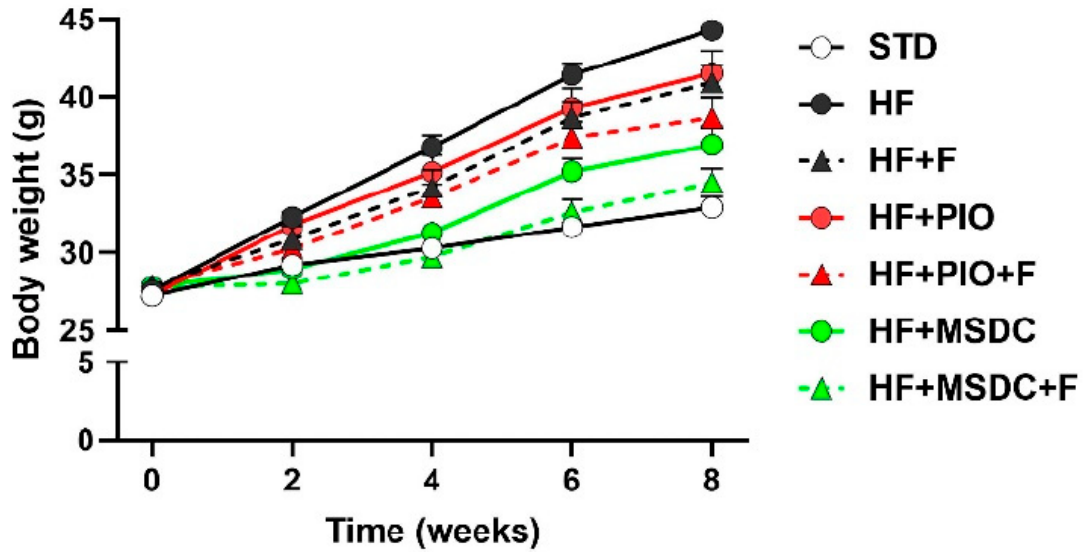
Figure 4.1.1 Body weight during the dietary interventions. Data are pooled from two separate experiments (*n* = 16-19). Data are means ± SEM. STD: standard chow diet; HF: high-fat diet; F: *n*-3 PUFA; PIO: pioglitazone; MSDC: MSDC-0602K.

The food consumption was not affected by any of the interventions (Table 4.1.1). The increase in body weight was reflected in the weight of eWAT. All the interventions except HF+PIO suppressed the effect of HF feeding on the expansion of eWAT. The weight of scWAT increased in response to HF diet feeding; however, none of the intervention led to significant suppression of the obesogenic effect. Mice in all the HF diet fed groups except HF+MSDC+F displayed increased levels of TAG in the liver compared to STD group. TAG content in the liver was lowered in HF+F and HF+PIO+F groups compared to HF group. The weight of the liver reflected the hepatic TAG content as in all treated groups except for HF+PIO group it was lower compared to HF group. HF diet increased plasmatic levels of NEFA, TAG and cholesterol in comparison with STD group. All the interventions lowered plasmatic NEFA, TAG and cholesterol levels with the strongest effect observed in the HF+MSDC+F group (Table 4.1.1). Histological analysis of eWAT revealed that HF diet feeding caused adipocyte hypertrophy resulting in an increase in the size of adipocytes in eWAT. Only in HF+MSDC+F group adipocyte size was lower compared to HF group (Figure 4.1.2 A, B).

Table 4.1.1 General metabolic parameters in mice fed experimental diets. Cumulative energy intake was assessed during the first 7 weeks of dietary interventions. Data are pooled from two separate experiments (n = 16-19). Data are means ± SEM. *—Significantly different from STD ($p \leq 0.05$, t-test); a—significantly different from HF; b—significantly different from HF+F; c—significantly different from HF+PIO; d—significantly different from HF+PIO+F; e—significantly different from HF+MSDC ($p \leq 0.05$, one-way ANOVA). STD: standard chow diet; HF: high-fat diet; F: *n*-3 PUFA; PIO: pioglitazone; MSDC: MSDC-0602K; eWAT: epididymal white adipose tissue; TAG: triacylglycerols; NEFA: non-esterified fatty acid; CHOL: cholesterol.

|	STD	HF	HF + F	HF + PIO	HF + PIO + F	HF + MSDC	HF + MSDC + F
Energy balance							
Body weight initial g)	27.2 ± 0.40	27.6 ± 0.40	27.9 ± 0.49	27.3 ± 0.47	27.9 ± 0.48	27.8 ± 0.42	27.8 ± 0.50
Body weight final (g)	32.9 ± 0.70	44.3 ± 0.64 *	41.0 ± 1.13 *	41.5 ± 1.42 *	38.6 ± 1.35 *,a	36.9 ± 1.16 *,a	34.5 ± 0.91 abc
Body weight gain (g)	5.50 ± 0.44	16.1 ± 0.63 *	12.0 ± 0.75 *,a	13.3 ± 1.17 *	10.1 ± 1.11 *,a	8.27 ± 0.94 abc	6.02 ± 0.58 abcd
Cumulative food intake (MJ/animal)	3.86 ± 0.06	4.59 ± 0.11 *	4.21 ± 0.18	4.57 ± 0.25 *	4.17 ± 0.15	4.75 ± 0.20 *	4.81 ± 0.32 *
Tissues							
eWAT weight (mg)	833 ± 73	2489 ± 84 *	1977 ± 88 *,a	2252 ± 168 *	1734 ± 142 *,ac	1511 ± 123 *,ac	1171 ± 117 *,abcd
scWAT weight (mg)	403 ± 34	1398 ± 87 *	1283 ± 137 *	1614 ± 288 *	1191 ± 84 *	1097 ± 96 *	936 ± 78 *
Liver weight (mg)	1763 ± 43	1793 ± 63	1563 ± 58 *,a	1613 ± 84 *	1425 ± 58 *a	1477 ± 58 *a	1418 ± 33 *,a
Liver TAG content (mg/g)	33.2 ± 1.16	93.4 ± 8.03 *	57.0 ± 4.96 *,a	112 ± 17.6 *,b	48.6 ± 5.77 *,ac	67.9 ± 10.0 *c	42.4 ± 5.58 ac
Plasma (random fed state)							
NEFA (mmol/l)	0.50 ± 0.05	0.66 ± 0.04 *	0.38 ± 0.03 *,a	0.42 ± 0.02 a	0.34 ± 0.03 *,a	0.38 ± 0.04 *,a	0.22 ± 0.02 *,abce
TAG (mmol/l)	1.39 ± 0.06	1.79 ± 0.05 *	1.05 ± 0.09 *,a	0.99 ± 0.06 *,a	0.82 ± 0.06 *,a	0.89 ± 0.06 *,a	0.54 ± 0.04 *,abce
Cholesterol (mmol/l)	2.81 ± 0.33	4.61 ± 0.14 *	3.40 ± 0.12 a	3.91 ± 0.10 *,ab	2.91 ± 0.13 ac	3.40 ± 0.13 ac	2.55 ± 0.07 abce

Immunohistochemical analysis determined the degree of inflammation based on the amount of CLS in eWAT (Figure 4.1.2 C, D). HF diet increased the infiltration of macrophages into eWAT resulting in increased amount of CLS. All the interventions except HF+F reduced the amount of CLS with HF+MSDC+F treatment being able to reduce the degree of inflammation to the same level as in STD group (Figure 4.1.2 C, D).
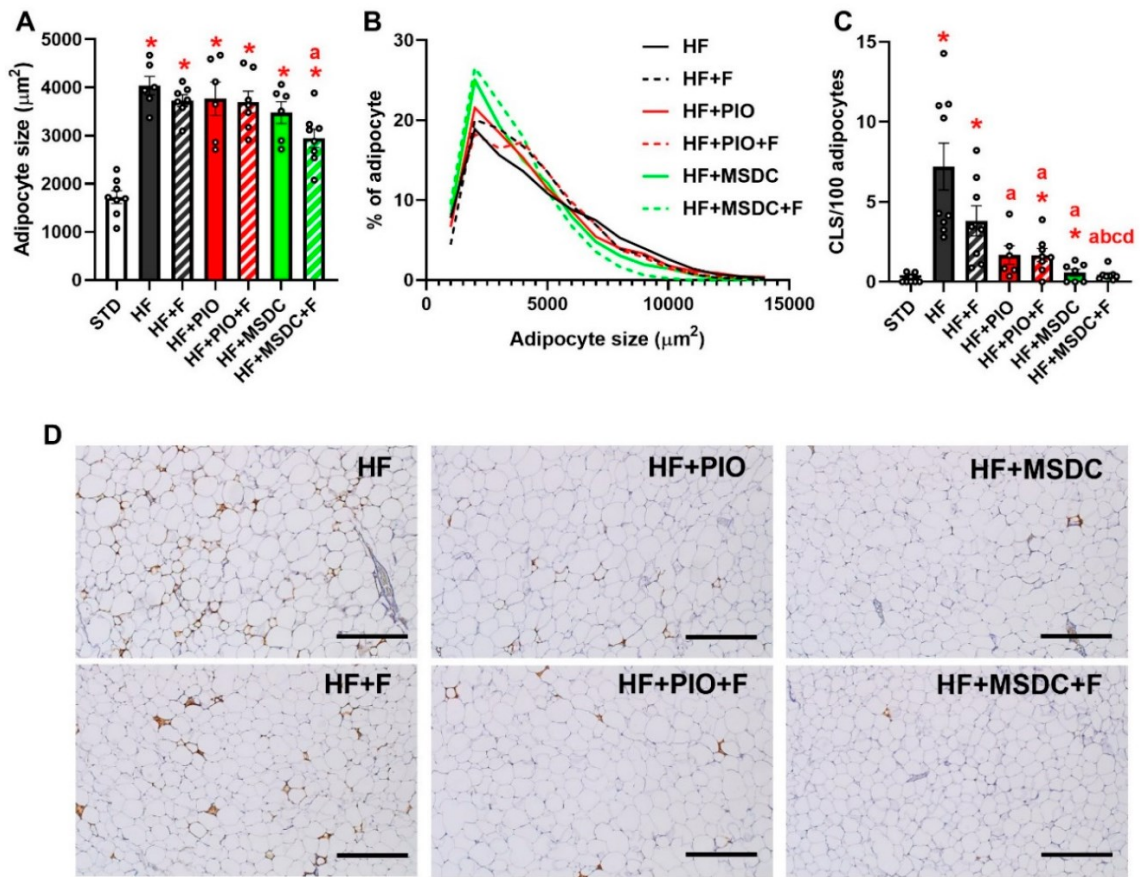
Figure 4.1.2 Histological and immunohistochemical analyses of eWAT. Adipocyte size was determined from hematoxylin and eosin stained sections and expressed either as a mean (**A**) or as a histogram (**B**). The amount of CLS was assessed using antibody against Mac-2 and expressed as the number of CLS/100 adipocytes (**C**). CLS are visualised by reddish colour in representative histological sections (**D**, scale bar = 200 μm). Data are means ± SEM. *— Significantly different from STD ($p \leq 0.05$, t-test); a—significantly different from HF; b— significantly different from HF+F; c—significantly different from HF+PIO; d—significantly different from HF+PIO+ F ($p \leq 0.05$, one-way ANOVA). STD: standard chow diet; HF: high-fat diet; F: *n*-3 PUFA; PIO: pioglitazone; MSDC: MSDC-0602K.

HF diet feeding led to the increase in plasmatic levels of both glucose and insulin after overnight fasting (Figure 4.1.3 A, B). All the interventions lowered fasting insulin levels with HF+PIO+F and HF+MSDC+F exhibiting the strongest effect (Figure 4.1.3 B). Fasting glycemia was lowered in mice from HF+F group and even greater effect was in HF+MSDC and HF+MSDC+F groups (Figure 4.1.3 A). HOMA index calculated from fasting glycemia and fasting insulinemia values was increased compared to STD group in all HF diet fed groups except for HF+MSDC+F group. Glucose clearance determined during IGTT was ameliorated by HF diet (Figure 4.1.3 D). All the intervention with the exception of HF+F increased the rate of glucose clearance that was blunted by HF diet feeding (Figure 4.1.3 E).
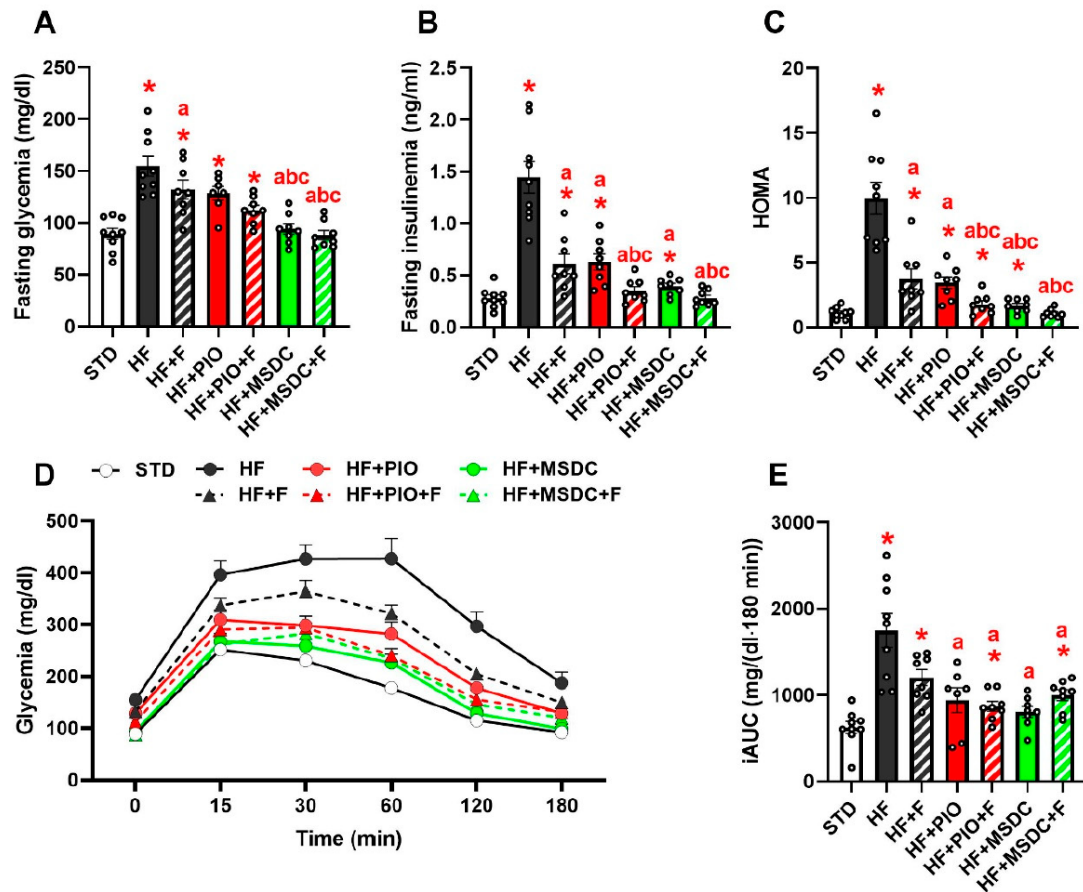
Figure 4.1.3 Parameters of glucose homeostasis in mice fed experimental diets. Fasting glycemia (**A**) and fasting insulinemia values (**B**) were used for the calculation of HOMA index (**C**). Glucose clearance was determined by IGTT and expressed as three-hour blood glucose response curve (**D**) and corresponding iAUC (**E**). Data are means ± SEM ($n = 8$). *— Significantly different from STD ($p \leq 0.05$, t-test); a—significantly different from HF; b— significantly different from HF+F; c—significantly different from HF+PIO ($p \leq 0.05$, one-way ANOVA). STD: standard chow diet; HF: high-fat diet; F: *n*-3 PUFA; PIO: pioglitazone; MSDC: MSDC-0602K; HOMA: homeostatic model assessment; IGTT: intraperitoneal glucose tolerance test; iAUC: incremental area under the curve.

4.1.2 Determination of the rate of TAG/FA cycling in eWAT *in vivo*

High rate of TAG/FA cycling contributes to the maintenance of healthy metabolic properties of WAT in obesity [209]. The aim of this study was to learn whether combined treatment with *n*-3 PUFA and TZDs could exert its beneficial effects through the stimulation of the rate of TAG/FA cycling in eWAT. Therefore, the rate of TAG/FA cycling in eWAT was determined by the analysis of ^{2}H enrichment of TAG by NMR spectroscopy, allowing for separate evaluations of ^{2}H enrichment of glycerol and fatty acyl methyl moieties of TAG, which reflects synthetic rates of G3P and fatty acids [210]. The ^{2}H enrichment of glycerol was evaluated separately for both *sn* 1 + 3 and *sn* 2 position. ^{2}H enrichment of glycerol on all positions was reduced by HF diet with stronger effect at *sn* 2 position (Figure 4.1.4 A, B). However, deceleration of this reduction was observed in both combined interventions, i.e.

HF+PIO+F and HF+MSDC+F. In the HF+MSDC and HF+MSDC+F groups, enrichment at *sn* 1 + 3 positions was even restored to the same level as in STD group (Figure 4.1.4 A). The enrichment of fatty acyl methyl moieties was strongly suppressed in all HF diet-fed groups (Figure 4.1.4 C). In HF+PIO and HF+PIO+F groups the fatty acyl enrichment level was increased in comparison with HF group. Treatments with *n*-3 PUFA and TZDs therefore partially rescued the rate of TAG/FA cycling suppressed by HF diet (Figure 4.1.4 C).
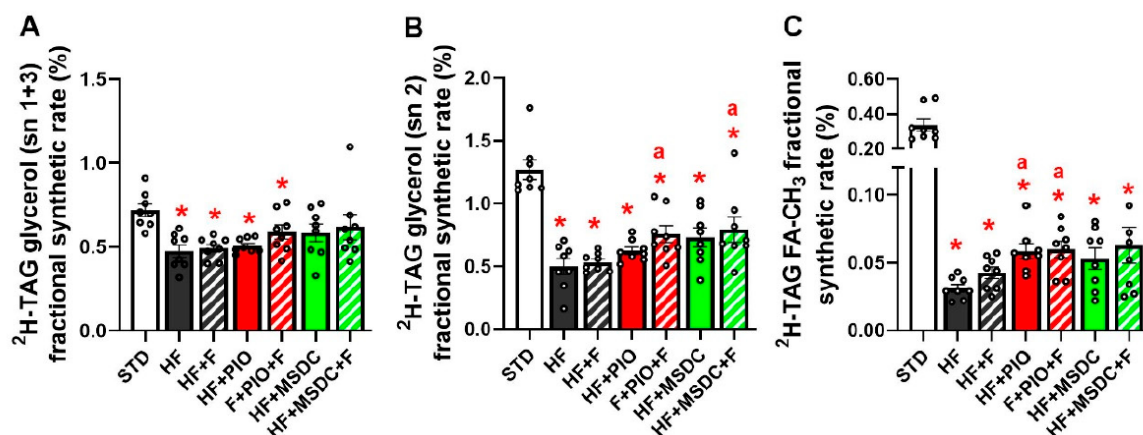
Figure 4.1.4 Fractional synthetic rates of TAG and fatty acids. Evaluation of ^{2}H enrichment of glycerol moieties at *sn* 1 + 3 positions (**A**), *sn* 2 position (**B**) and ^{2}H enrichment of fatty acid methyl moieties of TAGs (**C**) performed by NMR spectroscopy. Data are means ± SEM (*n* = 8). *—Significantly different from STD ($p \leq 0.05$, t-test); a—significantly different from HF ($p \leq 0.05$, one-way ANOVA). TAG: triacylglycerols; NMR: nuclear magnetic resonance; STD: standard chow diet; HF: high-fat diet; F: *n*-3 PUFA; PIO: pioglitazone; MSDC: MSDC-0602K.

Another approach, LC-MS analysis, was used in order to determine ^{2}H enrichment of individual fatty acids in various TAG species. In total, 62 TAG species were evaluated. Although, the degree of total ^{2}H enrichment was decreased in all HF diet groups compared to STD group; however, the enrichment of individual fatty acids in different TAG species largely varied between the interventions (Figure 4.1.5). The number of ^{2}H enriched TAG species in HF diet groups with interventions increased in the following order: HF+PIO < HF+PIO+F < HF+F < HF+MSDC < HF+MSDC+F. According to LC-MS analysis, HF+MSDC+F treatment had the highest stimulatory effect on the rate of TAG/FA cycling decreased by HF diet (Figure 4.1.5).
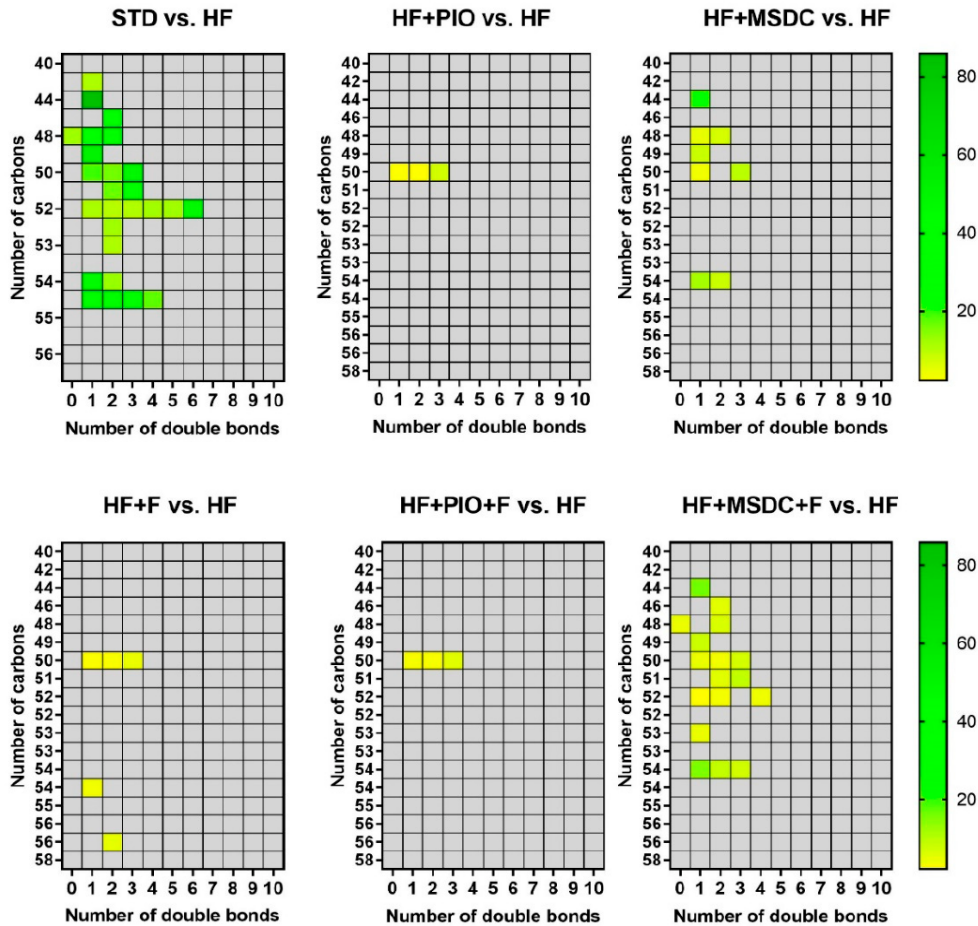
Figure 4.1.5 ^{2}H enrichment of various TAG species. In total, 62 different TAG species were evaluated. The ratio between the mean ^{2}H enrichment of TAG in the respective intervention group in comparison with HF group is plotted only if the difference was significant ($p \leq 0.05$, t-test). Data are means $\pm$ SEM ($n = 8$). STD: standard chow diet; HF: high-fat diet; F: n-3 PUFA; PIO: pioglitazone; MSDC: MSDC-0602K; TAG: triacylglycerols.

4.1.3 Gene expression analysis in eWAT

The gene expression of key markers of metabolic pathways in eWAT was evaluated. First, PLS-DA was performed. In order to get a global view on effects of the interventions, mice from STD group were excluded from the analysis. Groups treated with different TZDs (PIO and MSDC) were analysed separately against HF and HF+F groups. The analysis of HF, HF+F, HF+PIO and HF+PIO+F groups revealed a separation within component 1, which was responsible for 45% of all the variations between HF group and interventions including PIO, i.e. HF+PIO and HF+PIO+F (Figure 4.1.6 A). The analysis of HF, HF+F, HF+MSDC and HF+MSDC+F groups revealed a separation within component 1, which described 71% of all the variations between HF group and interventions including MSDC, i.e. HF+MSDC and HF+MSDC+F (Figure 4.1.6 B). Both TZDs therefore greatly affected the expression of metabolic genes in eWAT with MSDC having a stronger effect. On the other hand, the analysis detected only a minor effect of n-3 PUFA. According to variable importance in

projection (VIP) scores, the most discriminative factor throughout the whole analysis was the expression of the gene for PEPCK (*Pck1*), one of the key enzymes involved in fatty acid re-esterification [23, 210] (Figure 4.1.6. C, D).
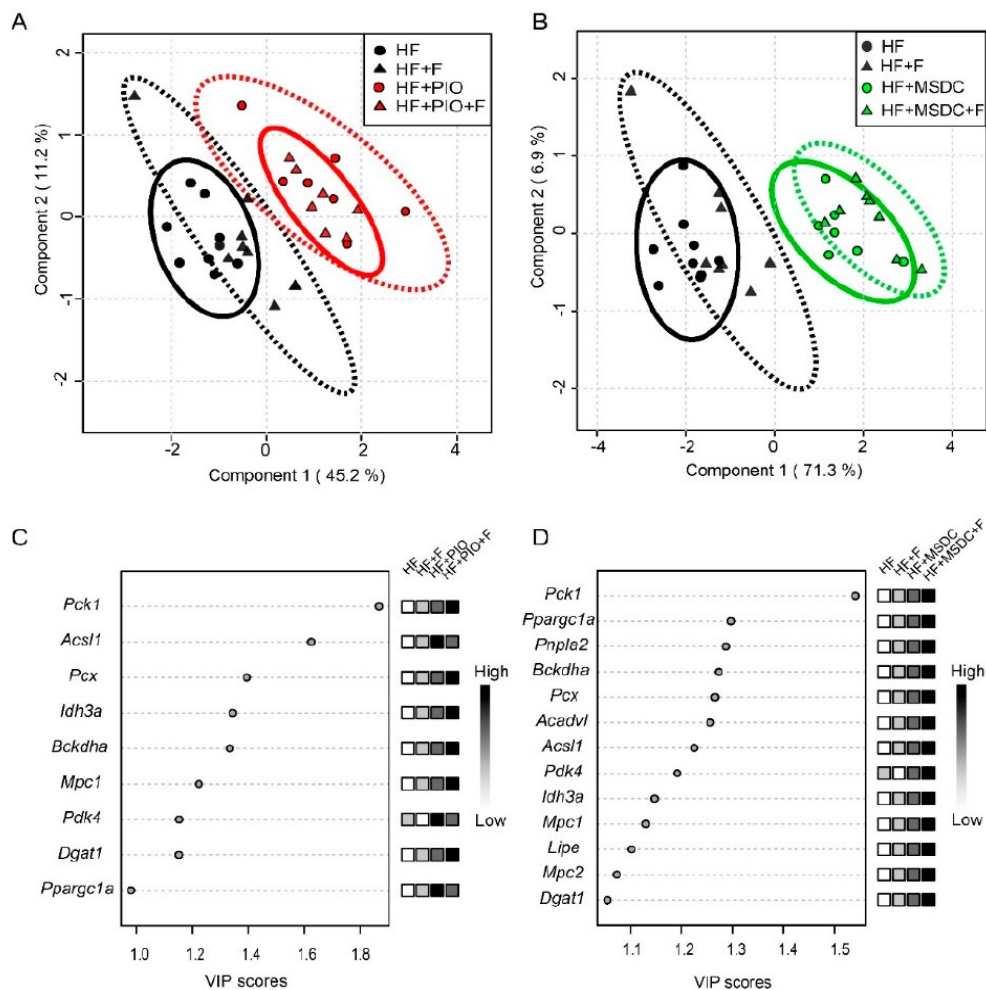
Figure 4.1.6 Partial least squares discriminant analysis (PLS-DA) of gene expression in eWAT. In total, 24 different genes were analysed. Score plots illustrating results of analyses focused on the separation of mice in HF, HF+F, HF+PIO and HF+PIO+F groups (**A**) and on the separation of mice in HF, HF+F, HF+MSDC and HF+MSDC+F groups (**B**). Corresponding variable importance in projection (VIP) plots (**C, D**) with VIP > 1.0 are shown in (**C** for **A**) and (**D** for **B**). STD: standard chow diet; HF: high-fat diet; F: *n*-3 PUFA; PIO: pioglitazone; MSDC: MSDC-0602K; *Acadvl*: acyl-Coenzyme A dehydrogenase; *Acsl1*: acyl-CoA synthetase long-chain family member 1; *Bckdha*: branched chain ketoacid dehydrogenase E1, alpha polypeptide; *Dgat1*: diacylglycerol O-acyltransferase 1; *Idh3a*: isocitrate dehydrogenase 3 (NAD(+)) alpha; *Lipe*: hormone sensitive lipase; *Mpc1*: mitochondrial pyruvate carrier 1; *Mpc2*: mitochondrial pyruvate carrier 2; *Pck1*: phosphoenolpyruvate carboxykinase 1, cytosolic; *Pcx*: pyruvate carboxylase; *Pdk4*, pyruvate dehydrogenase kinase, isoenzyme 4; *Pnpla2*, patatin-like phospholipase domain-containing protein 2 (adipose triglyceride lipase); *Ppargc1a*: peroxisome proliferator-activated receptor gamma coactivator 1 alpha.

The expression of particular genes involved in the regulation of eWAT metabolism was analysed using RT-qPCR. The expression of the gene for PPARγ (*Pparg)*, the key regulator of lipogenesis and adipocyte differentiation, was decreased by HF diet with none of the interventions being able to restore its expression levels (Figure 4.1.7 A). The expression of *Pgc-1a/Ppargc1a*, an important regulator of mitochondrial oxidation and biogenesis and target of PPARγ, was decreased by HF diet even more than the expression of *Pparg*. However, the expression of *Pgc-1a* was upregulated in HF+PIO group and even more in HF+MSDC and HF+MSDC+F groups compared to HF group (Figure 4.1.7 A). The expression of *Lpl*, the marker of fatty acid uptake, was suppressed by HF diet and HF+MSDC+F was the only intervention with the ability to restore LPL gene expression to the same level as in STD group. The expression of *Cd36*, another marker of fatty acid uptake, was not affected by HF diet; however, it was upregulated in HF+MSDC and HF+MSDC+F groups (Figure 4.1.7 B). The expression of key lipases, i.e. *Atgl/Pnpla2* and *Hsl/Lipe* was suppressed by HF diet and partially restored in HF+PIO and HF+MSDC groups. Moreover, the expression of both lipases was increased in HF+MSDC+F group to a higher level compared to STD group (Figure 4.1.7 C).

The expression of lipogenic genes was measured in order to determine the effects of interventions on the activity of TAG/FA cycling in eWAT. The expression of *Fas/Fasn* was strongly suppressed by HF diet and none of the interventions affected its expression levels (Figure 4.1.7 D). The expression of *Elovl5* followed the same pattern as the expression of the gene for FAS. The expression of *Gk*, the marker of glyceroneogenesis, was upregulated by HF diet and its expression was even more increased by TZD-containing interventions without *n*-3 PUFA (HF+PIO and HF+MSDC; Figure 4.1.7 E). As mentioned above, the expression of the gene for PEPCK (*Pck1*) differed greatly among the interventions. Although HF diet downregulated Pck1 expression, all TZD-containing interventions decelerated this reduction. Moreover, *Pck1* expression was restored to the same level as in STD group in both MSDC-containing interventions (Figure 4.1.7 E). The expression of the gene for PC, another marker of glyceroneogenesis, was suppressed by HF diet and all TZD-containing interventions except for HF+PIO+F suppressed the decrease of its expression levels. The expression of genes responsible for the regulation of fatty acid re-esterification, namely DGAT1 and DGAT2, were downregulated by HF diet. All the interventions increased the expression of *Dgat1*, with the strongest effect in HF+MSDC+F group compared to HF group. In the case of *Dgat2* expression, HF+MSDC+F was the only group where the level of expression was restored to the same level as in STD group (Figure 4.1.7 E).
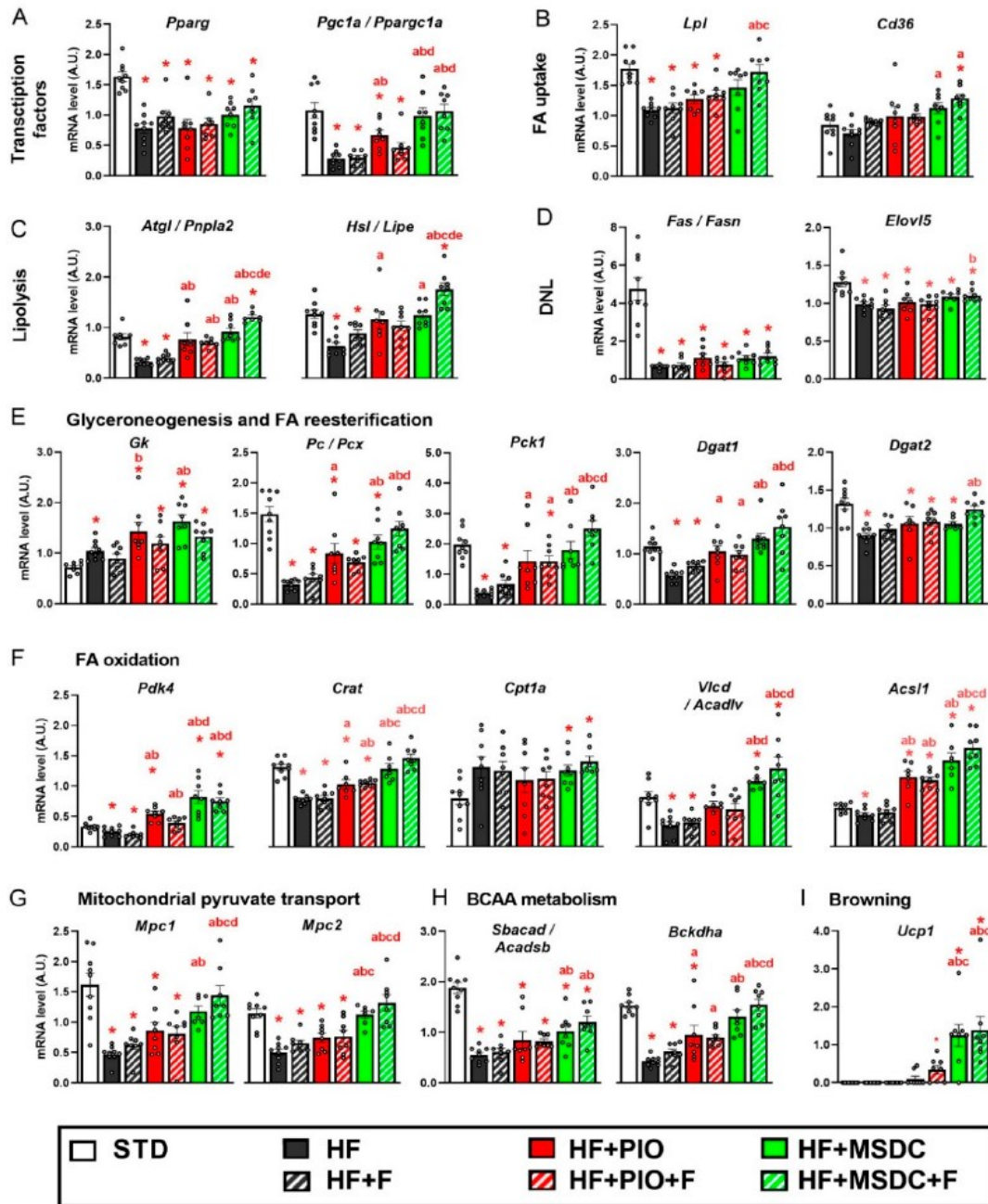
Figure 4.1.7 The expression of key metabolic genes in eWAT. The expression of genes involved in the regulation of different metabolic pathways (**A-I**). The gene expression was evaluated using RT-qPCR and data were normalized to the geometric mean signal of four reference genes (see 3.4). Data are means ± SEMs (*n* = 8). *—Significantly different from STD ($p \leq 0.05$, t-test); a—significantly different from HF; b—significantly different from HF+F; c—significantly different from HF+PIO; d—significantly different from HF+PIO+F; e—significantly different from HF+MSDC ($p \leq 0.05$, one-way ANOVA). STD: standard chow diet; HF: high-fat diet; F: *n*-3 PUFA; PIO: pioglitazone; MSDC: MSDC-0602K; FA: fatty acids, DNL: *de novo* lipogenesis; BCAA: branched-chain amino acids; *Acadsb*: acyl-Coenzyme A dehydrogenase, short/branched chain; *Acadvl*: acyl-Coenzyme A dehydrogenase; *Acsl1*: acyl-CoA synthetase long-chain family member 1; *Bckdha*: branched chain ketoacid

dehydrogenase E1, alpha polypeptide; *Cd36*: Cd36 antigen; *Cpt1*: carnitine palmitoyltransferase 1a; *Crat*: carnitine acetyltransferase; *Dgat1*: diacylglycerol O-acyltransferase 1; *Dgat2*: diacylglycerol O-acyltransferase 2; *Elovl5*: fatty acid elongase 5; *Fas/Fasn*: fatty acid synthase; *Gk*: glycerol kinase; *Lipe/Hsl*: hormone sensitive lipase; *Lpl*: lipoprotein lipase; *Mpc1*: mitochondrial pyruvate carrier 1; *Mpc2*: mitochondrial pyruvate carrier 2; *Pck1*: phosphoenolpyruvate carboxykinase 1, cytosolic; *Pcx/Pc*: pyruvate carboxylase; *Pdk4*: pyruvate dehydrogenase kinase, isoenzyme 4; *Pnpla2/Atgl*: patatin-like phospholipase domain-containing protein 2 (adipose triglyceride lipase); *Pparg*: peroxisome proliferator-activated receptor gamma; *Pgc-1a/Ppargc1a*: peroxisome proliferator-activated receptor gamma coactivator 1 alpha; *Ucp1*: uncoupling protein 1.

Next, we analysed the expression of genes involved in the control of fatty acid catabolism. The gene expression of genes for PDK4 and CRAT, enzymes supporting fatty acid utilization as a substrate for mitochondrial oxidation, was downregulated by HF diet. The expression of both *Pdk4* and *Crat* was increased by all TZD-containing interventions, with the strongest effect in HF+MSDC+F group as compared with HF group (Figure 4.1.8.F). The gene expression for CPT1α, which is required for the transport of fatty acids into mitochondrial matrix, was upregulated by HF diet with no effects of any interventions. The expression of the gene for VLCAD (*Acadlv*), an enzyme directly involved in β-oxidation, was supressed by HF diet. All TZD-containing interventions increased *Acadlv* expression with HF+MSDC and HF+MSDC+F groups having even higher gene expression levels than STD group. The expression of the gene for ACSL1, another enzyme involved in fatty acid catabolism, was slightly decreased by HF diet and strongly upregulated by all TZD-containing interventions (Figure 4.1.7 F).

The expression of *Mpc1* and *Mpc2*, genes for two forms of mitochondrial pyruvate carrier, was suppressed by HF diet and only in HF+MSDC and HF+MSDC+F groups it was restored to the same level as in STD group (Figure 4.1.7 G). The expression of genes for ACADSB and BCKDHA, enzymes involved in the regulation of BCAA metabolism, was suppressed by HF diet. PIO elevated the expression of *Bckdha*, while both MSDC-containing interventions restored the expression of both *Acadsb* and *Bckdha* to the same level as in STD group (Figure 4.1.7 H). The expression of the gene for UCP1, the protein responsible for BAT thermogenesis, was not detectable in STD, HF and HF+F groups. On the other hand, *Ucp1* expression was greatly increased in HF+MSDC and HF+MSDC+F groups (Figure 4.1.7 I).

The gene expression analysis revealed that HF diet had a general suppressive effect on metabolic pathways in eWAT. However, the expression levels of *Cd36*, *Cpt1α* and *Gk* were upregulated by HF diet and they were further increased in response to MSDC. TZD-containing interventions generally increased gene expression levels suppressed by HF diet with MSDC having stronger effect compared to PIO. *n*-3 PUFA tended to enhance the stimulatory effect of MSDC on most of the genes. Significant additive effects of *n*-3 PUFA and MSDC were observed on the expression of *Atgl/Pnpla2* and *Hsl/Lipe*. On the other hand, no additive effects of *n*-3 PUFA and PIO were observed. Moreover, combined treatment with PIO and *n*-3 PUFA decreased the expression of certain genes, e.g. *Pgc-1a/Ppargc1a*, *Gk* and *Pdk4* (Figure 4.1.7). Combined treatment with *n*-3 PUFA and MSDC had generally the strongest effect on the recovery of gene expression in eWAT suppressed by HF diet.

In conclusion, we observed additive beneficial effects of combined treatment with *n*-3 PUFA and TZDs on the improvement of metabolic health in mice fed obesogenic HF diet. The modulation of intrinsic metabolic processes in WAT, namely TAG/FA cycling by *n*-3 PUFA and TZDs seems to have an important role in the mediation of these beneficial effects. Combined treatment with *n*-3 PUFA and MSDC had the strongest ability to counteract the detrimental effects of HF diet on metabolic health of mice.

4.2 Publication B: Effects of GPR-10 deletion on the whole-body energy homeostasis in mice

The second aim of this thesis is addressed in publication B. We aimed to characterize the effects of GPR-10 deletion in CNS on metabolic processes in other organs especially in adipose tissue. GPR-10 is believed to affect energy homeostasis due to its abundant expression in brain areas involved in the regulation of food intake and energy expenditure. We characterized general metabolic parameters with a focus on lipid metabolism in GPR-10 KO mice as well as in their WT littermates of both genders. We used *in vivo* analyses such as INCA, OGTT and *ex vivo* analyses such as RT-qPCR and histological analyses.

4.2.1 Characterization of general parameters related to energy homeostasis

GPR-10 deficient mice and their WT littermates of both genders were on C57BL/6J genetic background. They were either fed STD or they were assigned to obesogenic HF diet at the age of 12 weeks and fed HF diet for a period of 28 weeks. The average food consumption per day expressed in kJ was higher in animals fed HF diet compared to animals fed STD. GPR-10 KO mice of both genders fed HF diet had higher food consumption compared to WT mice fed HF diet (Table 4.2.1). Body weight reflected food consumption and it was increased in all groups fed HF diet compared to animals on STD. GPR-10 deletion affected body weight only in males fed STD and it was increased in KO males compared to WT. The weight of eWAT was increased in response to HF diet in WT mice of both genders as well as in KO females. GPR-10 KO mice of both genders fed STD had higher weight of eWAT compared to WT mice. The weight of scWAT increased in response to HF diet in mice of both genders and genotypes. GPR-10 deletion resulted in increase of scWAT weight only in males fed STD. The weight of iBAT increased in response to HF diet in both genders and genotypes; however, no differences between KO and WT mice were observed. The weight of the liver was increased in GPR-10 KO males fed both STD as well as on HF diet compared to WT males. HF diet increased the liver weight only in males, while no differences between any groups were observed in females (Table 4.2.1).

Table 4.2.1 General metabolic parameters of WT and GPR-10 KO mice fed different diets. Food intake was monitored weekly for the period of 28 weeks. Body weight and the weight of tissues were assessed after the sacrifice at the age of 38 weeks. Data are means ± SEM (n = 6-8). *—Significantly different from WT mice (*p ≤ 0.05, ** p ≤ 0.01, unpaired t-test); #—significantly different from mice on STD (# p ≤ 0.05, ## p ≤ 0.01, ### p ≤ 0.001, unpaired t-test). GPR-10 KO mice: GPR-10 knockout mice; WT: wild-type mice; STD: standard chow diet; HFD: high-fat diet; FI: food intake; BW: body weight; gWAT: gonadal white adipose tissue; scWAT: subcutaneous white adipose tissue; BAT: interscapular brown adipose tissue.

Group	Average FI [kJ] per day	BW [g] (38 weeks)	gWAT [g]	scWAT [g]	BAT [g]	liver [g]
WT male STD	49.22 ± 1.87	33.57 ± 2.16	0.83 ± 0.22	0.28 ± 0.06	0.12 ± 0.02	1.46 ± 0.06
GPR10 KO male STD	51.70 ± 1.01	39.54 ± 1.48 *	1.60 ± 0.16 *	0.48 ± 0.06 *	0.18 ± 0.02	1.93 ± 0.12 **
WT male HFD	60.69 ± 0.83 ###	53.17 ± 2.14 ###	1.61 ± 0.11 #	1.36 ± 0.15 ###	0.32 ± 0.02 ###	2.55 ± 0.20 ###
GPR10 KO male HFD	65.82 ± 1.99 ###, *	56.13 ± 0.57 ###	1.49 ± 0.09	1.29 ± 0.06 ###	0.30 ± 0.02 ###	3.74 ± 0.19 ###, **
WT female STD	44.22 ± 0.43	26.51 ± 1.01	0.45 ± 0.02	0.24 ± 0.02	0.08 ± 0.01	1.15 ± 0.06
GPR10 KO female STD	46.59 ± 2.47	29.19 ± 1.65	1.03 ± 0.24 *	0.39 ± 0.07	0.10 ± 0.01	1.31 ± 0.06
WT female HFD	53.75 ± 1.26 ###	44.01 ± 2.42 ###	3.02 ± 0.38 ###	1.47 ± 0.21 ###	0.16 ± 0.02 ###	1.31 ± 0.11
GPR10 KO female HFD	59.70 ± 0.97 ###, **	48.71 ± 4.01 ###	4.05 ± 0.62 ##	1.53 ± 0.17 ###	0.21 ± 0.03 ##	1.63 ± 0.18

### 4.2.2 Characterization of whole-body energy metabolism *in vivo*

GPR-10 deletion affected the plasmatic levels of major markers of glucose and lipid metabolism assessed by OGTT (Table 4.2.2). Fasting glucose levels were elevated in response to HF diet only in GPR-10 KO females. Moreover, GPR-10 KO males fed STD had higher fasting glucose levels compared to WT mice. Fasting insulin levels were greatly elevated in response to HF diet in mice of both genders and genotypes. Both GPR-10 KO males and females fed HF diet had increased fasting insulin levels compared to WT mice fed HF diet, while there were no differences between genotypes in STD groups. 30 minutes after the glucose administration levels of insulin were elevated in all groups fed HF diet compared to mice fed STD; however, there were no differences between genotypes in any of the groups. The decrease in plasmatic NEFA levels due to the glucose administration, i.e. the difference

between fasting NEFA levels and NEFA levels 30 minutes after glucose gavage (ΔNEFA) was smaller in WT males fed HF diet compared to WT males fed STD. No effect of HF diet on ΔNEFA was detected in GPR-10 KO males. In females ΔNEFA was supressed by HF diet in both genotypes with greater effect in WT mice. Moreover, in females fed STD, ΔNEFA was decreased in GPR-10 KO mice compared to WT mice. Plasmatic TAG levels were mildly increased in response to HF diet in females and no difference between dietary groups was detected in males. However, GPR-10 KO males fed HF diet had increased TAG levels compared to WT males fed the same diet. HOMA-IR index was increased in both genders in response to HF diet. GPR-10 KO mice of both genders in HF diet groups had higher HOMA-IR index compared to WT mice with more pronounced effect in males. Plasmatic leptin levels reflected the increase in body weight and they were increased in response to HF diet. In GPR-10 KO males fed STD, leptin levels were increased compared to WT males, while no differences between genotypes were detected in other groups (Table 4.2.2).

Table 4.2.2 Metabolic parameters in plasma during OGTT in WT and GPR-10 KO mice fed different diets. Determination of plasmatic parameters related to energy metabolism. Data are means ± SEM (n = 6-8). *—Significantly different from WT mice (*$p \leq 0.05$, ** $p \leq 0.01$, unpaired t-test); #—significantly different from mice fed STD (#$p \leq 0.05$, ## $p \leq 0.01$, ### $p \leq 0.001$, unpaired t-test). GPR-10 KO mice: GPR-10 knockout mice; WT: wild-type mice; STD: standard chow diet; HFD: high-fat diet; NEFA: non-esterified fatty acid; HOMA-IR: homeostatic model assessment; TAG: triacylglycerol.

| Group	Glucose 0 min [mmol/l]	Insulin 0 min [ng/ml]	Insulin 30 min [ng/ml]	Δ NEFA [mol/l]	HOMA-IR	leptin 0 min [ng/ml]	TAG 0 min [mmol/l]
WT male STD	8.64 ± 0.37	0.67 ± 0.22	1.61 ± 0.43	0.41 ± 0.03	46.69 ± 16.57	3.95 ± 1.74	0.57 ± 0.06
GPR10 KO male STD	10.16 ± 0.37 *	1.24 ± 0.21	3.32 ± 0.94	0.25 ± 0.07	97.57 ± 17.80	12.81 ± 2.96 *	0.57 ± 0.04
WT male HFD	8.83 ± 0.34	2.30 ± 0.19 ###	5.73 ± 0.52 ###	0.15 ± 0.03 ###	154.86 ± 12.14 ###	31.9 ± 11.41 ###	0.53 ± 0.05
GPR10 KO male HFD	9.74 ± 0.43	3.12 ± 0.24 ###, *	8.96 ± 1.64 #	0.16 ± 0.04	223.01 ± 16.66 ###, **	33.05 ± 1.39 ###	0.68 ± 0.03 *
WT female STD	7.46 ± 0.44	0.27 ± 0.06	0.85 ± 0.12	0.48 ± 0.05	15.81 ± 3.91	2.94 ± 0.55	0.59 ± 0.04
GPR10 KO female STD	8.16 ± 0.34	0.37 ± 0.07	1.07 ± 0.17	0.32 ± 0.03 *	23.58 ± 4.86	6.86 ± 2.10	0.46 ± 0.08
WT female HFD	8.76 ± 0.51	0.77 ± 0.08 ###	2.03 ± 0.17 ###	0.22 ± 0.04 ##	52.20 ± 6.23 ###	27.41 ± 3.65 ###	0.69 ± 0.03
GPR10 KO female HFD	9.70 ± 0.37 ##	1.25 ± 0.17 ###, *	3.30 ± 0.66 ##	0.22 ± 0.03 #	94.52 ± 14.45 ###, *	33.68 ± 3.82 ###	0.68 ± 0.02 #

For the detection of whole-body energy expenditure and fuel preference, INCA was performed at the age of 24 weeks. HF diet decreased RQ in both male and female WT mice compared to mice fed STD (Figure 4.2.1 A, B). HF diet resulted in decreased RQ also in GPR-10 KO female mice, while no effect was observed in GPR-10 KO males. Decreased RQ indicates greater utilization of lipids as an oxidative fuel, which corresponds with the composition of HF diet. Higher RQ during the night in mice fed STD indicates the feeding period of the animals when carbohydrates are oxidised as a fuel (Figure 4.2.1 A, B). energy expenditure was increased in response to HF diet in both male and female WT mice. There were no differences in energy expenditure between the genotypes (Figure 4.2.1 C, D).
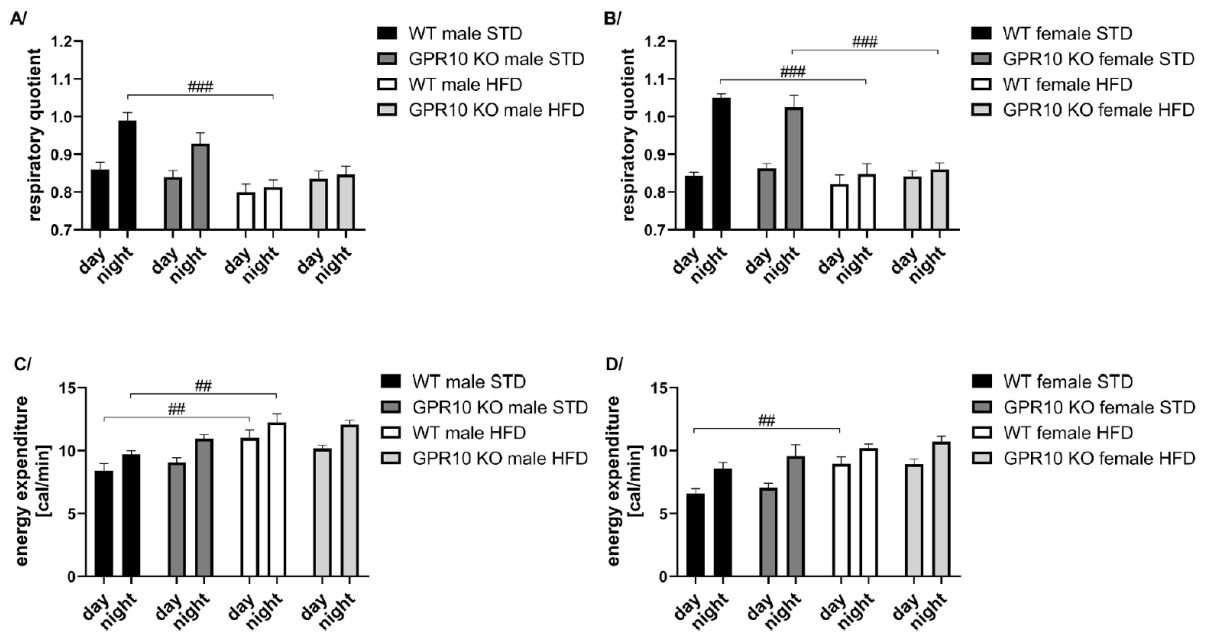
Figure 4.2.1 Respiratory quotient and energy expenditure in WT and GPR-10 KO mice fed different diets. Respiratory quotient in male (**A**) and female (**B**) and energy expenditure in male (**C**) and female (**D**) WT and GPR-10 KO mice fed STD and HF diet measured by INCA at the age of 24 weeks. Day stands for a period between 6 a.m. and 6 p.m. Data are means ± SEM (*n* = 6-8). Significance is ## $p \leq 0.01$, ### $p \leq 0.001$, as determined by two-way ANOVA followed by Tukey's multiple comparisons test. GPR-10 KO mice: GPR-10 knockout mice; WT: wild-type mice; STD: standard chow diet; HFD: high-fat diet.

4.2.3 Histological and biochemical analyses of the liver

Histological analyses revealed liver steatosis as a result of HF diet feeding (Figure 4.2.2). The effect of HF diet was more pronounced in males compared to females and no effect of GPR-10 deletion was detected. The degree of liver steatosis was determined as a percentage of lipid droplets with WT mice fed STD being calculated as 100% (Figure 4.2.2 A, B). HF diet resulted in an increased hepatic TAG content with a greater effect in males. Hepatic TAG content was increased in GPR-10 KO mice of both genders in STD groups compared to WT mice, while in HF diet groups no differences between genotypes were detected (Figure 4.2.2 C, D). Liver TAG content was only partly reflected in the weight of the liver. In females no effect of diet or genotype was detected, while in males GPR-10 deletion increased the liver weight in both STD and HF diet groups and HF diet itself also increased the liver weight in both genotypes in male mice (Table 4.2.1).
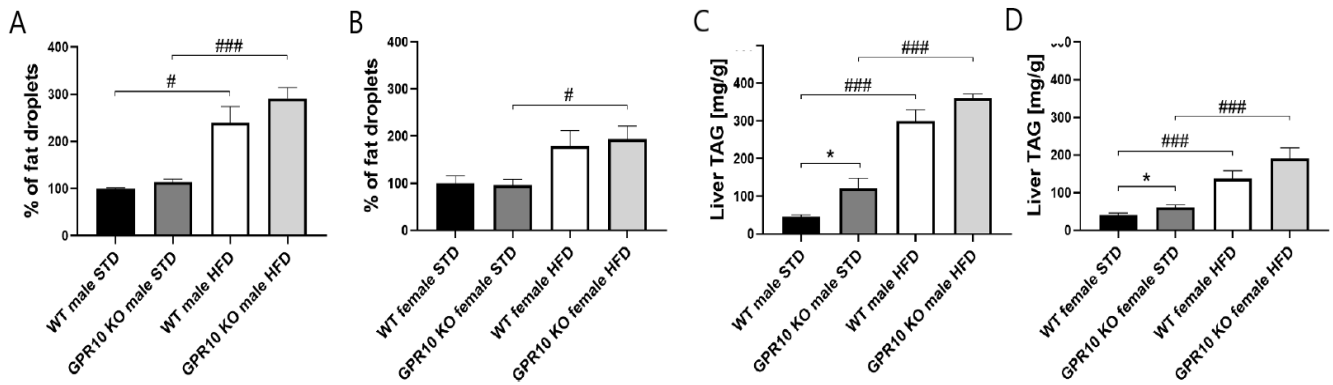
Figure 4.2.2 Quantification of hepatic lipid content in WT and GPR-10 KO mice fed different diets. Quantification of liver steatosis in male (**A**) and female (**B**) WT and GPR-10 KO mice fed STD and HF diet represented by % of lipid droplets (WT mice on STD being set as 100%). Liver TAG levels in male (**C**) and female (**D**) WT and GPR-10 KO mice fed STD and HF diet. Data are means ± SEM (n = 4-8). Significance is * $p \leq 0.05$ GPR-10 KO vs WT on the same diet, # $p \leq 0.05$, ### $p \leq 0.001$ HFD vs STD of the same genotype, as determined by unpaired t-test. GPR-10 KO mice: GPR-10 knockout mice; WT: wild-type mice; STD: standard chow diet; HFD: high-fat diet; TAG: triacylglycerol.

### 4.2.4 Gene expression analysis

The gene expression of key markers of lipid and glucose metabolism was determined in scWAT, liver, eWAT and in iBAT of WT and GPR-10 KO mice fed STD using RT-qPCR. In scWAT the expression of genes for PPARα and PPARγ, major regulators of lipid metabolism, was decreased in GPR-10 KO males compared to WT males, while the expression of *Ppargc1a*, one of the important targets of PPARγ, was not affected (Figure 4.2.3 A). On the other hand, the expression of *Ppara*, *Pparg* as well as *Ppargc1a* increased in scWAT of GPR-10 KO females compared to WT females (Figure 4.2.3 B). The expression of lipogenic genes in scWAT was also affected by GPR-10 deletion with different effects in males and females. The expression of *Fasn* was strongly suppressed in GPR-10 KO males compared to their WT littermates, while no effect was observed in females. In addition, the expression of genes for DGAT1 and DGAT2, enzymes regulating the final stage of TAG synthesis, was decreased in GPR-10 KO males compared to WT males. The expression of genes for SCD1 and MLXIPL, two other enzymes involved in the regulation of lipogenesis, was also decreased in GPR-10 KO males in comparison with WT males (Figure 4.2.3 C). In GPR-10 KO females the expression of genes for DGAT2 and MLXIPL was upregulated compared to WT females. The expression of *Pck2*, the gene for mitochondrial isoform of PEPCK and another marker of lipogenesis in WAT, was also increased in GPR-10 KO females compared to WT females. The expression of the gene for GLUT4 (*Slc2a4*), which is an enzyme responsible for the transport of glucose into adipocytes and the promotion of lipogenesis, was again increased in GPR-10 KO females in comparison with WT females (Figure 4.2.3 D). Increased expression of genes involved in the control of lipid metabolism in scWAT of GPR-10 KO females seems to prevent the expansion of scWAT depot observed in GPR-10 KO males.

scWAT
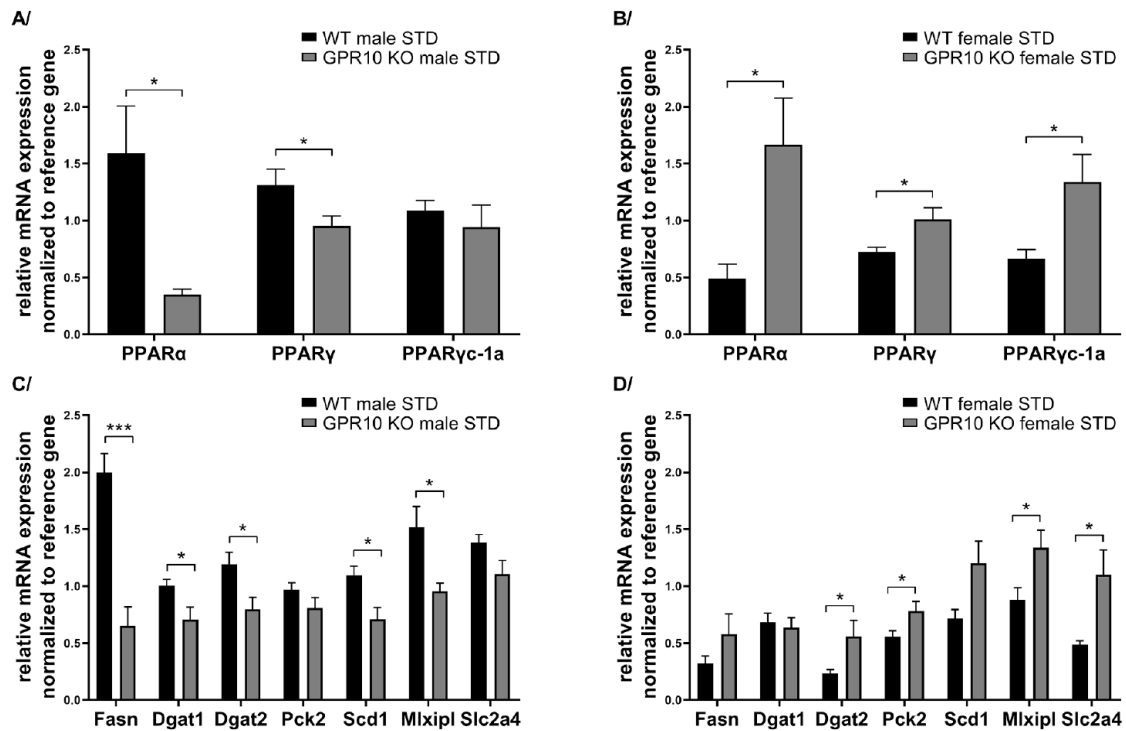
Figure 4.2.3 The expression of metabolic genes in scWAT of WT and GPR-10 KO mice. The expression of genes for PPARα/γ and PGC-1α (PPARγc-1a) transcriptional regulators in scWAT of male (**A**) and female (**B**) WT and GPR-10 KO mice; the expression of key lipogenic genes in scWAT of male (**C**) and female (**D**) WT and GPR-10 KO mice. Data are means ± SEM (*n* = 7-8). Significance is * p ≤ 0.05, *** p ≤ 0.001 GPR-10 KO vs WT mice, as determined by unpaired t-test. GPR-10 KO mice: GPR-10 knockout mice WT: wild-type mice; STD: standard chow diet; scWAT: subcutaneous white adipose tissue; *Dgat1*: diacylglycerol O-acyltransferase 1; *Dgat2*: diacylglycerol O-acyltransferase 2; *Fasn*: fatty acid synthase; *Mlxipl*: MLX interacting protein like (carbohydrate response element binding protein); *Pck2*: phosphoenolpyruvate carboxykinase 1, mitochondrial; *Ppara*: peroxisome proliferator-activated receptor alpha; *Pparγ*: peroxisome proliferator-activated receptor gamma; *Pparγc-1a*: peroxisome proliferator-activated receptor gamma coactivator 1 alpha; *Scd1*: stearoyl-Coenzyme A desaturase 1; *Slc2a4*: solute carrier family 2 (facilitated glucose transporter), member 4.

In the liver, the expression of genes for PPARα, PPARγ and PGC-1α (PPARγc-1a) was again increased in GPR-10 KO females compared to their WT littermates (Figure 4.2.4 B), while no differences between genotypes were detected in males (Figure 4.2.4 A). In GPR-10 KO males the expression of the gene for NRF1, which is an important regulator of mitochondrial oxidative functions, was decreased compared to WT mice (Figure 4.2.4 C). In GPR-10 KO females the gene expression for the key lipogenic enzyme FAS (*Fasn*) was supressed in comparison with their WT littermates (Figure 4.2.4 D). Levels of other metabolic genes in the liver did not differ significantly between the genotypes.
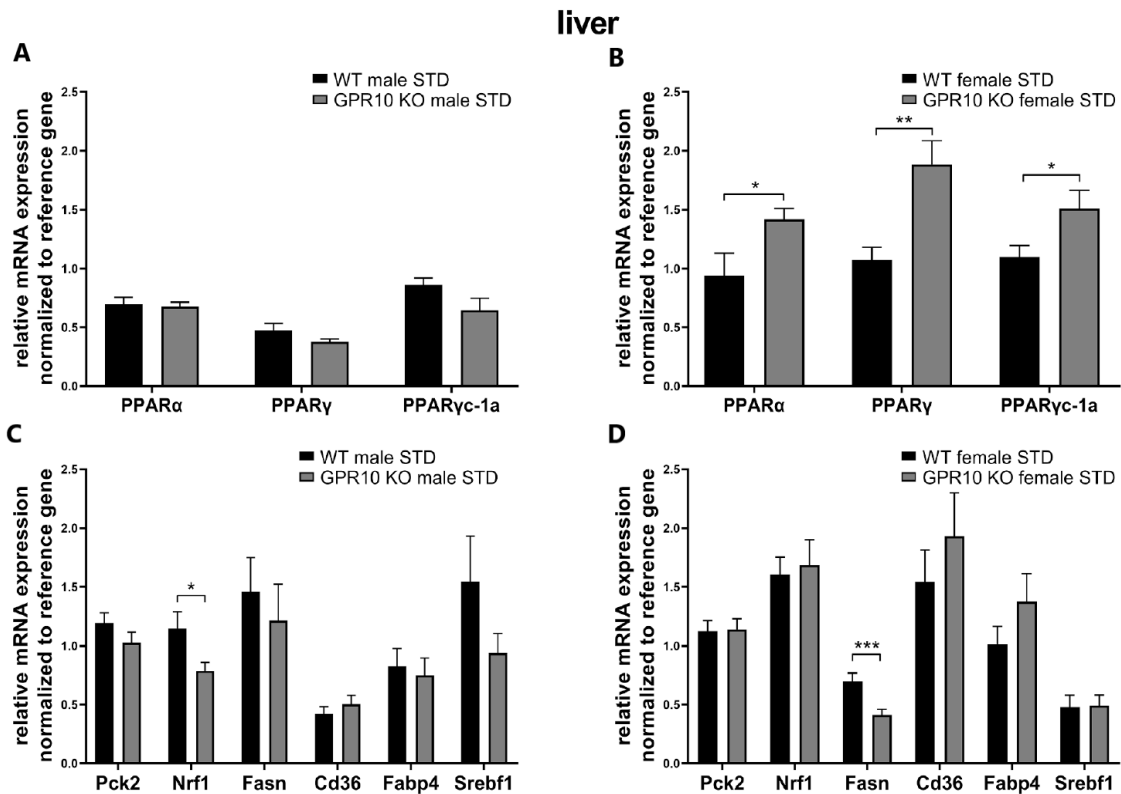
Figure 4.2.4 The expression of metabolic genes in the liver of WT and GPR-10 KO mice.
The expression of genes for PPARα/γ and PGC-1α (PPARγc-1a) transcriptional regulators in the liver of male (**A**) and female (**B**) WT and GPR-10 KO mice; the expression of key genes controlling energy metabolism in the liver of male (**C**) and female (**D**) WT and GPR-10 KO mice. Data are means ± SEM (*n* = 7-8). Significance is * p ≤ 0.05, ** p ≤ 0.01, *** p ≤ 0.001 GPR-10 KO vs WT mice, as determined by unpaired t-test. GPR-10 KO mice: GPR-10 knockout mice; WT: wild-type mice; STD: standard chow diet; *Cd36*: Cd36 antigen; *Fabp4*: fatty acid binding protein 4; *Fasn*: fatty acid synthase; *Nrf1*: nuclear respiratory factor 1; *Pck2*: phosphoenolpyruvate carboxykinase 1, mitochondrial; *Ppara*: peroxisome proliferator-activated receptor alpha; *Pparγ*: peroxisome proliferator-activated receptor gamma; *Pparγc-1a*: peroxisome proliferator-activated receptor gamma coactivator 1 alpha; *Srebf1*: sterol regulatory element binding transcription factor 1.

In eWAT GPR-10 KO males displayed decreased expression of *Pparγc-1a* and *Mlxipl* compared to WT males. GPR-10 KO females displayed upregulated expression of genes for PPARγ and SCD1, which are both critical for the regulation of lipogenesis (Data not shown). No significant differences were observed in the expression of metabolic genes in iBAT (Data not shown). GPR-10 KO males generally displayed downregulation of metabolic genes, while in GPR-10 KO females the expression of key metabolic genes was upregulated in the liver and in WAT. This could contribute to the gender-specific differences in an excessive fat accumulation connected with GPR-10 deletion as it was observed only in GPR-10 KO males.

In conclusion, GPR-10 deletion resulted in changes of lipid metabolism and deterioration of insulin sensitivity in mice of both genders; with more pronounced effect in males. GPR-10 KO males displayed increased body weight probably due to an increased amount of WAT,

while in females no differences between genotypes were detected. The weights of WAT depots in GPR-10 KO female mice were not increased by GPR-10 deletion possibly due to a compensatory increase in the expression of genes involved in the regulation of lipid metabolism.

4.3 Publication C: Effects of adipose tissue-specific PGC-1β deletion on the control of thermogenesis

Publication C deals with the third aim of this thesis. We aimed to characterize the role of PGC-1β in adipose tissue under conditions with different requirements for thermogenesis. It was reported that mice with whole-body deletion of PGC-1β displayed impaired thermogenesis [212]. In this study we used mice with PGC-1β deletion exclusively in adipocytes (PGC-1β-AT-KO) and their WT littermates in order to investigate whether cold sensitivity of whole-body PGC-1β ablated mice is due to a defect in BAT thermogenesis.

4.3.1 Characterization of general metabolic parameters in WT and PGC-1β-AT-KO mice

PGC-1β-AT-KO male mice as well as their WT littermates were on C57BL/6J genetic background and they were fed STD diet. Two-months old mice were first maintained at thermoneutral temperature (30 °C) for 10 days and thereafter exposed to cold (6 °C) for 2 (2-day-CE) or 7 days (7-day-CE) with control group staying at 30 °C for the whole time (Table 4.3.1.). Food consumption was increased by CE with no differences between genotypes except a mild increase in PGC-1β-AT-KO mice at 2-day-CE group. Body weight did not differ between any of the groups; on the other hand, body weight gain was decreased by CE in both 2-day-CE and 7-day-CE groups with KO mice in 2-day-CE group having lower BW gain compared to WT mice. The weight of eWAT and scWAT depots did not differ among the groups. The weight of iBAT displayed transient decrease after 2-day-CE with recovery of the amount of iBAT after 7-day-CE only in WT mice. In PGC-1β-AT-KO mice the weight of iBAT was not restored after 7 days of CE and remained lighter than in the control group (30 °C). In addition, the weight of iBAT was increased in PGC-1β-AT-KO mice compared to WT mice in all the groups with the biggest difference in 30 °C group. The weight of the liver did not differ among the groups, while the hepatic TAG content was slightly increased in 7-day-CE group compared to 30 °C group without any effect of genotype. The weight of quadriceps muscle slightly decreased in response to 7 days of CE, while the TAG content in the muscle did not differ among the groups. Plasmatic levels of TAG and NEFA were transiently declined after 2 days of CE and their levels were restored after 7 days of CE. However, in PGC-1β-AT-KO mice both TAG and NEFA levels were restored only partially after 7 days of CE resulting in lower levels of these metabolites in 7-day-CE group compared to WT mice. Glucose and insulin levels did not differ between the genotypes (Table 4.3.1).

Table 4.3.1 General metabolic parameters in WT and PGC-1β-AT-KO mice maintained at 30 °C or exposed to cold. Data are means ± SEM (n = 12-15), Statistical analysis was performed using two-way ANOVA (p≤0.05). *Significant difference compared to 30 °C within the genotype; # significant difference between genotype within the same temperature. KO: adipose tissue-specific PGC-1β knockout mice; WT: wild-type mice; 30 °C: mice adapted to thermoneutral conditions; 2-day-CE: mice exposed to cold for 2 days; 7-day-CE: mice exposed to cold for 7 days; AT: adipose tissue; eWAT: epididymal white adipose tissue; scWAT: subcutaneous white adipose tissue; iBAT: interscapular brown adipose tissue; TAG: triacylglycerols; NEFA: non-esterified fatty acids.

|	WT			KO		
	30 °C	2-day-CE	7-day-CE	30 °C	2-day-CE	7-day-CE
Food consumption (g day^{-1})	2.6 ± 0.1	4.6 ± 0.3[a]	5.6 ± 0.2[a,b]	2.6 ± 0.1	5.3 ± 0.2[a,c]	5.7 ± 0.2[a]
Body weight (g)	27.5 ± 0.6	26.6 ± 0.4	27.2 ± 0.4	27.7 ± 0.6	27.1 ± 0.5	27.0 ± 0.5
Body weight gain (g)	0.21 ± 0.13	-0.82 ± 0.13[a]	-0.19 ± 0.16[b]	0.11 ± 0.13	-1.35 ± 0.26[a,c]	-0.24 ± 0.19[b]
Weight of AT depots						
eWAT (mg)	498 ± 27	464 ± 30	423 ± 17	439 ± 30	460 ± 32	387 ± 21
scWAT (mg)	292 ± 15	241 ± 11	256 ± 11	270 ± 18	265 ± 24	245 ± 12
iBAT (mg)	107 ± 4	65 ± 3[a]	97 ± 4[b]	168 ± 10[c]	86 ± 4[a,c]	112 ± 4[a,b,c]
Liver						
Weight (mg)	1110 ± 37	n.d.	1128 ± 40	1134 ± 34	n.d.	1170 ± 33
TAG (mg per g tissue)	20.2 ± 1.1	n.d.	24.4 ± 1.1[a]	21.5 ± 0.8	n.d.	26.3 ± 0.9[a]
Quadriceps muscle						
Weight (mg)	235 ± 7	n.d.	198 ± 5[a]	226 ± 8	n.d.	204 ± 7[a]
TAG (mg per g tissue)	13.5 ± 1.6	n.d.	10.8 ± 0.8	10.2 ± 1	n.d.	10 ± 0.7
Plasma levels						
TAG (mmol l^{-1})	0.94 ± 0.07	0.43 ± 0.03[a]	0.80 ± 0.10[b]	0.99 ± 0.06	0.40 ± 0.02[a]	0.55 ± 0.05[a,b,c]
NEFA (mmol l^{-1})	0.39 ± 0.03	0.27 ± 0.03[a]	0.44 ± 0.03[b]	0.37 ± 0.02	0.25 ± 0.02[a]	0.33 ± 0.05[b,c]
Glucose (mg dl^{-1})	191 ± 8	n.d.	217 ± 9	182 ± 10	n.d.	236 ± 17[a]
Insulin (ng ml^{-1})	0.49 ± 0.11	0.67 ± 0.1	0.39 ± 0.04	0.37 ± 0.06	0.60 ± 0.08	0.47 ± 0.07

4.3.2 Cold tolerance test and noradrenaline test in indirect calorimetry

PGC-1β-AT-KO mice and their WT littermates adapted to 30 °C were acutely exposed to 5 °C and their core body temperature was measured in INCA. Decline in core body temperature between 1st and 2nd hour of CE was more pronounced in PGC-1β-AT-KO mice compared to WT mice (Figure 4.3.1 A). The core body temperature of WT mice stabilised at 33 °C after 2 hours of CE, while in PGC-1β-AT-KO mice core body temperature decreased to 28 °C after 2 hours of CE as was observed in the whole body PGC-1β KO mice [109]. Despite the marked decrease of body temperature in the initial phase of CE, PGC-1β-AT-KO mice are able to survive in cold.

In order to assess the effect of PGC-1β deletion on adrenergically-stimulated energy expenditure, NE-test was performed in INCA (Figure 4.3.1 B). WT and PGC-1β-AT-KO mice adapted to 30 °C or exposed to cold for 7 days were anaesthetized by pentobarbital and their whole-body oxygen consumption was measured at 33 °C 30 minutes before (basal condition) and 60 minutes after norepinephrine application. Under basal conditions, oxygen consumption

was increased in cold exposed groups with no differences between genotypes. After norepinephrine administration, oxygen consumption increased in all groups. In mice adapted to 30 °C PGC-1β-AT-KO animals tended to have lower oxygen consumption in response to norepinephrine compared to WT mice, while in mice exposed to cold there was significantly reduced oxygen consumption in PGC-1β-AT-KO mice compared to WT littermates (4.3.1 B and C).
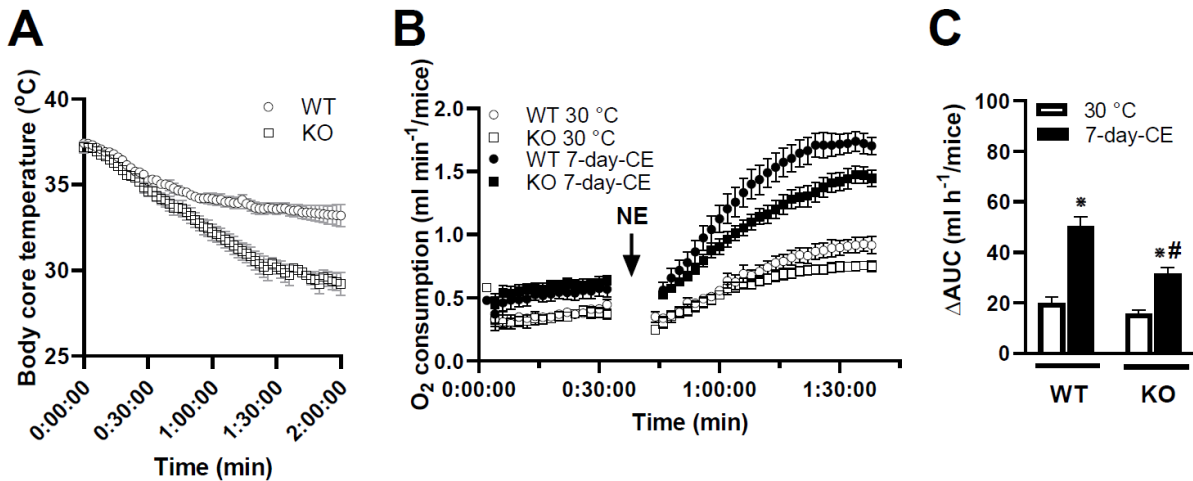

Figure 4.3.1 Effect of PGC-1β ablation on thermogenesis. Cold tolerance test **(A)** and NE-test **(B, C)** measured using INCA. Data are means ± SEM (n = 6-9), Statistical analysis was performed using one **(A)** or two-way **(B, C)** ANOVA (p≤0.05). *Significant difference compared to 30 °C within the genotype; # significant difference between genotype within the same temperature. KO: adipose tissue-specific PGC-1β knockout mice; WT: wild-type mice; 30 °C: mice adapted to thermoneutral conditions; 7-day-CE: mice exposed to cold for 7 days; NE: norepinephrine; ΔAUC: delta area under the curve.

4.3.3 Gene expression and protein levels of UCP1 in iBAT

To investigate the cause of increased cold sensitivity (Figure 4.3.1 A) and impaired thermogenesis (4.3.1 B, C) of PGC-1β-AT-KO mice, we measured mRNA and protein levels of UCP1 as the most important protein responsible for NST in BAT. UCP1 mRNA levels were negligible in mice maintained at 30 °C, while 2 days of CE markedly increased their levels. However, in 7-day-CE group *Ucp1* expression levels declined again (Figure 4.3.2 A). No differences were found between genotypes except higher *Ucp1* level in PGC-1β-AT-KO mice compared to WT in 2-day-CE group.

In order to learn whether the gene expression levels reflect protein content we evaluated UCP1 protein levels in mice from 30 °C and 7-day-CE group. CE resulted in considerable increase in UCP1 protein levels; however, no differences between genotypes were detected in any of the groups (Figure 4.3.2 B) even if the protein levels were normalised to the weight of iBAT (Figure 4.3.2 C).
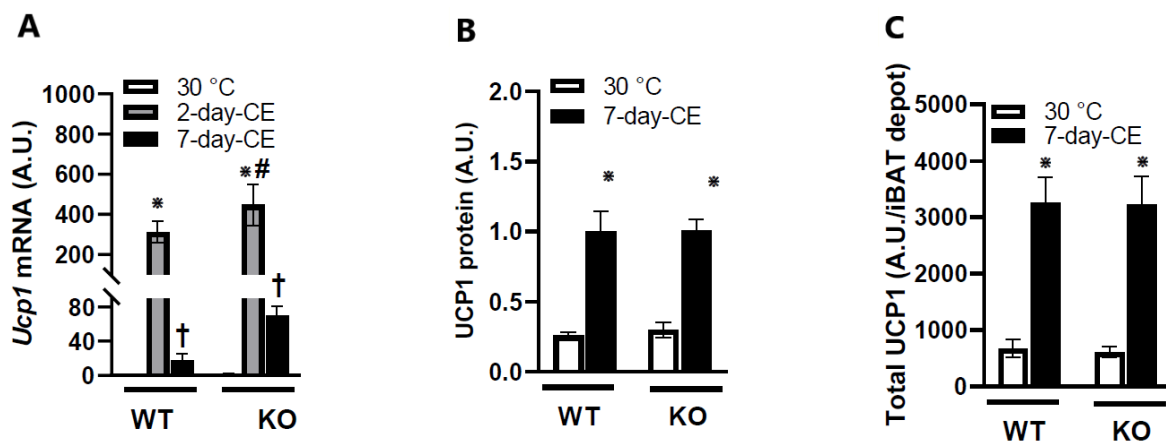
Figure 4.3.2 Gene expression and protein levels of UCP1 in iBAT of WT and PGC-1β-AT-KO mice maintained at 30 °C or exposed to cold. Data are means ± SEM (n = 8-15), Statistical analysis was performed using two-way ANOVA (p≤0.05). *Significant difference compared to 30 °C within the genotype; †significant difference in comparison to 2-day-CE within the genotype; # significant difference between genotype within the same temperature. KO: adipose tissue-specific PGC-1β knockout mice; WT: wild-type mice; 30 °C: mice adapted to thermoneutral conditions; 7-day-CE: mice exposed to cold for 7 days; iBAT: interscapular brown adipose tissue; UCP1: uncoupling protein 1.

4.3.4 Immunohistochemical analyses of iBAT

Immunohistochemical analyses of iBAT were performed in order to characterize the nature of iBAT enlargement in PGC-1β-AT-KO mice. We analysed the size of both brown adipocytes and lipid droplets in adipocytes using light microscopy (Figure 4.3.3). Brown adipocytes of both WT and PGC-1β-AT-KO mice from 30 °C adopted white-like phenotype with one or few large lipid droplets. The size of adipocytes (Figure 4.3.3.A, B) and also lipid droplets in adipocytes (4.3.3 C, D) from PGC-1β-AT-KO mice maintained at 30 °C was increased compared to WT mice. In 7-day-CE group brown adipocytes of PGC-1β-AT-KO mice, but not WT mice, were smaller compared to 30 °C group, while the size of lipid droplets was markedly reduced due to CE to the same level in both genotypes (Figure 4.3.3 C, D). The significant increase in the size of brown adipocytes and more importantly lipid droplets in adipocytes of PGC-1β-AT-KO mice from 30 °C might explain higher iBAT weight of these animals.
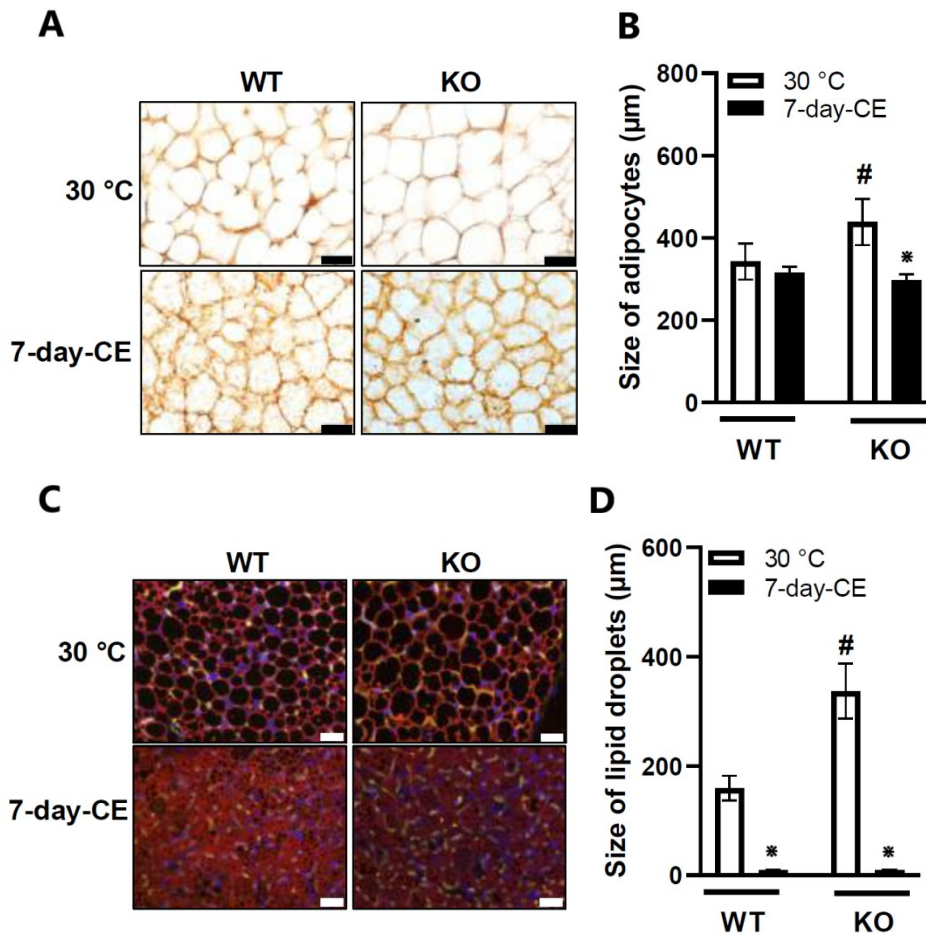
Figure 4.3.3 Morphology of adipocytes in iBAT of WT and PGC-1β-AT-KO mice maintained at 30 °C or exposed to cold. Size of adipocytes **(A, B)** and lipid droplets **(C, D)** Data are means ± SEM ($n = 4$). Statistical analysis was performed using two-way ANOVA ($p \leq 0.05$). *Significant difference compared to 30 °C within the genotype; # significant difference between genotype within the same temperature. KO: adipose tissue-specific PGC-1β knockout mice; WT: wild-type mice; 30 °C: mice adapted to thermoneutral conditions; 7-day-CE: mice exposed to cold for 7 days.

4.3.5 Gene expression analysis in iBAT

To characterize the effect of PGC-1β deletion on metabolic processes in BAT, we measured the expression of various genes controlling lipid metabolism and mitochondrial functions in iBAT. Most of the measured genes followed similar pattern with transient upregulation after 2 days of CE, followed by more or less pronounced reduction in the gene expression level after 7 days of CE. The expression of genes for transcriptional factors PGC-1α, PPARα as well as PPARγ was increased in PGC-1β-AT-KO mice in 7-day-CE group compared to WT mice (Figure 4.3.4 A).
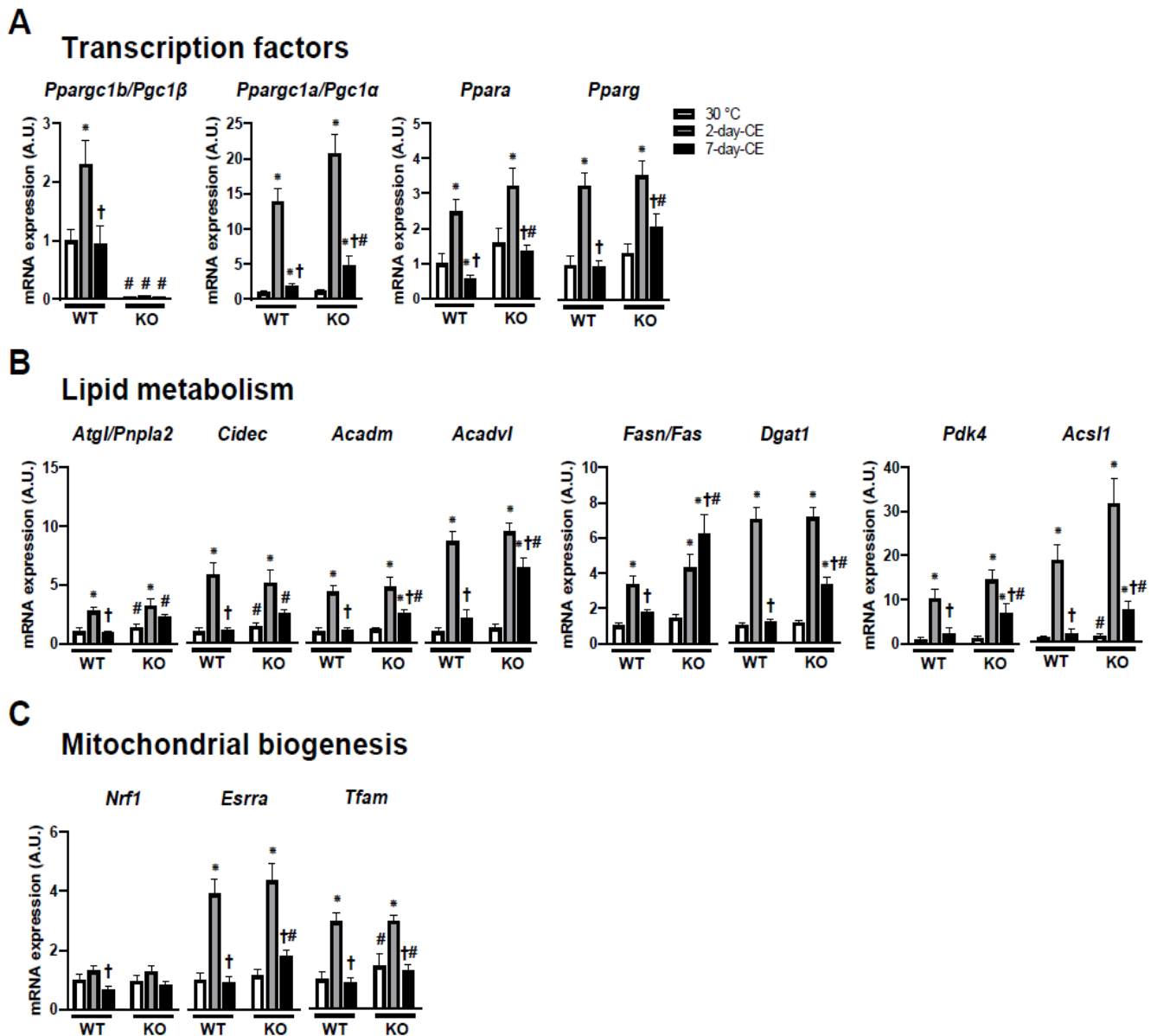
Figure 4.3.3 The effect of PGC-1β deletion on the expression of major metabolic genes in iBAT. Data are means ± SEM (*n* = 7-8). Statistical analysis was performed using two-way ANOVA (p≤0.05). *Significant difference compared to 30 °C within the genotype; †significant difference in comparison to 2-day-CE within the genotype; # significant difference between genotype within the same temperature. KO: adipose tissue-specific PGC-1β knockout mice; WT: wild-type mice; 30 °C: mice adapted to thermoneutral conditions; 2-day-CE: mice exposed to cold for 2 days; 7-day-CE: mice exposed to cold for 7 days. *Acadm*: acyl-Coenzyme A dehydrogenase, medium chain; *Acadvl*: acyl-Coenzyme A dehydrogenase; *Acsl1*: acyl-CoA synthetase long-chain family member 1; Cidec: cell death-inducing DFFA-like effector c; *Dgat1*: diacylglycerol O-acyltransferase 1; *Essra:* estrogen related receptor alpha; *Fas/Fasn*: fatty acid synthase; *Nrf1*: nuclear respiratory factor 1; *Pdk4*: pyruvate dehydrogenase kinase, isoenzyme 4; *Pnpla2/Atgl*: patatin-like phospholipase domain-containing protein 2 (adipose triglyceride lipase); *Ppara*: peroxisome proliferator-activated receptor alpha; *Pparg*: peroxisome proliferator-activated receptor gamma; *Pgc-1α/Ppargc1a*:

peroxisome proliferator-activated receptor gamma coactivator 1 alpha; *Pgc-1β/Ppargc1b*: peroxisome proliferator-activated receptor gamma coactivator 1 alpha; *Tfam*: transcription factor A, mitochondrial.

Next, we measured genes involved in the control of lipid catabolism. The expression of genes for ATGL (*Atgl/Pnpla2)* and CIDEC was increased in PGC-1β-AT-KO mice compared to WT mice in both 30 °C as well as in 7-day-CE group. The expression of genes for ACADM and ACADVL, enzymes with an important role in fatty acid catabolism, was increased in PGC-1β-AT-KO mice in 7-day-CE group compared to WT mice. Other two genes important for the process of fatty acid oxidation, *Pdk4* and *Acsl1*, were upregulated in PGC-1β-AT-KO mice compared to WT mice in 7-day-CE group and in the case of *Acsl1* also in 30 °C group.

The expression of the gene for FAS, the major enzyme controlling *de novo* lipogenesis, was increased in PGC-1β-AT-KO mice in 7-day-CE group compared to WT mice. Surprisingly, the expression of *Fas/Fasn* in PGC-1β-AT-KO mice from 7-day-CE group was even higher compared to PGC-1β-AT-KO mice from 2-day-CE group, which is a different pattern than we observed in all other metabolic genes. The expression of the gene for DGAT1, which is an important enzyme for TAG synthesis, was again increased in PGC-1β-AT-KO mice in 7-day-CE group compared to WT mice (Figure 4.3.4 B).

The expression of genes involved in the regulation of mitochondrial oxidative functions, such as *Nrf1*, *Esrra* and *Tfam*, followed the same pattern as other metabolic genes with transient increase in response to CE. The gene expression of *Esrra* and *Tfam* was upregulated in PGC-1β-AT-KO mice in 7-day-CE group compared to WT mice. In addition, the expression of *Tfam* was also increased in PGC-1β-AT-KO mice from 30 °C compared to WT mice (Figure 4.3.4 C).

In conclusion, increased levels of genes involved in the control of lipid metabolism and mitochondrial functions in BAT of PGC-1β-AT-KO mice exposed to cold copy the expression levels of PGC-1α, the main regulator of adaptive thermogenic program, and suggest compensatory mechanism of PGC-1β ablation.

4.3.6 Gene expression and protein levels of mitochondrial dynamics regulators in iBAT

Mitochondrial dynamics (fusion and fission) affect mitochondrial function; therefore, we aimed to quantify mRNA and protein levels of their important regulators (Figure 4.3.5). The expression of the gene for MFN2, protein controlling the fusion of mitochondrial outer membrane, followed the same pattern as other metabolic genes with transient increase in response to CE. In PGC-1β-AT-KO mice from 7-day-CE group *Mfn2* expression was increased compared to WT mice. The expression of the gene for OPA1, which is responsible for the fusion of inner mitochondrial membrane, also had the same pattern as other metabolic genes in iBAT; however, no differences between genotypes were detected.

On the level of protein, we measured levels of MFN2, DRP1 and long and short forms of OPA1, L-OPA1 and S-OPA1 respectively. DRP1 is a protein involved in the control of mitochondrial fission and S-OPA1 is believed to be responsible for the maintenance of mitochondrial cristae shape and OXPHOS function during mitochondrial fusion events (see

1.3.3). There were no differences in the protein levels of MFN2, DRP1 and S-OPA1 in any of the groups. Protein levels of L-OPA1 were reduced in response to CE with no difference between genotypes. On the other hand, in mice from 30 °C L-OPA1 protein levels were decreased in PGC-1β-AT-KO mice compared to WT mice. Decreased protein content of L-OPA1 might contribute to the impairment of interactions between mitochondria and the surface of lipid droplet resulting in higher amount of lipid stored in the droplet.
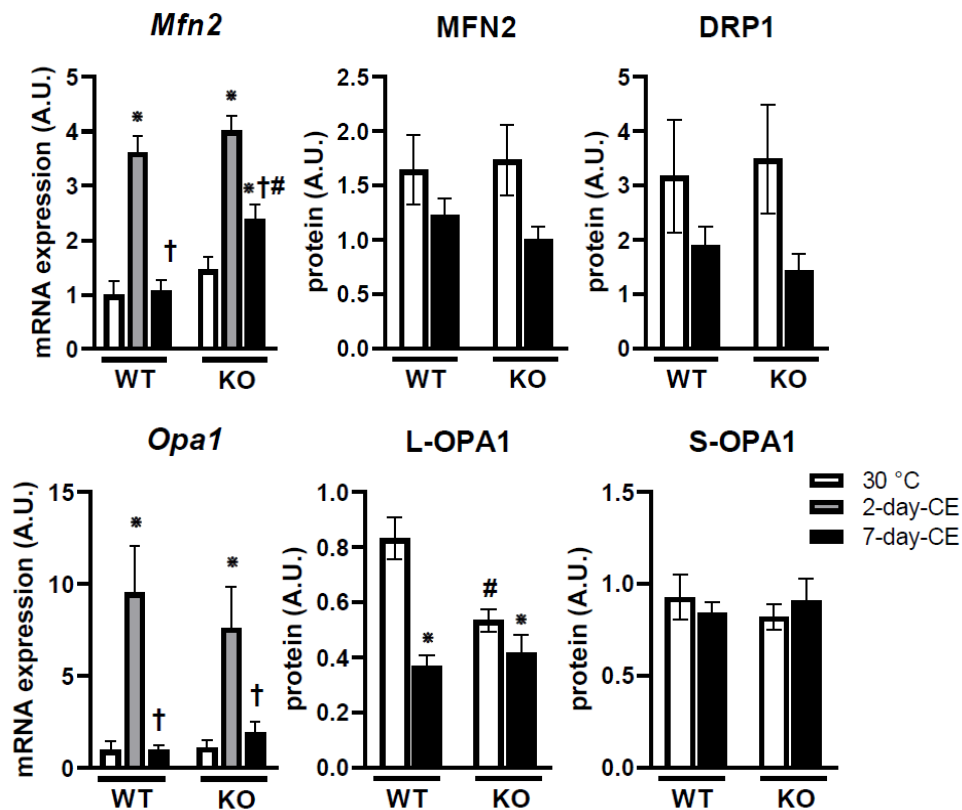
Figure 4.3.5 The mRNA and protein levels of the main regulators of mitochondrial dynamics in iBAT. Data are means ± SEM ($n = 7$-8). Statistical analysis was performed using two-way ANOVA (p≤0.05). *Significant difference compared to 30 °C within the genotype; †significant difference in comparison to 2-day-CE within the genotype; # significant difference between genotype within the same temperature. KO: adipose tissue-specific PGC-1β knockout mice; WT: wild-type mice; 30 °C: mice adapted to thermoneutral conditions; 2-day-CE: mice exposed to cold for 2 days; 7-day-CE: mice exposed to cold for 7 days; DRP1: dynamin-related protein 1; MFN2: mitofusin 2; L-OPA1: optic atrophy 1, mitochondrial dynamin-like GTPase, long isoform; S-OPA1: optic atrophy 1, mitochondrial dynamin-like GTPase, short isoform.

4.3.7 Electron microscopy analysis of iBAT

To investigate the potential effect of altered mitochondrial morphology on the control of lipid accumulation in brown adipocytes, we performed electron microscopy of iBAT samples (Figure 4.3.6). We evaluated the size of lipid droplets, mitochondrial length and calculated the

percentage of contact between mitochondria and the surface of lipid droplets. The magnification used in light microscopy was insufficient to detect differences in the size of lipid droplets in 7-day-CE group as the size of lipid droplets was markedly reduced by CE. On the other hand, electron microscopy used very high magnification, which together with a large size of lipid droplets in samples from mice at 30 °C only enabled to evaluate samples from 7-day-CE group. The data from light microscopy (Figure 4.3.3) were consistent with the data from electron microscopy (Figure 4.3.6) and they both showed that CE reduced the size of lipid droplets in brown adipocytes without any differences between genotypes (Figure 4.3.6 A, C). Mitochondrial length was also reduced in response to CE; however, the reduction was more pronounced in WT mice compared to PGC-1β-AT-KO mice (Figure 4.3.6 B). The quantitative analysis of the contact area between mitochondria and the surface of lipid droplets revealed decrease in contacts due to CE to the same level in both genotypes (Figure 4.3.6 D). On the other hand, in mice from 30 °C the contact area was decreased in PGC-1β-AT-KO mice compared to WT mice. This result could be associated with the protein levels of L-OPA1 and suggests a defect in lipid combustion linked with an impaired communication between mitochondria and lipid droplets.
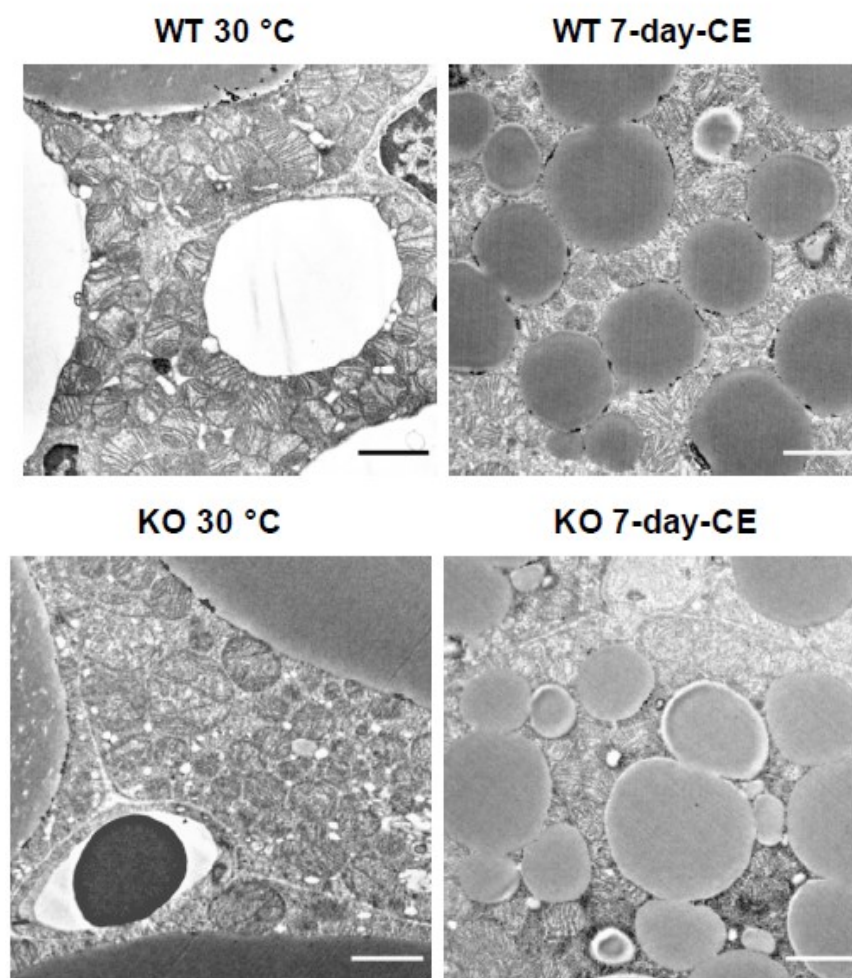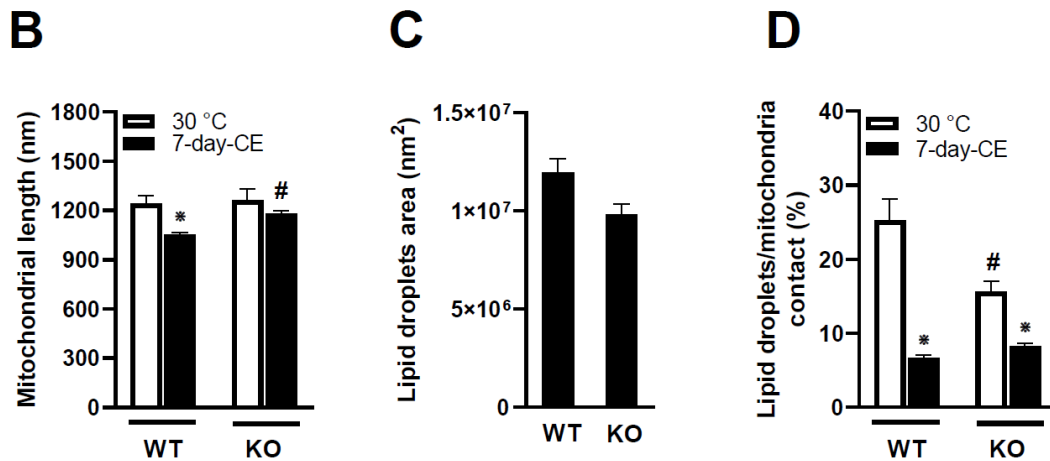
Figure 4.3.6 Electron microscopy analysis of iBAT of WT and PGC-1β-AT-KO mice maintained at 30 °C or exposed to cold. Representative electron microscopy images (**A**), length of mitochondria (**B**), the size of lipid droplets (**C**) and quantification of the contact area between mitochondria and the surface of lipid droplets. Data are means ± SEM (*n* = 5), Statistical analysis was performed using two-way ANOVA (p≤0.05). *Significant difference compared to 30 °C within the genotype; # significant difference between genotype within the same temperature. KO: adipose tissue-specific PGC-1β knockout mice; WT: wild-type mice; 30 °C: mice adapted to thermoneutral conditions; 7-day-CE: mice exposed to cold for 7 days.

In summary, our results demonstrate that PGC-1β has a unique function in the control of communication between mitochondria and the surface of lipid droplets during lipolysis in brown adipocytes. PGC-1β-AT-KO mice displayed enlarged iBAT probably due to increased lipid deposition in the depot with the strongest effect in mice maintained at thermoneutral conditions. This suggests that in the stimulated state PGC-1β deletion is partially compensated by upregulation of PGC-1α. However, PGC-1α does not compensate the absence of PGC-1β sufficiently as PGC-1β-AT-KO mice exposed to cold displayed reduced maximal thermogenic capacity of BAT.

5 Discussion

5.1 Publication A

The principal finding of this study was that combined treatment with *n*-3 PUFA and TZDs exerted additive beneficial effects on the metabolic health of mice fed obesogenic HF diet. HF diet generally impaired metabolic health of mice and blunted metabolic processes in eWAT. We observed that combined treatment with *n*-3 PUFA and both TZDs (PIO and MSDC) modulated metabolic functions of eWAT. In particular, it stimulated the activity of TAG/FA cycling in eWAT, decreased eWAT inflammation and increased the expression of genes involved in the control of eWAT metabolic functions. Combined treatment with *n*-3 PUFA and TZDs had also beneficial effects on the whole-body level. It reduced body weight gain and adiposity and positively influenced glucose homeostasis as reflected by an increase in insulin sensitivity and decrease in fasting glucose and insulin levels. Such results are of a great interest concerning that the treatment only with PIO resulted in the increase of body weight and adiposity [195]. However, we observed that treatment only with MSDC also decreased body weight gain and adiposity. Our findings show that the systemic improvement of metabolic health impaired by HF diet could be mediated by the modulation of eWAT metabolism.

One of the specific aims of this study was to compare effects of PIO and MSDC as both TZDs activate different pathways. PIO exerts its effects through the stimulation of PPARγ [200], while MSDC, a second generation TZD, acts mostly as an inhibitor of MPC [199]. Our previous studies showed additive effects of *n*-3 PUFA and PIO or rosiglitazone on the improvement of insulin sensitivity and other parameters of metabolic health in obese mice [202, 207, 208]. MSDC has a very low binding affinity to PPARγ, and that is supposed to limit adverse effects that accompany treatment with classical TZDs. On the other hand, *n*-3 PUFA act as a PPARγ ligand and the combined treatment with *n*-3 PUFA and MSDC is therefore of a particular interest.

In our study the activity of TAG/FA cycling, one of the intrinsic metabolic processes of WAT, was suppressed by HF diet in eWAT. High activity of TAG/FA cycling is one of the markers of healthy WAT [209]. TAG/FA cycling serves as a tool for the buffering of plasmatic NEFA since high plasmatic concentrations of NEFA can damage non-adipose tissues [213, 214]. Decreased TAG/FA activity in WAT therefore lowers the ability of WAT to buffer NEFA and to prevent from lipotoxic damage of other tissues. Increased activity of TAG/FA cycling in adipocytes stimulates the rate of both lipolysis and fatty acid re-esterification; moreover, higher TAG/FA cycling activity is associated with higher ATP consumption and with higher rate of fatty acid catabolism [47]. Stimulation of TAG/FA cycling generally increases the rate of energy metabolism in adipocytes and our study demonstrated that it also impacts the energy homeostasis on the whole-body level.

The labelling of TAG by ^{2}H *in vivo* in mice allowed us to measure the rate of glyceroneogenesis and to examine the composition of individual TAG species. The data from LC-MS showed the highest number of deuterated TAG species in HF+MSDC+F group suggesting the highest increase in the rate of fatty acid re-esterification. This was further

supported by the highest increase in the expression of genes involved in TAG synthesis (*Dgat1* and *Dgat2*) and in glyceroneogenesis (*Pc* and *Pck1*) in HF+MSDC+F group. These results are in accordance with studies that reported increased glyceroneogenesis in response to TZDs [23, 215]. The expression of the gene for GK, the enzyme responsible for the direct phosphorylation of glycerol, was increased the most in HF+MSDC group compared to HF group. The increase in the rate of fatty acid re-esterification by MSDC was therefore probably even higher than estimated by LC-MS and NMR spectroscopy as additional pathway could generate glycerol-3-phospate. On the other hand, *Gk* expression levels are generally low in WAT, so the contribution of GK was probably rather minor.

The increase in the rate of fatty acid re-esterification is accompanied by the increase in the rate of lipolysis to sustain TAG/FA cycling. This is supported by results from our gene expression analysis where the main lipolytic markers, *Atgl/Pnpla2* and *Hsl/Lipe*, had the highest expression levels again in HF+MSDC+F group. Several studies demonstrated that higher lipolysis is associated with higher rate of fatty acid oxidation [216, 217]. One of the links between higher activity of TAG/FA cycling in adipocytes and increased rate of fatty acid oxidation is an increased demand for ATP to fuel energy demanding futile cycling [218]. Another involved mechanism is the activation of PPAR receptors by their endogenous ligands: fatty acids liberated from lipolysed TAG. Activated PPAR receptors further transcriptionally activate genes involved in fatty acid oxidation [219]. The expression of *Pparg* was suppressed by HF diet and no interventions were able to restore its levels; however, the transcriptional activity of PPARγ was not determined. Nevertheless, the expression of genes for PDK4, CRAT, VLCAD and ACSL1, important regulators of fatty acid oxidation in adipocytes, was higher in both groups treated with MSDC compared to HF group, which was in accordance with the expression of both lipases. Moreover, the measurement of ^{14}C-palmitate oxidation in eWAT samples immediately after dissection confirmed that the highest rate of fatty acid oxidation was in HF+MSDC+F group (data shown in the supplement of publication A). In addition to the stimulation of TAG/FA cycling, combined treatment with *n*-3 PUFA and MSDC had the strongest potential to augment the capacity of white adipocytes to oxidise fatty acids.

The evaluation of ^{2}H enrichment of fatty acid methyls in TAG by NMR spectroscopy revealed a strong suppression of *de novo* lipogenesis in eWAT by HF diet. An increase in the rate of *de novo* lipogenesis was observed in groups treated with PIO; other interventions did not exert any stimulatory effects. In our study *n*-3 PUFA had no effect on lipogenesis in eWAT; moreover, there is an evidence that *n*-3 PUFA suppress the activity of FAS, the key lipogenic enzyme [220]. On the other hand, TZDs are believed to generally promote lipogenesis in WAT [182]. In particular, it was reported that PIO increased the gene expression of FAS, DGAT1 and PEPCK in human WAT [181, 195]. In our study TZD-containing interventions upregulated the expression of *Dgat1* and *Pck1*; however, the expression of *Fas* was strongly suppressed by HF diet and no interventions restored its levels. Therefore, the increase of *de novo* lipogenesis by PIO was likely mediated by different mechanisms than the upregulation of *Fas* expression.

HF diet resulted in a low-grade eWAT inflammation as determined by the amount of CLS formed by macrophages infiltrated into the tissue. In all the groups except for HF+F, the amount of CLS was reduced with the strongest effect in HF+MSDC+F group where the

eWAT inflammation was at the same level as in STD group. It was reported that in visceral WAT depots the amount of CLS positively correlated with adipocyte size [177]. In our study the adipocyte size was increased in all the groups fed HF diet in comparison with STD group and only in HF+MSDC+F group mice had smaller adipocytes compared to HF group. These results document that combined treatment with n-3 PUFA and MSDC has the ability to reduce adipocyte hypertrophy induced by HF diet and even completely abolish low-grade eWAT inflammation.

All TZD-containing interventions except for HF+PIO reduced body weight gain and the weight of eWAT. Increased energy expenditure due to high energy requirements of futile TAG/FA cycling could possibly explain how TZDs affect whole-body energy homeostasis [47]. Indeed, the combined treatment with n-3 PUFA and MSDC had the strongest effect on both the stimulation of TAG/FA cycling and the reduction of body weight gain and adiposity. Although energy requirements of TAG/FA cycling in WAT are considered to be quite minor in human [49] in rodents the rate of TAG/FA cycling in WAT is supposed to be the main determinant of the flux of circulating fatty acids and therefore has considerable energy costs [221]. Another systemic effect of TZDs was the improvement of glucose homeostasis impaired by HF diet. As determined by IGTT, all TZD-containing interventions stimulated glucose clearance impaired by HF diet and decreased fasting plasma insulin levels. Increased glucose clearance resulting in higher glucose uptake into adipocytes could further support lipogenesis and act as a possible mechanism how TZDs stimulate the activity of TAG/FA cycling.

Further investigation is required to identify exact mechanisms how n-3 PUFA and TZDs exert their additive beneficial effects. Our previous studies demonstrated the ability of n-3 PUFA to stimulate fatty acid oxidation in eWAT [190, 222]. Stimulation of mitochondrial biogenesis and oxidative capacity through transcriptional coactivator PGC-1α seems to be one of the mechanisms involved. Effects of TZDs on eWAT metabolism seem to be very diverse. Effects of PIO are largely mediated through the stimulation of PPARγ and its various targets, while MSDC rather act through the inhibition of MPC1 and MPC2. Both mechanisms result in the stimulation of lipid catabolism in adipocytes and increased activity of TAG/FA cycling. The combination of n-3 PUFA and MSDC had the strongest ability to (i) reverse HF diet-mediated suppression of the expression of metabolic genes in eWAT, (ii) stimulate the activity of TAG/FA cycling in eWAT and (iii) to improve the parameters of metabolic health on the whole-body level impaired by HF diet. Our study showed that the combined treatment with n-3 PUFA and MSDC has a great potential for the alleviation of metabolic disorders associated with diet-induced obesity and the stimulation of TAG/FA cycling in WAT seems to be the key mechanism involved.

5.2 Publication B

In this study we demonstrated that GPR-10 gene deletion in mice altered lipid homeostasis and metabolic functions in the liver and WAT in a gender-specific manner. GPR-10 is a receptor for anorexigenic neuropeptide PrRP and it is predominantly expressed in hypothalamus and in the brainstem. GPR-10 deletion resulted in increased body weight in

male mice fed STD, while no difference in females was observed. In mice fed STD, higher weight of eWAT was observed in GPR-10 KO mice of both genders, while the weight of scWAT was increased only in GPR-10 KO males. The weight of the liver was higher in GPR-10 KO males on both STD and HF diets compared to their WT littermates. On the other hand, there were no differences in the liver weight between any groups in females. In mice of both genders HF diet increased body weight and the weights of eWAT, scWAT and iBAT depots compared to mice fed STD; however, there were no differences between genotypes. HF diet also resulted in an increase in plasmatic leptin levels, fasting insulin levels, hepatic TAG content and generally impaired metabolic health of the animals. However, in most of the parameters HF diet masked the effects of GPR-10 deletion, which is in accordance with previous study with GPR-10 deficient mice [133]. Results that are going to be discussed further therefore relate only to mice fed STD. GPR-10 deletion in males had a stronger effect on fat deposition compared to females, which probably explains increased body weight only in GPR-10 KO males. These findings oppose results from previous studies with GPR-10 KO mice, where body weight and adiposity increased similarly in both genders or it was even higher in females [133, 134].

Results from OGTT demonstrated that important plasmatic parameters of glucose and lipid homeostasis were deteriorated by GPR-10 deletion. Fasting glucose levels were elevated only in GPR-10 KO males and there were no differences between females. In OGTT 30 minutes after the glucose administration plasmatic NEFA levels decreased due to insulin-mediated inhibition of lipolysis that reduced fatty acid release from WAT. There was a trend towards lower ΔNEFA (i.e. the difference between fasting NEFA levels and NEFA levels 30 minutes after the glucose gavage) in GPR-10 KO males compared to WT males and in GPR-10 KO females ΔNEFA was even significantly lower in comparison with WT females. These results suggest that GPR-10 deletion is associated with a defect in insulin-mediated regulation of fatty acid buffering by WAT. It remains to be identified whether this effect is due to an insufficient insulin secretion from pancreatic β-cells or there is a defect in regulatory pathways in WAT. Unsurprisingly, plasmatic leptin levels reflected the amount of WAT and were elevated in GPR-10 KO males compared to their WT littermates, while no differences were detected in females.

Leptin has been previously shown to interact with PrRP in the regulation of food intake [223]. Leptin secreted by WAT regulates food intake through transcription factor STAT3 resulting in the stimulation of the expression of anorexigenic POMC in hypothalamic neurons [156]. GPR-10 KO males displayed increased activation of STAT3 by phosphorylation as was determined using western blotting in hypothalamus (data shown in the supplement of publication B). Higher circulating leptin levels in GPR-10 KO males could be responsible for this effect. However, there were no differences in food intake between genotypes neither in males nor in females. Moreover, the measurement of energy expenditure by INCA did not identify any differences between genotypes in any of the groups. These results again oppose observations from previous studies, where higher adiposity in GPR-10 KO mice was interpreted as a consequence of higher food intake and decreased energy expenditure respectively [133, 134]. In these studies, differences in described parameters were generally not that major; therefore, contrasting data obtained in our study might be due to a different experimental design.

GPR-10 deletion affected metabolic functions of the liver. Although the degree of liver steatosis was similar in all mice regardless of the gender or genotype, hepatic TAG content was increased in GPR-10 KO mice of both genders with a stronger effect in males and the liver weight was also higher only in GPR-10 KO males. Gene expression analysis in the liver did not reveal any major differences between genotypes in males. In females; however, we observed an increased expression of genes for transcription regulators PPARα, PPARγ and PGC-1α, which are critical for the control of hepatic lipid metabolism and they all stimulate lipid catabolism in the liver [224]. Higher expression of these genes in the liver of GPR-10 KO females could therefore reduce TAG accumulation resulting in smaller genotype differences in hepatic TAG content compared to males. The expression of the gene for FAS was also greatly upregulated in GPR-10 KO females. In addition to its role in lipogenesis, hepatic FAS was reported to stimulate fatty acid catabolism through interaction with PPARα, which could further reduce TAG accumulation in the liver [225].

GPR-10 deficiency altered the expression of central metabolic genes in scWAT. The expression of genes for PPARα, PPARγ and PGC-1α was upregulated in scWAT of GPR-10 KO females compared to their WT littermates. Contrastingly, the gene expression of PPARα and PPARγ was decreased in scWAT of GPR-10 KO males compared to WT males. Moreover, GPR-10 deletion in females resulted in higher expression of genes associated with *de novo* lipogenesis and fatty acid re-esterification, namely *Dgat2*, *Pck2*, *Mlxipl* and *Slc2a4*, while in GPR-10 KO males the expression of *Dgat1*, *Dgat2*, *Scd1*, *Mlxipl* and especially *Fas* was lower than in WT males. Similarly as in the liver, higher expression of these metabolic regulators in WAT of GPR-10 KO females could counteract excessive lipid accumulation and protect them from increased adiposity that manifested in GPR-10 KO males. This is in accordance with our previous study, where we observed that increased *de novo* lipogenesis and fatty acid re-esterification in WAT could contribute to the lean phenotype of mice resistant to diet-induced obesity [44]. Similar effects, though less pronounced than in scWAT, were observed also in eWAT of GPR-10 KO mice. Altered gene expression of the key metabolic regulators in biggest WAT depots might have a great impact on systemic lipid homeostasis.

In conclusion, GPR-10 deletion in mice altered energy homeostasis, which manifested as increased body weight and adiposity in males, while no major changes in these parameters were detected in females. In GPR-10 KO females excessive fat deposition was possibly prevented by compensatory increase in the expression of genes controlling lipid metabolism in the liver and WAT. Effects on food intake and energy expenditure observed in previous studies with GPR-10 deficient mice were not confirmed in our study. Further investigation is therefore necessary to identify mechanisms connecting GPR-10 deficiency in CNS with disruption of lipid homeostasis particularly in the liver and WAT and to reveal the nature of differential response to GPR-10 deletion in males and females.

5.3 Publication C

Results of this study demonstrate that PGC-1β has a unique function in the control of lipid metabolism and thermogenesis in brown adipocytes. We examined male mice with adipose tissue specific PGC-1β deletion (PGC-1β-AT-KO) at the thermoneutral temperature (30 °C)

and under the conditions of CE. Previous study reported that mice with whole-body PGC-1β deficiency exposed to cold developed abnormal hypothermia and morbidity, suggesting a critical role of PGC-1β in thermoregulatory thermogenesis [212]. Our PGC-1β-AT-KO mice displayed hypothermia upon acute CE; however, they were able to survive CE for 7 days (and probably even longer). The ability to maintain sufficient body temperature in cold environment therefore does not seem to be dependent on the presence of PGC-1β in adipose tissue. As assessed by NE-test in INCA, PGC-1β-AT-KO mice displayed decreased maximal thermogenic capacity of BAT compared to their WT littermates despite having the same levels of UCP1 in iBAT. This is in accordance with another study with whole-body PGC-1β KO mice [109]. PGC-1β in adipose tissue therefore seems to contribute to the regulation of thermogenesis.

Despite obvious alterations of BAT thermogenic functions in cold-exposed mice, the most pronounced effects of PGC-1β deletion were observed at 30 °C. Substantial phenotype difference between PGC-1β-AT-KO mice and their WT littermates was the weight of iBAT, which was higher in PGC-1β-AT-KO mice in all experimental groups with the most pronounced effect at 30 °C. The size of adipocytes and also lipid droplets in adipocytes in iBAT was increased in PGC-1β-AT-KO mice at 30 °C compared to their WT littermates suggesting that higher iBAT weight of PGC-1β-AT-KO mice from 30 °C is probably due to an increased lipid deposition. The size of lipid droplets in iBAT was reduced by CE and further detailed analysis by electron microscopy confirmed that there were no differences between genotypes in cold-exposed mice.

The expression of various metabolic genes in iBAT was elevated in PGC-1β-AT-KO mice compared to WT mice. Most of the genotype differences were observed in 7-day-CE group and only a few genes differed between the genotypes at 30 °C. Metabolic functions of BAT are blunted at thermoneutral temperature due to the inactivity of NST; therefore, low levels of gene expression and less genotype differences were detected in mice at 30 °C. However, expressions of *Cidec*, gene involved in the regulation of TAG accumulation in the lipid droplet [32] and *Atgl/Pnpla2*, the gene for the key lipolytic enzyme were upregulated in PGC-1β-AT-KO mice at 30 °C. Furthermore, the expression of *Acsl1*, was also increased in PGC-1β-AT-KO mice and it was reported that an overexpression of this gene increased fatty acid uptake and their incorporation into TAG [226]. These alterations in gene expression could possibly contribute to higher lipid deposition in iBAT of PGC-1β-AT-KO mice. The expression of *Cidec*, *Atgl/Pnpla2, Acsl1* and other metabolic genes was increased also in iBAT of PGC-1β-AT-KO mice in 7-day-CE group where no difference in lipid droplet size was detected. The upregulation of metabolic gene levels in iBAT of PGC-1β-AT-KO mice in 7-day-CE group could be due to an increased expression of the gene for PGC-1α. PGC-1α is the master regulator of BAT thermogenic program, it was greatly upregulated in response to CE in our study and it might compensate the absence of PGC-1β in the stimulated state [102]. Indeed it was reported that in mice the expression of *Pgc1α* was strongly increased in BAT already after 6 hours of CE [108]. Compensatory upregulation of the gene for PGC-1α might also explain that PGC-1β deletion in our mice had no effect on the expression of genes for the enzymes of mitochondrial respiratory chain (data not shown). This is in contrast with previous study with PGC-1β-AT-KO mice, where no PGC-1α gene upregulation was observed and genes associated with mitochondrial respiratory chain were decreased in WAT and BAT of

PGC-1β-AT-KO mice [204]. However, this study used different experimental design (mice were raised at 30 °C) and Cre recombinase used for PGC-1β deletion was expressed under aP2 promoter (specific for adipose tissue and macrophages) and therefore this model might differ from our PGC-1β-AT-KO mice.

PGC-1α directly stimulates transcription rates of key mitochondrial metabolic genes in brown adipocytes including *Ucp1*, *Nrf1* and *Tfam* [100, 227]. In iBAT of PGC-1β-AT-KO mice in 7-day-CE group the increased expression of *Pgc1α* was reflected by upregulation of *Ppara*, *Pparg* and other genes associated with mitochondrial oxidation and biogenesis including *Ucp1* and *Tfam*. Despite the upregulation of *Ucp1* expression, UCP1 protein levels in iBAT of PGC-1β-AT-KO mice did not differ from WT mice. Therefore, the function of UCP1 in NST does not seem to be affected by PGC-1β deletion and decreased thermogenic capacity of BAT is probably caused by other mechanisms.

CE greatly increases mitochondrial energy requirements, which also affects mitochondrial dynamics and mitochondrial shape. Expressions of *Mfn2*, which encodes the regulator of outer mitochondrial membrane fusion, and *Opa1*, another mitochondrial dynamics marker were upregulated in iBAT from PGC-1β-AT-KO mice in 7-day-CE group. However, there was no effect of PGC-1β deletion on MFN2 protein levels in any of the groups. On the other hand, protein levels of L-OPA1 form were reduced in PGC-1β-AT-KO mice in 30 °C group compared to WT mice, while no difference was observed in cold-exposed animals. OPA1 is involved in the regulation of mitochondrial dynamics, similarly as MFN2 [116, 228] and it also contributes to the control of energy metabolism. Particularly S-OPA1 form has been shown to maintain the structure of mitochondrial cristae in order to preserve the proper function of respiratory chain in changing mitochondrial network [115]. Both S-OPA and L-OPA forms are required for optimal fusion of mitochondria. Moreover, it was suggested that OPA1 has a role in the control of lipolysis in adipocytes as AKAP and it could mediate the interaction between mitochondria and lipid droplets [36]. Both PGC-1α and PGC-1β interact with proteins responsible for the control of mitochondrial dynamics, in particular with MFN2 [118, 119]. The fact that the compensatory upregulation of *Pgc1α* expression in 7-day-CE group reduced the effects of PGC-1β deletion is in accordance with the study proposing unique role of PGC-1β in the regulation of basal mitochondrial functions [109]. It was further proposed that in the stimulated state *Pgc1α* expression increased and it seems to have the main role in the regulation of metabolic genes that interact with both PGC-1α and PGC-1β [229]. As the protein levels of L-OPA1 were reduced in PGC-1β-AT-KO mice only at 30 °C, we assume that the absence of PGC-1β affected L-OPA1 protein expression and resulted in the excessive lipid deposition in brown adipocytes due to impaired regulation of lipid metabolism. Sufficient L-OPA1 content in cold-exposed PGC-1β-AT-KO mice could be possibly maintained due to the upregulated *Pgc1α* expression.

Finally, we examined effects of PGC-1β ablation on mitochondrial length and the contact between mitochondria and the surface of lipid droplets, which can influence the rate of lipolysis in brown adipocytes. The mitochondrial length was decreased by CE which is accordance with previously published study [111], where adrenergic stimulation induced mitochondrial fragmentation. However, the mitochondrial length was slightly increased in PGC-1β-AT-KO mice in 7-day-CE group compared to WT mice. This could possibly reflect increased expression of *Mfn2* and *Opa1*; however, it is not in line with protein levels of

mitochondrial dynamics regulators, which were not affected by PGC-1β deletion in cold-exposed mice. On the other hand, the percentage of the contact between mitochondria and lipid droplets was decreased in PGC-1β-AT-KO mice at 30 °C which is in accordance with reduced L-OPA1 expression. Based on these findings we propose that L-OPA1 has a role in mediating the interaction between the mitochondrion and the surface of lipid droplet in brown adipocytes. Under the basal conditions this function is controlled by PGC-1β and its absence cannot be compensated by PGC-1α.

Our findings demonstrated that the absence of PGC-1β in adipose tissue of mice results in the impairment of thermogenic and metabolic functions of BAT. The compensatory increase in *Pgc1α* expression probably reduced the effect of PGC-1β deletion under the conditions of CE. However, it did not compensate it fully as cold-exposed PGC-1β-AT-KO mice showed decreased adrenergically-stimulated thermogenic capacity of BAT, despite having normal UCP1 protein levels. On the other hand, the most pronounced effects of PGC-1β deletion were observed under basal conditions. At the thermoneutral temperature brown adipocytes of PGC-1β-AT-KO mice displayed higher lipid deposition possibly due to decreased interactions between mitochondria and lipid droplets, which blunted the rate of lipid catabolism. We propose a novel function of OPA1 in mediating the mitochondrion/lipid droplet interaction in brown adipocytes. PGC-1β seems to contribute to the control of this function of L-OPA1 and therefore under basal conditions the presence of PGC-1β in brown adipocytes is required to preserve fully functional lipid metabolism in BAT.

6   Conclusion

Based on the specific aims of the thesis, following conclusions can be made:

1) The treatment of obese mice with *n*-3 PUFA and TZDs was shown to modulate WAT metabolism, which exerted beneficial effects on the whole-body level. HF diet suppressed the rate of metabolic processes in eWAT including the activity of TAG/FA cycling resulting in decreased ability of eWAT to buffer metabolites from the circulation. The combined treatment with *n*-3 PUFA and TZDs partially rescued the activity of TAG/FA cycling, stimulated the rate of metabolic processes in eWAT including fatty acid oxidation and reduced eWAT inflammation. In addition, combined interventions with *n*-3 PUFA and TZDs reduced body weight gain and improved markers of insulin sensitivity in obese mice. The increased activity of TAG/FA cycling in eWAT seems to contribute to these systemic effects. In most of the measured parameters the effects of MSDC were more pronounced compared to PIO; moreover, *n*-3 PUFA further augmented the effects of both TZDs. The combination of *n*-3 PUFA and MSDC had the strongest additive beneficial effects and therefore seems to have a great potential for the treatment of metabolic disorders associated with diet-induced obesity.

2) GPR-10 deficiency in CNS affected energy metabolism in the liver and in WAT. HF diet increased body weight, adiposity and generally impaired metabolic health of mice; however, HF diet masked the effects of GPR-10 deletion, which were only apparent in mice fed STD. GPR-10 deletion affected energy metabolism in mice of both genders fed STD with a stronger effect in males. GPR-10 KO males had higher body weight compared to their WT littermates probably due to increased weight of WAT depots. The increase in adiposity was possibly prevented in GPR-10 KO females due to the upregulation of the expression of genes controlling lipid metabolism in the liver and WAT. Moreover, GPR-10 KO mice of both genders displayed defects in insulin-mediated regulation of WAT metabolism and increased hepatic TAG content compared to WT mice. Unlike in previous studies with GPR-10 KO mice, no effects on energy expenditure and food intake were detected. Particular mechanisms that link GPR-10 deletion with altered energy metabolism in the liver and WAT therefore need to be further identified.

3) PGC-1β deficiency in adipose tissue affected thermogenic and metabolic functions of BAT with strongest effects in mice under basal conditions (30 °C). PGC-1β-AT-KO mice exposed to cold for 7 days displayed decreased maximal thermogenic capacity of BAT upon adrenergic stimulation. Other effects of PGC-1β deletion in cold-exposed mice were less pronounced possibly due to the compensatory increase of *Pgc1α* expression in iBAT, which was followed by increased expression of other metabolic genes. *Ucp1* expression displayed the same pattern as *Pgc1α* expression, while UCP1 protein levels did not differ between genotypes in any of the groups. The weight of iBAT was increased in all PGC-1β-AT-KO mice compared to WT mice with the biggest difference in 30 °C group. The enlargement of iBAT could be explained by higher lipid deposition as PGC-1β-AT-KO mice at 30 °C displayed larger lipid droplets in brown adipocytes possibly due to decreased interactions between mitochondria and lipid

droplets resulting in lower rate of lipid catabolism. We identified the L-OPA1 form as a protein involved in mediating the mitochondrion/lipid droplet interaction and PGC-1β seems to control its protein expression under basal conditions. PGC-1β is therefore necessary for the proper function of lipid metabolism in BAT under basal conditions as well as for the control of BAT thermogenic function.

7   List of all publications

Publication A

Bardova K*, **Funda J***, Pohl R, Cajka T, Hensler M, Kuda O, Janovska P, Adamcova K, Irodenko I, Lenkova L, Zouhar P, Horakova O, Flachs P, Rossmeisl M, Colca J, Kopecky J. Additive Effects of Omega-3 Fatty Acids and Thiazolidinediones in Mice Fed a High-Fat Diet: Triacylglycerol/Fatty Acid Cycling in Adipose Tissue. *Nutrients*. 2020;12(12):3737. IF = 5.717 (2020)

* These authors contributed equally

My personal contribution to this publication was supervising animal experiments and taking care of animals. I participated in dissection of animals after their sacrifice, in glucose tolerance tests and in writing the manuscript. I was also responsible for the preparation of samples for the *in vivo* determination of TAG synthesis and *de novo* lipogenesis, namely the isolation of TAG for NMR Spectroscopy.

Publication B

Prazienkova V, **Funda J**, Pirnik Z, Karnosova A, Hruba L, Korinkova L, Neprasova B, Janovska P, Benzce M, Kadlecova M, Blahos J, Kopecky J, Zelezna B, Kunes J, Bardova K, Maletinska L. GPR10 gene deletion in mice increases basal neuronal activity, disturbs insulin sensitivity and alters lipid homeostasis. *Gene*. 2021;774:145427. IF = 3.47 (2020)

My personal contribution to this publication included supervising animal experiments and taking care of animals. I participated in dissection of animals after their sacrifice, in glucose tolerance tests and I also performed the implantation surgeries prior to INCA experiments. In addition, I performed the gene expression analyses and statistical analyses.

Publication C – under review

Funda J, Villena J, Bardova K, Adamcova K, Irodenko I, Flachs P, Jedlickova I, Rossmeisl M, Kopecky J, Janovska P. Adipose tissue-specific ablation of PGC-1β impairs thermogenesis in brown fat

My personal contribution to this publication mostly included scheduling and supervising animal experiments as well as taking care of animals and dissecting them after the sacrifice. I performed the implantation surgeries prior to INCA experiments, the gene expression analyses and statistical analyses. I also participated in the measuring of plasma parameters and tissue TAG content, western blotting analyses and in writing the manuscript.

Zouhar P, Janovska P, Stanic S, Bardova K, **Funda J**, Haberlova B, Andersen B, Rossmeisl M, Cannon B, Kopecky J, Nedergaard J. A pyrexic effect of FGF21 independent of energy expenditure and UCP1. *Mol Metab*. 2021;53:101324. IF = 7.422 (2020)

My personal contribution to this publication included western blotting analyses and I also performed the implantation surgeries prior to INCA experiments. The publication is not a part of this dissertation thesis.

References

[1]   B. Cannon and J. Nedergaard, "Brown Adipose Tissue: Function and Physiological Significance," *Physiol Rev*, vol. 84, no. 1, pp. 277–359, 2004.

[2]   M. Krssak *et al.*, "Intramyocellular lipid concentrations are correlated with insulin sensitivity in humans: a 1H NMR spectroscopy study," *Diabetologia*, vol. 42, no. 1, pp. 113–116, 1999.

[3]   L. O. Ohlson *et al.*, "The influence of body fat distribution on the incidence of diabetes mellitus. 13.5 Years of follow-up of the participants in the study of men born in 1913," *Diabetes*, vol. 34, no. 10, pp. 1055–1058, 1985.

[4]   F. Item and D. Konrad, "Visceral fat and metabolic inflammation: The portal theory revisited," *Obes. Rev.*, vol. 13, no. SUPPL.2, pp. 30–39, 2012.

[5]   M. Blüher, "Metabolically healthy obesity," *Endocrine Reviews*, vol. 41, no. 3. Endocrine Society, pp. 405–420, 2020.

[6]   M. J. Lee, Y. Wu, and S. K. Fried, "Adipose tissue heterogeneity: Implication of depot differences in adipose tissue for obesity complications," *Mol. Aspects Med.*, vol. 34, no. 1, pp. 1–11, 2013.

[7]   C. T. Herz and F. W. Kiefer, "Adipose tissue browning in mice and humans," *J. Endocrinol.*, vol. 241, no. 3, pp. R97–R109, 2019.

[8]   M. Giralt and F. Villarroya, "White, brown, beige/brite: Different adipose cells for different functions?," *Endocrinology*, vol. 154, no. 9, pp. 2992–3000, 2013.

[9]   P. Seale *et al.*, "PRDM16 Controls a Brown Fat/Skeletal Muscle Switch," *Nature*, vol. 454, no. 7207, pp. 961–967, 2008.

[10]   J. Kopecký, M. Rossmeisl, P. Flachs, K. Bardová, and P. Brauner, "Mitochondrial uncoupling and lipid metabolism in adipocytes," *Biochem. Soc. Trans.*, vol. 29, no. 6, pp. 791–797, 2001.

[11]   A. Smorlesi, A. Frontini, A. Giordano, and S. Cinti, "The adipose organ: White-brown adipocyte plasticity and metabolic inflammation," *Obes. Rev.*, vol. 13, no. SUPPL.2, pp. 83–96, 2012.

[12]   S. Cinti, "Transdifferentiation properties of adipocytes in the adipose organ," *Am. J. Physiol. - Endocrinol. Metab.*, vol. 297, no. 5, pp. E977–E986, 2009.

[13]   K. Virtanen, M. E. Lidell, J. Orava, H. Mikael, W. Rickard, and N. Tarja, "Functional Brown Adipose Tissue in Healthy Adults," *N. Engl. J. Med.*, vol. 360, pp. 1518–25, 2009.

[14]   J. Nedergaard, T. Bengtsson, and B. Cannon, "Unexpected evidence for active brown adipose tissue in adult humans," *Am. J. Physiol. - Endocrinol. Metab.*, vol. 293, no. 2, pp. 444–452, 2007.

[15]   M. C. Zingaretti *et al.*, "The presence of UCP1 demonstrates that metabolically active adipose tissue in the neck of adult humans truly represents brown adipose tissue," *FASEB J.*, vol. 23, no. 9, pp. 3113–3120, 2009.

[16]   V. A. Drover *et al.*, "CD36 mediates both cellular uptake of very long chain fatty acids and their intestinal absorption in mice," *J. Biol. Chem.*, vol. 283, no. 19, pp. 13108–13115, 2008.

[17]   M. Furuhashi and G. S. Hotamisligil, "Fatty acid-binding proteins: Role in metabolic diseases and potential as drug targets," *Nat. Rev. Drug Discov.*, vol. 7, no. 6, pp. 489–503, 2008.

[18]   O. Catalina-Rodriguez *et al.*, "The mitochondrial citrate transporter, CIC, is essential for mitochondrial homeostasis," *Oncotarget*, vol. 3, no. 10, pp. 1220–1235, 2012.

[19]   K. H. G. Verschueren *et al.*, "Structure of ATP citrate lyase and the origin of citrate synthase in the Krebs cycle," *Nature*, vol. 568, no. 7753, pp. 571–575, 2019.

[20] S. J. Wakil, "Fatty Acid Synthase, A Proficient Multifunctional Enzyme," *Biochemistry*, vol. 28, no. 11, pp. 4523–4530, 1989.

[21] T. Matsuzaka and H. Shimano, "Elovl6: A new player in fatty acid metabolism and insulin sensitivity," *J. Mol. Med.*, vol. 87, no. 4, pp. 379–384, 2009.

[22] C. K. Nye, R. W. Hanson, and S. C. Kalhan, "Glyceroneogenesis is the dominant pathway for triglyceride glycerol synthesis in vivo in the rat," *J. Biol. Chem.*, vol. 283, no. 41, pp. 27565–27574, 2008.

[23] L. Reshef *et al.*, "Glyceroneogenesis and the triglyceride/fatty acid cycle," *J. Biol. Chem.*, vol. 278, no. 33, pp. 30413–30416, 2003.

[24] C. Eberhardt, P. W. Gray, and L. W. Tjoelker, "Human lysophosphatidic acid acyltransferase: cDNA cloning, expression, and localization to chromosome 9q34.3," *J. Biol. Chem.*, vol. 272, no. 32, pp. 20299–20305, 1997.

[25] C. L. E. Yen, S. J. Stone, S. Koliwad, C. Harris, and R. V. Farese, "DGAT enzymes and triacylglycerol biosynthesis," *J. Lipid Res.*, vol. 49, no. 11, pp. 2283–2301, 2008.

[26] R. A. Coleman and D. P. Lee, "Enzymes of triacylglycerol synthesis and their regulation," *Prog. Lipid Res.*, vol. 43, no. 2, pp. 134–176, 2004.

[27] V. Bezaire *et al.*, "Contribution of adipose triglyceride lipase and hormone-sensitive lipase to lipolysis in hMADS adipocytes," *J. Biol. Chem.*, vol. 284, no. 27, pp. 18282–18291, 2009.

[28] V. Large *et al.*, "Decreased expression and function of adipocyte hormone-sensitive lipase in subcutaneous fat cells of obese subjects," *J. Lipid Res.*, vol. 40, no. 11, pp. 2059–2065, 1999.

[29] C. Kim, N.-H. Xuong, and S. S. Taylor, "Crystal Structure of a Complex Between the Catalytic and Regulatory (RIα) Subunits of PKA," *Science (80-.)*., vol. 307, no. 5710, pp. 690–696, 2005.

[30] C. Sztalryd and D. L. Brasaemle, "The perilipin family of lipid droplet proteins - Gatekeepers of intracellular lipolysis," *Biochim. Biophys. Acta*, vol. 1862, no. 10 Pt B, pp. 1221–1232, 2017.

[31] J. T. Tansey *et al.*, "Perilipin ablation results in a lean mouse with aberrant adipocyte lipolysis, enhanced leptin production, and resistance to diet-induced obesity," *Proc Natl Acad Sci U S A*, vol. 98, no. 11, pp. 6494–6499, 2001.

[32] V. Puri *et al.*, "Fat-specific protein 27, a novel lipid droplet protein that enhances triglyceride storage," *J. Biol. Chem.*, vol. 282, no. 47, pp. 34213–34218, 2007.

[33] T. H. M. Grahn, Y. Zhang, M.-J. Lee, and A. G. Sommer, "FSP27 and PLIN1 interaction promotes the formation of large lipid droplets in human adipocytes," *Biochem Biophys Res Commun*, vol. 432, no. 2, pp. 296–301, 2013.

[34] C. Sztalryd *et al.*, "Perilipin A is essential for the translocation of hormone-sensitive lipase during lipolytic activation," *J. Cell Biol.*, vol. 161, no. 6, pp. 1093–1103, 2003.

[35] J. Zhang, C. J. Hupfeld, S. S. Taylor, J. M. Olefsky, and R. Y. Tsien, "Insulin disrupts β-adrenergic signalling to protein kinase A in adipocytes," *Nature*, vol. 437, no. 7058, pp. 569–573, 2005.

[36] G. Pidoux *et al.*, "Optic atrophy 1 is an A-kinase anchoring protein on lipid droplets that mediates adrenergic control of lipolysis," *EMBO J.*, vol. 30, no. 21, pp. 4371–4386, 2011.

[37] R. Zechner *et al.*, "FAT SIGNALS - Lipases and lipolysis in lipid metabolism and signaling," *Cell Metab.*, vol. 15, no. 3, pp. 279–291, 2012.

[38] E. A. Newsholme, J. R. Arch, B. Brooks, and B. Surholt, "The role of substrate cycles in metabolic regulation.," *Biochem. Soc. Trans.*, vol. 11, no. 1, pp. 52–56, 1983.

[39] G. Solinas *et al.*, "The direct effect of leptin on skeletal muscle thermogenesis is mediated by substrate cycling between de novo lipogenesis and lipid oxidation," *FEBS*

Lett., vol. 577, no. 3, pp. 539–544, 2004.

[40] N. C. Bal and M. Periasamy, "Uncoupling of sarcoendoplasmic reticulum calcium ATPase pump activity by sarcolipin as the basis for muscle non-shivering thermogenesis," *Philos. Trans. R. Soc. B Biol. Sci.*, vol. 375, no. 1793, 2020.

[41] V. A. Hammond and D. G. Johnston, "Substrate cycling between triglyceride and fatty acid in human adipocytes," *Metabolism*, vol. 36, no. 4, pp. 308–313, 1987.

[42] T. Wang, Y. Zang, W. Ling, B. E. Corkey, and W. Guo, "Metabolic partitioning of endogenous fatty acid in adipocytes," *Obes. Res.*, vol. 11, no. 7, pp. 880–887, 2003.

[43] D. Zhou, D. Samovski, A. L. Okunade, P. D. Stahl, N. a. Abumrad, and X. Su, "CD36 level and trafficking are determinants of lipolysis in adipocytes," *FASEB J.*, vol. 26, no. 11, pp. 4733–4742, 2012.

[44] P. Flachs *et al.*, "Induction of lipogenesis in white fat during cold exposure in mice: Link to lean phenotype," *Int. J. Obes.*, vol. 41, no. 3, pp. 372–380, 2017.

[45] T. Hashimoto *et al.*, "Active involvement of micro-lipid droplets and lipid droplet-associated proteins in hormone-stimulated lipolysis in adipocytes," *J. Cell Sci.*, vol. 125, pp. 6127–6136, 2012.

[46] R. L. Baldwin, "Metabolic functions affecting the contribution of adipose tissue to total energy expenditure.," *Fed. Proc.*, vol. 29, no. 3, pp. 1277–1283, 1970.

[47] M. Veliova *et al.*, "Blocking mitochondrial pyruvate import in brown adipocytes induces energy wasting via lipid cycling," *EMBO Rep.*, vol. 21, no. 12, pp. 1–17, 2020.

[48] M. D. Jensen, K. Ekberg, and B. R. Landau, "Lipid metabolism during fasting.," *Am. J. Physiol.*, vol. 281, no. 4, pp. E789–E793, 2001.

[49] P. Flachs, M. Rossmeisl, O. Kuda, and J. Kopecky, "Stimulation of mitochondrial oxidative capacity in white fat independent of UCP1: A key to lean phenotype," *Biochim. Biophys. Acta - Mol. Cell Biol. Lipids*, vol. 1831, no. 5, pp. 986–1003, 2013.

[50] H. A. Hostetler *et al.*, "Acyl-CoA binding proteins interact with the acyl-CoA binding domain of mitochondrial carnitine palmitoyl transferase I," *Mol Cell Biochem*, vol. 355, no. 1–2, pp. 135–148, 2011.

[51] B. K. Smith *et al.*, "Identification of a novel malonyl-CoA IC50 for CPT-1: implications for predicting in vivo fatty acid oxidation rates," *Biochem. J.*, vol. 448, no. 1, 2012.

[52] G. J. van der Vusse, "Albumin as Fatty Acid Transporter," *Drug Metab. Pharmacokinet.*, vol. 24, no. 4, pp. 300–307, 2009.

[53] S. Park *et al.*, "Role of the pyruvate dehydrogenase complex in metabolic remodeling: Differential pyruvate dehydrogenase complex functions in metabolism," *Diabetes Metab. J.*, vol. 42, pp. 270–281, 2018.

[54] H. S. Kwon and R. A. Harris, "Mechanisms responsible for regulation of pyruvate dehydrogenase kinase 4 gene expression," *Adv. Enzyme Regul.*, vol. 44, pp. 109–121, 2004.

[55] A. G. Cordente *et al.*, "Redesign of carnitine acetyltransferase specificity by protein engineering," *J. Biol. Chem.*, vol. 279, no. 32, pp. 33899–33908, 2004.

[56] D. M. Muoio *et al.*, "Muscle-specific Deletion of Carnitine Acetyltransferase Compromises Glucose Tolerance and Metabolic Flexibility," *Cell Metab.*, vol. 15, no. 5, pp. 764–777, 2012.

[57] N. M. Vacanti *et al.*, "Regulation of substrate utilization by the mitochondrial pyruvate carrier," *Mol. Cell*, vol. 56, no. 3, pp. 425–435, 2014.

[58] A. S. Divakaruni *et al.*, "Thiazolidinediones are acute, specific inhibitors of the mitochondrial pyruvate carrier," *Proc Natl Acad Sci U S A*, vol. 110, no. 14, pp. 5422–5427, 2013.

[59] B. Cannon and J. Nedergaard, "Nonshivering thermogenesis and its adequate

measurement in metabolic studies," *J. Exp. Biol.*, vol. 214, no. 2, pp. 242–253, 2011.

[60] B. R. M. Kingma, A. J. H. Frijns, L. Schellen, and W. D. van Marken Lichtenbelt, "Beyond the classic thermoneutral zone: Including thermal comfort," *Temperature*, vol. 1, no. 2, pp. 142–149, 2014.

[61] T. Hoang, M. D. Smith, and M. Jelokhani-Niaraki, "Expression, folding, and proton transport activity of human uncoupling protein-1 (ucp1) in lipid membranes," *J. Biol. Chem.*, vol. 288, no. 51, pp. 36244–36258, 2013.

[62] A. M. Bertholet and Y. Kirichok, "UCP1: a transporter for H+ and fatty acid anions," *Biochimie*, vol. 134, pp. 28–34, 2017.

[63] S. Rousset *et al.*, "The Biology of Mitochondrial Uncoupling Proteins," *Diabetes*, vol. 53, no. 1, pp. S130–S135, 2004.

[64] P. G. Crichton, Y. Lee, and E. R. S. Kunji, "The molecular features of uncoupling protein 1 support a conventional mitochondrial carrier-like mechanism," *Biochimie*, vol. 134, pp. 35–50, 2017.

[65] K. S. Echtay, E. Winkler, and M. Klingenberg, "Coenzyme Q is an obligatory cofactor for uncoupling protein function.," *Nature*, vol. 408, no. 30, pp. 609–613, 2000.

[66] M. Mar González-Barroso, C. Fleury, F. Bouillaud, D. G. Nicholls, and E. Rial, "The uncoupling protein UCP1 does not increase the proton conductance of the inner mitochondrial membrane by functioning as a fatty acid anion transporter," *J. Biol. Chem.*, vol. 273, no. 25, pp. 15528–15532, 1998.

[67] P. Jezek, D. E. Orosz, M. Modriansky, and K. D. Garlid, "Transport of anions and protons by the mitochondrial uncoupling protein and its regulation by nucleotides and fatty acids. A new look at old hypotheses," *J. Biol. Chem.*, vol. 269, no. 42, pp. 26184–26190, 1994.

[68] A. S. Divakaruni and M. D. Brand, "The regulation and physiology of mitochondrial proton leak.," *Physiology*, vol. 26, no. 3, pp. 192–205, 2011.

[69] G. Barbatelli *et al.*, "The emergence of cold-induced brown adipocytes in mouse white fat depots is determined predominantly by white to brown adipocyte transdifferentiation," *Am. J. Physiol. - Endocrinol. Metab.*, vol. 298, pp. 1244–1253, 2010.

[70] Q. A. Wang, C. Tao, R. K. Gupta, and P. E. Scherer, "Tracking adipogenesis during white adipose tissue development, expansion and regeneration," *Nat Med*, vol. 19, no. 10, pp. 1338–1344, 2013.

[71] G. V. Denis and M. S. Obin, "'Metabolically healthy obesity': Origins and implications," *Mol. Aspects Med.*, vol. 34, no. 1, pp. 59–70, 2013.

[72] Y. D. Tchoukalova, S. B. Votruba, T. Tchkonia, N. Giorgadze, J. L. Kirkland, and M. D. Jensen, "Regional differences in cellular mechanisms of adipose tissue gain with overfeeding," *Proc Natl Acad Sci U S A*, vol. 107, no. 42, pp. 18226–18231, 2010.

[73] R. Drolet *et al.*, "Hypertrophy and hyperplasia of abdominal adipose tissues in women," *Int. J. Obes.*, vol. 32, no. 2, pp. 283–291, 2008.

[74] K. Sun, C. M. Kusminski, and P. E. Scherer, "Adipose tissue remodeling and obesity," *J. Clin. Invest.*, vol. 121, no. 6, pp. 2094–2101, 2011.

[75] S. P. Weisberg, D. McCann, M. Desai, M. Rosenbaum, R. L. Leibel, and A. W. Ferrante, "Obesity is associated with macrophage accumulation in adipose tissue," *J. Clin. Invest.*, vol. 112, no. 12, pp. 1796–1808, 2003.

[76] J. Y. Kim *et al.*, "Obesity-associated improvements in metabolic profile through expansion of adipose tissue," *J. Clin. Invest.*, vol. 117, no. 9, pp. 2621–2637, 2007.

[77] P. Hallgren, L. Sjostrom, H. Hedlund, L. Lundell, and L. Olbe, "Influence of age, fat cell weight, and obesity on O2 consumption of human adipose tissue," *Am. J. Physiol. - Endocrinol. Metab.*, vol. 256, no. 4, pp. E467–E474, 1989.

[78] H. Böttcher and P. Fürst, "Decreased white fat cell thermogenesis in obese individuals," *Int. J. Obes.*, vol. 21, pp. 439–444, 1997.

[79] H. J. Choo *et al.*, "Mitochondria are impaired in the adipocytes of type 2 diabetic mice," *Diabetologia*, vol. 49, no. 4, pp. 784–791, 2006.

[80] J. Naukkarinen *et al.*, "Characterising metabolically healthy obesity in weight-discordant monozygotic twins," *Diabetologia*, vol. 57, pp. 167–176, 2014.

[81] H. S. Cheng, W. R. Tan, Z. S. Low, C. Marvalim, J. Y. H. Lee, and N. S. Tan, "Exploration and Development of PPAR Modulators in Health and Disease An Update of Clinical Evidence," *Int. J. Mol. Sci.*, vol. 20, no. 20, 2019.

[82] J. N. Feige, L. Gelman, C. Tudor, Y. Engelborghs, W. Wahli, and B. Desvergne, "Fluorescence imaging reveals the nuclear behavior of peroxisome proliferator-activated receptor/retinoid X receptor heterodimers in the absence and presence of ligand," *J. Biol. Chem.*, vol. 280, no. 18, pp. 17880–17890, 2005.

[83] W. Cao, A. V. Medvedev, K. W. Daniel, and S. Collins, "β-adrenergic activation of p38 MAP kinase in adipocytes: cAMP induction of the uncoupling protein 1 (UCP1) gene requires p38 map kinase," *J. Biol. Chem.*, vol. 276, no. 29, pp. 27077–27082, 2001.

[84] S. Yu and J. K. Reddy, "Transcription coactivators for peroxisome proliferator-activated receptors," *Biochim. Biophys. Acta - Mol. Cell Biol. Lipids*, vol. 1771, no. 8, pp. 936–951, 2007.

[85] M. Rakhshandehroo *et al.*, "Comprehensive analysis of PPARα-dependent regulation of hepatic lipid metabolism by expression profiling," *PPAR Res.*, vol. 2007, 2007.

[86] T. C. Leone, C. J. Weinheimer, and D. P. Kelly, "A critical role for the peroxisome proliferator-activated receptor α (PPARα) in the cellular fasting response: The PPARα-null mouse as a model of fatty acid oxidation disorders," *Proc. Natl. Acad. Sci. U. S. A.*, vol. 96, no. 13, pp. 7473–7478, 1999.

[87] X. Yang *et al.*, "Nuclear Receptor Expression Links the Circadian Clock to Metabolism," *Cell*, vol. 126, no. 4, pp. 801–810, 2006.

[88] M. M. Mihaylova *et al.*, "Fasting Activates Fatty Acid Oxidation to Enhance Intestinal Stem Cell Function during Homeostasis and Aging," *Cell Stem Cell*, vol. 22, no. 5, pp. 769-778.e4, 2018.

[89] G. D. Barish, V. A. Narkar, and R. M. Evans, "PPARδ: A dagger in the heart of the metabolic syndrome," *J. Clin. Invest.*, vol. 116, no. 3, pp. 590–597, 2006.

[90] P. Tontonoz, E. Hu, J. Devine, E. G. Beale, and B. M. Spiegelman, "PPAR gamma 2 regulates adipose expression of the phosphoenolpyruvate carboxykinase gene," *Mol. Cell. Biol.*, vol. 15, no. 1, pp. 351–357, 1995.

[91] K. Schoonjans *et al.*, "Induction of the acyl-coenzyme A synthetase gene by fibrates and fatty acids is mediated by a peroxisome proliferator response element in the C promoter," *Journal of Biological Chemistry*, vol. 270, no. 33. pp. 19269–19276, 1995.

[92] S. Ranganathan and P. A. Kern, "Thiazolidinediones Inhibit Lipoprotein Lipase Activity in Adipocytes," *J. Biol. Chem.*, vol. 273, no. 40, pp. 26117–26122, 1998.

[93] H. J. Lim *et al.*, "PPARγ activation induces CD36 expression and stimulates foam cell like changes in rVSMCs," *Prostaglandins Other Lipid Mediat.*, vol. 80, pp. 165–174, 2006.

[94] J. C. Yoon *et al.*, "Peroxisome Proliferator-Activated Receptor γ Target Gene Encoding a Novel Angiopoietin-Related Protein Associated with Adipose Differentiation," *Mol. Cell. Biol.*, vol. 20, no. 14, pp. 5343–5349, 2000.

[95] S. R. Thoennes, P. L. Tate, T. M. Price, and M. W. Kilgore, "Differential transcriptional activation of peroxisome proliferator-activated receptor gamma by omega-3 and omega-6 fatty acids in MCF-7 cells," *Mol. Cell. Endocrinol.*, vol. 160, pp. 67–73, 2000.

[96] P. C. Calder, "Marine omega-3 fatty acids and inflammatory processes: Effects, mechanisms and clinical relevance," *Biochim. Biophys. Acta - Mol. Cell Biol. Lipids*, vol. 1851, no. 4, pp. 469–484, 2014.

[97] P. Flachs, M. Rossmeisl, and J. Kopecky, "The effect of n-3 fatty acids on glucose homeostasis and insulin sensitivity," *Physiol. Res.*, vol. 63, no. Suppl. 1, pp. 93–118, 2014.

[98] S. H. Koo *et al.*, "PGC-1 promotes insulin resistance in liver through PPAR-α-dependent induction of TRB-3," *Nat. Med.*, vol. 10, no. 5, pp. 530–534, 2004.

[99] S. Kleiner, V. Nguyen-Tran, O. Baré, X. Huang, B. Spiegelman, and Z. Wu, "PPARδ agonism activates fatty acid oxidation via PGC-1α but does not increase mitochondrial gene expression and function," *J. Biol. Chem.*, vol. 284, no. 28, pp. 18624–18633, 2009.

[100] P. Puigserver, Z. Wu, C. W. Park, R. Graves, M. Wright, and B. M. Spiegelman, "A cold-inducible coactivator of nuclear receptors linked to adaptive thermogenesis," *Cell*, vol. 92, no. 6, pp. 829–839, 1998.

[101] U. Andersson and R. C. Scarpulla, "PGC-1-Related Coactivator, a Novel, Serum-Inducible Coactivator of Nuclear Respiratory Factor 1-Dependent Transcription in Mammalian Cells," *Mol. Cell. Biol.*, vol. 21, no. 11, pp. 3738–3749, 2001.

[102] M. J. Barberá, A. Schlüter, N. Pedraza, R. Iglesias, F. Villarroya, and M. Giralt, "Peroxisome proliferator-activated receptor α activates transcription of the brown fat uncoupling protein-1 gene. A link between regulation of the thermogenic and lipid oxidation pathways in the brown fat cell," *J. Biol. Chem.*, vol. 276, no. 2, pp. 1486–1493, 2001.

[103] J. Lin *et al.*, "Defects in adaptive energy metabolism with CNS-linked hyperactivity in PGC-1α null mice," *Cell*, vol. 119, no. 1, pp. 121–135, 2004.

[104] J. V. Virbasius and R. C. Scarpulla, "Activation of the human mitochondrial transcription factor A gene by nuclear respiratory factors: A potential regulatory link between nuclear and mitochondrial gene expression in organelle biogenesis," *Proc Natl Acad Sci U S A*, vol. 91, no. 4, pp. 1309–1313, 1994.

[105] K. T. Chambers *et al.*, "PGC-1β and ChREBP partner to cooperatively regulate hepatic lipogenesis in a glucose concentration-dependent manner," *Mol. Metab.*, vol. 2, no. 3, pp. 194–204, 2013.

[106] J. Lin *et al.*, "Hyperlipidemic effects of dietary saturated fats mediated through PGC-1β coactivation of SREBP," *Cell*, vol. 120, no. 2, pp. 261–273, 2005.

[107] J. C. Yoon *et al.*, "Control of hepatic gluconeogenesis through the transcriptional coactivator PGC-1," *Nature*, vol. 413, pp. 131–138, 2001.

[108] J. Lin, P. Puigserver, J. Donovan, P. Tarr, and B. M. Spiegelman, "Peroxisome proliferator-activated receptor γ coactivator 1β (PGC-1β), a novel PGC-1-related transcription coactivator associated with host cell factor," *J. Biol. Chem.*, vol. 277, no. 3, pp. 1645–1648, 2002.

[109] C. J. Lelliott *et al.*, "Ablation of PGC-1β results in defective mitochondrial activity, thermogenesis, hepatic function, and cardiac performance," *PLoS Biol.*, vol. 4, no. 11, pp. 2042–2056, 2006.

[110] M. Boutant *et al.*, "Mfn2 is critical for brown adipose tissue thermogenic function," *EMBO J.*, vol. 36, no. 11, pp. 1543–1558, 2017.

[111] J. D. Wikstrom *et al.*, "Hormone-induced mitochondrial fission is utilized by brown adipocytes as an amplification pathway for energy expenditure," *EMBO J.*, vol. 33, no. 5, pp. 418–436, 2014.

[112] M. Liesa and O. S. Shirihai, "Mitochondrial Dynamics in the Regulation of Nutrient Utilization and Energy Expenditure," *Cell Metab.*, vol. 17, no. 4, pp. 491–506, 2013.

[113] D. E. Kelley, J. He, E. V. Menshikova, and V. B. Ritov, "Dysfunction of mitochondria in human skeletal muscle in type 2 diabetes," *Diabetes*, vol. 51, no. 10, pp. 2944–2950, 2002.

[114] A. Zorzano, M. Liesa, and M. Palacín, "Role of mitochondrial dynamics proteins in the pathophysiology of obesity and type 2 diabetes," *Int. J. Biochem. Cell Biol.*, vol. 41, no. 10, pp. 1846–1854, 2009.

[115] H. Lee, S. B. Smith, and Y. Yoon, "The short variant of the mitochondrial dynamin OPA1 maintains mitochondrial energetics and cristae structure," *J. Biol. Chem.*, vol. 292, no. 17, pp. 7115–7130, 2017.

[116] S. Pich *et al.*, "The Charcot-Marie-Tooth type 2A gene product, Mfn2, up-regulates fuel oxidation through expression of OXPHOS system," *Hum. Mol. Genet.*, vol. 14, no. 11, pp. 1405–1415, 2005.

[117] S. Kameoka, Y. Adachi, K. Okamoto, M. Iijima, and H. Sesaki, "Phosphatidic Acid and Cardiolipin Coordinate Mitochondrial Dynamics," *Trends Cell Biol*, vol. 28, no. 1, pp. 67–76, 2018.

[118] M. Liesa *et al.*, "Mitochondrial fusion is increased by the nuclear coactivator PGC-1β," *PLoS One*, vol. 3, no. 10, 2008.

[119] F. X. Soriano, M. Liesa, D. Bach, D. C. Chan, M. Palacín, and A. Zorzano, "Evidence for a mitochondrial regulatory pathway defined by peroxisome proliferator-activated receptor-γ coactivator-1α, estrogen-related receptor-α, and mitofusin 2," *Diabetes*, vol. 55, no. 6, pp. 1783–1791, 2006.

[120] M. I. Hernández-Alvarez *et al.*, "Subjects With Early-Onset Type 2 Diabetes Show Defective Activation of the Skeletal," *Diabetes Care*, vol. 33, no. 3, pp. 645–651, 2010.

[121] G. Da Silva Xavier, G. A. Rutter, F. Diraison, C. Andreolas, and I. Leclerc, "ChREBP binding to fatty acid synthase and L-type pyruvate kinase genes is stimulated by glucose in pancreatic β-cells," *J. Lipid Res.*, vol. 47, no. 11, pp. 2482–2491, 2006.

[122] L. Eissing *et al.*, "De novo lipogenesis in human fat and liver is linked to ChREBP-β and metabolic health," *Nat. Commun.*, vol. 4, no. 1528, 2013.

[123] D. E. James, R. Brown, J. Navarro, and P. F. Pilch, "Insulin-regulatable tissues express a unique insulin-sensitive glucose transport protein," *Nature*, vol. 333, pp. 183–185, 1988.

[124] M. A. Herman *et al.*, "A novel ChREBP isoform in adipose tissue regulates systemic glucose metabolism," *Nature*, vol. 484, pp. 333–338, 2012.

[125] M. S. Brown and J. L. Goldstein, "The SREBP pathway: Regulation of cholesterol metabolism by proteolysis of a membrane-bound transcription factor," *Cell*, vol. 89, no. 3, pp. 331–340, 1997.

[126] J. D. Horton, I. Shimomura, M. S. Brown, R. E. Hammer, J. L. Goldstein, and H. Shimano, "Activation of cholesterol synthesis in preference to fatty acid synthesis in liver and adipose tissue of transgenic mice overproducing sterol regulatory element-binding protein-2," *J. Clin. Invest.*, vol. 101, no. 11, pp. 2331–2339, 1998.

[127] P. Matafome and R. Seiça, "The role of brain in energy balance" in *Adv. Neurobiol.*, vol. 19, pp. 33–48, 2017.

[128] R. S. Ahima and D. A. Antwi, "Brain Regulation of Appetite and Satiety," *Endocrinol. Metab. Clin. North Am.*, vol. 37, no. 4, pp. 811–823, 2008.

[129] B. Li *et al.*, "Altered features of neurotransmitters: NPY, α-MSH, and AgRP in type 2 diabetic patients with hypertension," *J. Int. Med. Res.*, vol. 48, no. 5, pp. 1–11, 2020.

[130] H. Matsumoto *et al.*, "Stimulation of corticotropin-releasing hormone-mediated adrenocorticotropin secretion by central administration of prolactin-releasing peptide in rats," *Neurosci. Lett.*, vol. 285, no. 3, pp. 234–238, 2000.

[131] C. B. Lawrence, F. Celsi, J. Brennand, and S. M. Luckman, "Alternative role for

prolactin-releasing peptide in the regulation of food intake," *Nat. Neurosci.*, vol. 3, no. 7, pp. 645–646, 2000.

[132] R. Fujii *et al.*, "Tissue distribution of prolactin-releasing peptide (PrRP) and its receptor," *Regul. Pept.*, vol. 83, no. 1, pp. 1–10, 1999.

[133] W. Gu, B. J. Geddes, C. Zhang, K. P. Foley, and A. Stricker-Krongrad, "The prolactin-releasing peptide receptor (GPR10) regulates body weight homeostasis in mice," *J. Mol. Neurosci.*, vol. 22, no. 1–2, pp. 93–103, 2004.

[134] M. Bjursell, M. Lennerås, M. Göransson, A. Elmgren, and M. Bohlooly-Y, "GPR10 deficiency in mice results in altered energy expenditure and obesity," *Biochem. Biophys. Res. Commun.*, vol. 363, no. 3, pp. 633–638, 2007.

[135] P. Seoane-Collazo *et al.*, "Hypothalamic-autonomic control of energy homeostasis," *Endocrine*, vol. 50, no. 2, pp. 276–291, 2015.

[136] R. Nogueiras *et al.*, "The central melanocortin system directly controls peripheral lipid metabolism," *J. Clin. Invest.*, vol. 117, no. 11, pp. 3475–3488, 2007.

[137] M. P. Ruffin and S. Nicolaidis, "Electrical stimulation of the ventromedial hypothalamus enhances both fat utilization and metabolic rate that precede and parallel the inhibition of feeding behavior," *Brain Res.*, vol. 846, pp. 23–29, 1999.

[138] S. J. Holt, H. V. Wheal, and D. A. York, "Hypothalamic control of brown adipose tissue in Zucker lean and obese rats. Effect of electrical stimulation of the ventromedial nucleus and other hypothalamic centres," *Brain Res.*, vol. 405, pp. 227–233, 1987.

[139] Y. C. Shi *et al.*, "Arcuate NPY controls sympathetic output and BAT function via a relay of tyrosine hydroxylase neurons in the PVN," *Cell Metab.*, vol. 17, pp. 236–248, 2013.

[140] R. G. McMurray and A. C. Hackney, "Interactions of metabolic hormones, adipose tissue and exercise," *Sport. Med.*, vol. 35, no. 5, pp. 393–412, 2005.

[141] S. Enocksson, M. Shimizu, F. Lönnqvist, J. Nordenström, and P. Arner, "Demonstration of an in vivo functional β3-adrenoceptor in man," *J. Clin. Invest.*, vol. 95, no. 5, pp. 2239–2245, 1995.

[142] G. R. Mullins *et al.*, "Catecholamine-induced lipolysis causes mTOR complex dissociation and inhibits glucose uptake in adipocytes," *Proc Natl Acad Sci U S A*, vol. 111, no. 49, pp. 17450–17455, 2014.

[143] N. H. McClenaghan, C. R. Barnett, F. P. M. M. O'Harte, and P. R. Flatt, "Mechanisms of amino acid-induced insulin secretion from the glucose-responsive BRIN-BD11 pancreatic B-cell line" *J. Endocrinol.*, vol. 151, no. 3, pp. 349–357, 1996.

[144] S. K. Fried, C. D. Russell, N. L. Grauso, and R. E. Brolin, "Lipoprotein lipase regulation by insulin and glucocorticoid in subcutaneous and omental adipose tissues of obese women and men," *J. Clin. Invest.*, vol. 92, pp. 2191–2198, 1993.

[145] G. Dimitriadis, P. Mitron, V. Lambadiari, E. Maratou, and S. A. Raptis, "Insulin effects in muscle and adipose tissue," *Diabetes Res. Clin. Pract.*, vol. 93, no. Suppl. 1, pp. 52–59, 2011.

[146] B. H. Jhun, A. L. Rampal, H. Liu, M. Lachaal, and C. Y. Jung, "Effects of insulin on steady state kinetics of GLUT4 subcellular distribution in rat adipocytes. Evidence of constitutive GLUT4 recycling," *J. Biol. Chem.*, vol. 267, no. 25, pp. 17710–17715, 1992.

[147] R. Belfort *et al.*, "Dose-response effect of elevated plasma free fatty acid on insulin signaling," *Diabetes*, vol. 54, no. 6, pp. 1640–1648, 2005.

[148] J. Yang, Y. Chi, B. R. Burkhardt, Y. Guan, and B. A. Wolf, "Leucine metabolism in regulation of insulin secretion from pancreatic beta cells," *Nutr. Rev.*, vol. 68, no. 5, pp. 270–279, 2010.

[149] C. B. Newgard *et al.*, "A Branched-Chain Amino Acid-Related Metabolic Signature

that Differentiates Obese and Lean Humans and Contributes to Insulin Resistance," *Cell Metab.*, vol. 9, no. 4, pp. 311–326, 2009.

[150] M. A. Herman, P. She, O. D. Peroni, C. J. Lynch, and B. B. Kahn, "Adipose tissue Branched Chain Amino Acid (BCAA) metabolism modulates circulating BCAA levels," *J. Biol. Chem.*, vol. 285, no. 15, pp. 11348–11356, 2010.

[151] C. B. Djurhuus *et al.*, "Effects of cortisol on lipolysis and regional interstitial glycerol levels in humans," *Am. J. Physiol. - Endocrinol. Metab.*, vol. 283, pp. 172–177, 2002.

[152] C. B. Djurhuus, C. H. Gravholt, S. Nielsen, S. B. Pedersen, N. Møller, and O. Schmitz, "Additive effects of cortisol and growth hormone on regional and systemic lipolysis in humans," *Am. J. Physiol. - Endocrinol. Metab.*, vol. 286, pp. 488–494, 2004.

[153] J. M. Deussing and A. Chen, "The corticotropin-releasing factor family: Physiology of the stress response," *Physiol. Rev.*, vol. 98, pp. 2225–2286, 2018.

[154] M. Fasshauer and M. Blüher, "Adipokines in health and disease," *Trends Pharmacol. Sci.*, vol. 36, no. 7, pp. 461–470, 2015.

[155] L. A. Tartaglia *et al.*, "Identification and expression cloning of a leptin receptor, OB-R," *Cell*, vol. 83, no. 7, pp. 1263–1271, 1995.

[156] S. H. Bates *et al.*, "STAT3 signalling is required for leptin regulation of energy balance but not reproduction," *Nature*, vol. 421, pp. 856–859, 2003.

[157] C. F. Elias *et al.*, "Leptin Differentially Regulates NPY and POMC Neurons Projecting to the Lateral Hypothalamic Area," *Neuron*, vol. 23, pp. 775–786, 1999.

[158] S. M. Harlan *et al.*, "Ablation of the leptin receptor in the hypothalamic arcuate nucleus abrogates leptin-induced sympathetic activation," *Circ Res*, vol. 108, no. 7, pp. 808–812, 2011.

[159] P. J. Enriori, P. Sinnayah, S. E. Simonds, C. G. Rudaz, and M. A. Cowley, "Leptin action in the dorsomedial hypothalamus increases sympathetic tone to brown adipose tissue in spite of systemic leptin resistance," *J. Neurosci.*, vol. 31, no. 34, pp. 12189–12197, 2011.

[160] R. V Considine *et al.*, "Serum Immunoreactive-Leptin Concentrations in Normal-Weight and Obese Humans," *N. Engl. J. Med.*, vol. 334, no. 5, pp. 292–295, 1996.

[161] D. L. Morris and L. Rui, "Recent advances in understanding leptin signaling and leptin resistance," *Am. J. Physiol. - Endocrinol. Metab.*, vol. 297, pp. E1247–E1259, 2009.

[162] T. Yamauchi *et al.*, "The fat-derived hormone adiponectin reverses insulin resistance associated with both lipoatrophy and obesity," *Nat. Med.*, vol. 7, no. 8, pp. 941–946, 2001.

[163] S. M. Furler, S. K. Gan, A. M. Poynten, D. J. Chisholm, L. V. Campbell, and A. D. Kriketos, "Relationship of adiponectin with insulin sensitivity in humans, independent of lipid availability," *Obesity*, vol. 14, no. 2, pp. 228–234, 2006, doi: 10.1038/oby.2006.29.

[164] K. Hotta *et al.*, "Plasma Concentrations of a Novel, Adipose-Specific Protein, Adiponectin, in Type 2 Diabetic Patients," *Arter. Thrombo Vasc Biol*, vol. 1, no. 1, pp. 1595–1599, 2000.

[165] A. Psilopanagioti, H. Papadaki, E. F. Kranioti, T. K. Alexandrides, and J. N. Varakis, "Expression of adiponectin and adiponectin receptors in human pituitary gland and brain," *Neuroendocrinology*, vol. 89, pp. 38–47, 2009.

[166] M. A. van Baak, R. G. Vink, N. J. T. Roumans, C. C. Cheng, A. C. Adams, and E. C. M. Mariman, "Adipose tissue contribution to plasma fibroblast growth factor 21 and fibroblast activation protein in obesity," *Int. J. Obes.*, vol. 44, pp. 544–547, 2020.

[167] A. Kharitonenkov *et al.*, "FGF-21 as a novel metabolic regulator," *J. Clin. Invest.*, vol. 115, pp. 1627–1635, 2005.

[168] T. Coskun *et al.*, "Fibroblast growth factor 21 corrects obesity in mice,"

Endocrinology, vol. 149, no. 12, pp. 6018–6027, 2008.

[169] C. Grunfeld *et al.*, "Persistence of the Hypertriglyceridemic Effect of Tumor Necrosis Factor Despite Development of Tachyphylaxis to Its Anorectic/Cachectic Effects in Rats," *Cancer Res.*, vol. 49, pp. 2554–2560, 1989.

[170] C. Mattacks, D. Sadler, and C. Pond, "The control of lipolysis in perinodal and other adipocytes by lymph node and adipose tissue-derived dendritic cells in rats," *Adipocytes*, vol. 1, no. 1, pp. 43–56, 2005.

[171] C. A. Mattacks and C. M. Pond, "Interactions of noradrenalin and tumour necrosis factor α, interleukin 4 and interleukin 6 in the control of lipolysis from adipocytes around lymph nodes," *Cytokine*, vol. 11, no. 5, pp. 334–346, 1999.

[172] C. M. Pond, C. A. Mattacks, and P. Prestrud, "Variability in the distribution and composition of adipose tissue in wild arctic foxes (Alopex lagopus) on Svalbard," *J. Zool.*, vol. 236, no. 4, pp. 593–610, 1995.

[173] S. W. Coppack, "Pro-inflammatory cytokines and adipose tissue," *Proc. Nutr. Soc.*, vol. 60, pp. 349–356, 2001.

[174] J. M. Wentworth *et al.*, "Pro-inflammatory CD11c+CD206+ adipose tissue macrophages are associated with insulin resistance in human obesity," *Diabetes*, vol. 59, no. 7, pp. 1648–1656, 2010.

[175] M. E. Shaul, G. Bennett, K. J. Strissel, A. S. Greenberg, and M. S. Obin, "Dynamic, M2-like remodeling phenotypes of CD11c+ adipose tissue macrophages during high-fat diet - Induced obesity in mice," *Diabetes*, vol. 59, no. 5, pp. 1171–1181, 2010.

[176] S. Fujisaka *et al.*, "M2 macrophages in metabolism," *Diabetol. Int.*, vol. 7, pp. 342–351, 2016.

[177] I. Murano *et al.*, "Dead adipocytes, detected as crown-like structures, are prevalent in visceral fat depots of genetically obese mice," *J. Lipid Res.*, vol. 49, pp. 1562–1568, 2008.

[178] A. C. MacKinnon *et al.*, "Regulation of Alternative Macrophage Activation by Galectin-3," *J. Immunol.*, vol. 180, pp. 2650–2658, 2008.

[179] A. Guilherme, J. V. Virbasius, V. Puri, and M. P. Czech, "Adipocyte dysfunctions linking obesity to insulin resistance and type 2 diabetes," *Nat Rev Mol Cell Biol*, vol. 9, no. 5, pp. 367–377, 2008.

[180] B. Grygiel-Górniak, "Peroxisome proliferator-activated receptors and their ligands: Nutritional and clinical implications - A review," *Nutr. J.*, vol. 13, no. 17, pp. 1–10, 2014.

[181] G. Ranganathan *et al.*, "The lipogenic enzymes DGAT1, FAS, and LPL in adipose tissue: effects of obesity, insulin resistance, and TZD treatment," *J. Lipid Res.*, vol. 47, no. 11, pp. 2444–2450, 2006.

[182] P. G. McTernan *et al.*, "Insulin and rosiglitazone regulation of lipolysis and lipogenesis in human adipose tissue in vitro," *Diabetes*, vol. 51, no. 5, pp. 1493–1498, 2002.

[183] F. Haman and D. P. Blondin, "Shivering thermogenesis in humans: Origin, contribution and metabolic requirement," *Temperature*, vol. 4, no. 3, pp. 217–226, 2017.

[184] A. L. Vallerand and I. Jacobs, "Rates of energy substrates utilization during human cold exposure," *Eur. J. Appl. Physiol. Occup. Physiol.*, vol. 58, pp. 873–878, 1989.

[185] S. M. Labbé *et al.*, "In vivo measurement of energy substrate contribution to cold-induced brown adipose tissue thermogenesis," *FASEB J.*, vol. 29, no. 5, pp. 2046–2058, 2015.

[186] S. W. Y. Ma and D. O. Foster, "Uptake of glucose and release of fatty acids and glycerol by rat brown adipose tissue in vivo," *Can J Physiol Pharmacol*, vol. 64, pp. 609–614, 1986.

[187] D. M. Sepa-Kishi, S. Jani, D. Da Eira, and R. B. Ceddia, "Cold acclimation enhances

UCP1 content, lipolysis, and triacylglycerol resynthesis, but not mitochondrial uncoupling and fat oxidation, in rat white adipocytes," *Am. J. Physiol. - Cell Physiol.*, vol. 316, no. 3, pp. C365–C376, 2019.

[188] P. Janovská, P. Flachs, L. Kazdová, and J. Kopecký, "Anti-obesity effect of n-3 polyunsaturated fatty acids in mice fed high-fat diet is independent of cold-induced thermogenesis," *Physiol. Res.*, vol. 62, no. 2, pp. 153–161, 2013.

[189] N. G. Løvsletten, S. S. Bakke, E. T. Kase, D. M. Ouwens, G. H. Thoresen, and A. C. Rustan, "Increased triacylglycerol - Fatty acid substrate cycling in human skeletal muscle cells exposed to eicosapentaenoic acid," *PLoS One*, vol. 13, no. 11, pp. 1–15, 2018.

[190] P. Flachs *et al.*, "Polyunsaturated fatty acids of marine origin upregulate mitochondrial biogenesis and induce β-oxidation in white fat," *Diabetologia*, vol. 48, no. 11, pp. 2365–2375, 2005.

[191] A. González-Périz *et al.*, "Obesity-induced insulin resistance and hepatic steatosis are alleviated by ω-3 fatty acids: a role for resolvins and protectins," *FASEB J.*, vol. 23, no. 6, pp. 1946–1957, 2009.

[192] E. Titos *et al.*, "Resolvin D1 and Its Precursor Docosahexaenoic Acid Promote Resolution of Adipose Tissue Inflammation by Eliciting Macrophage Polarization toward an M2-Like Phenotype," *J. Immunol.*, vol. 187, no. 10, pp. 5408–5418, 2011.

[193] E. Ricciotti and G. A. Fitzgerald, "Prostaglandins and inflammation," *Arterioscler. Thromb. Vasc. Biol.*, vol. 31, no. 5, pp. 986–1000, 2011.

[194] M. G. J. Balvers *et al.*, "Fish oil and inflammatory status alter the n-3 to n-6 balance of the endocannabinoid and oxylipin metabolomes in mouse plasma and tissues," *Metabolomics*, vol. 8, no. 6, pp. 1130–1147, 2012.

[195] I. Bogacka, H. Xie, G. A. Bray, and S. R. Smith, "The effect of pioglitazone on peroxisome proliferator-activated receptor-γ target genes related to lipid storage in vivo," *Diabetes Care*, vol. 27, no. 7, pp. 1660–1667, 2004.

[196] J. M. Lehmann, L. B. Moore, T. A. Smith-Oliver, W. O. Wilkison, T. M. Willson, and S. A. Kliewer, "An antidiabetic thiazolidinedione is a high affinity ligand for peroxisome proliferator-activated receptor gamma (PPAR gamma).," *J. Biol. Chem.*, vol. 270, no. 22, pp. 12953–12956, 1995.

[197] J. Choi *et al.*, "Obesity-linked phosphorylation of PPARγ by cdk5 is a direct target of the anti-diabetic PPARγ ligands," *Nature*, vol. 466, no. 7305, pp. 451–456, 2010.

[198] P. Raskin, M. Rendell, M. C. Riddle, J. F. Dole, M. I. Freed, and J. Rosenstock, "A Randomized Trial of Rosiglitazone Therapy in Patients With Inadequately Controlled Insulin-Treated Type 2 Diabetes," *Diabetes Care*, vol. 24, pp. 1226–1232, 2001.

[199] K. S. McCommis *et al.*, "Targeting the mitochondrial pyruvate carrier attenuates fibrosis in a mouse model of nonalcoholic steatohepatitis," *Hepatology*, vol. 65, no. 5, pp. 1543–1556, 2017.

[200] Z. Chen *et al.*, "Insulin resistance and metabolic derangements in obese mice are ameliorated by a novel peroxisome proliferator-activated receptor γ-sparing thiazolidinedione," *J. Biol. Chem.*, vol. 287, no. 28, pp. 23537–23548, 2012.

[201] S. A. Harrison *et al.*, "Insulin sensitizer MSDC-0602K in non-alcoholic steatohepatitis: A randomized, double-blind, placebo-controlled phase IIb study," *J. Hepatol.*, vol. 72, no. 4, pp. 613–626, 2020.

[202] O. Kuda *et al.*, "N-3 Fatty acids and rosiglitazone improve insulin sensitivity through additive stimulatory effects on muscle glycogen synthesis in mice fed a high-fat diet," *Diabetologia*, vol. 52, no. 5, pp. 941–951, 2009.

[203] C. H. S. Ruxton, S. C. Reed, M. J. A. Simpson, and K. J. Millington, "The health benefits of omega-3 polyunsaturated fatty acids - a review of the evience," *J Hum Nutr*

Diet., vol. 20, pp. 275–285, 2007.

[204] N. Enguix *et al.*, "Mice lacking PGC-1β in adipose tissues reveal a dissociation between mitochondrial dysfunction and insulin resistance," *Mol. Metab.*, vol. 2, no. 3, pp. 215–226, 2013.

[205] V. Kus *et al.*, "Induction of muscle thermogenesis by high-fat diet in mice: Association with obesity-resistance," *Am. J. Physiol. - Endocrinol. Metab.*, vol. 295, no. 2, pp. 356–367, 2008.

[206] J. Xia and D. S. Wishart, "Using metaboanalyst 3.0 for comprehensive metabolomics data analysis," *Curr. Protoc. Bioinforma.*, vol. 55, pp. 14.10.1-14.10.91, 2016.

[207] V. Kus *et al.*, "Unmasking differential effects of rosiglitazone and pioglitazone in the combination treatment with n-3 fatty acids in mice fed a high-fat diet," *PLoS One*, vol. 6, no. 11, 2011.

[208] O. Horakova *et al.*, "Preservation of Metabolic Flexibility in Skeletal Muscle by a Combined Use of n-3 PUFA and Rosiglitazone in Dietary Obese Mice," *PLoS One*, vol. 7, no. 8, 2012.

[209] M. Rydén, D. P. Andersson, S. Bernard, K. Spalding, and P. Arner, "Adipocyte triglyceride turnover and lipolysis in lean and overweight subjects," *J. Lipid Res.*, vol. 54, no. 10, pp. 2909–2913, 2013.

[210] I. R. Bederman, S. Foy, V. Chandramouli, J. C. Alexander, and S. F. Previs, "Triglyceride synthesis in epididymal adipose tissue- contribution of glucose and non-glucose carbon sources," *J. Biol. Chem.*, vol. 284, no. 10, pp. 6101–6108, 2009.

[211] S. Franckhauser *et al.*, "Increased Fatty Acid Re-esterification by PEPCK Overexpression in Adipose Tissue Leads to Obesity Without Insulin Resistance," *Diabetes*, vol. 51, pp. 624–630, 2002.

[212] J. Sonoda, I. R. Mehl, L. Chong, R. R. Nofsinger, and R. M. Evans, "PGC-1beta controls mitochondrial metabolism to modulate circadian activity, adaptive thermogenesis, and hepatic steatosis.," vol. 104, no. 12, pp. 5223–5228, 2006.

[213] M. Prentki and C. J. Nolan, "Islet β cell failure in type 2 diabetes," *J. Clin. Invest.*, vol. 116, no. 7, pp. 1802–1812, 2006.

[214] M. Prentki and S. R. M. Madiraju, "Glycerolipid Metabolism and Signaling in Health and Disease," *Endocr. Rev.*, vol. 29, no. 6, pp. 647–676, 2008.

[215] J. Tordjman, E. G. Beale, and C. Forest, "Thiazolidinediones Block Fatty Acid Release by Inducing Glyceroneogenesis in Fat Cells *," *J. Biol. Chem.*, vol. 278, no. 21, pp. 18785–18790, 2003.

[216] S. Kim, T. Tang, M. Abbott, J. A. Viscarra, Y. Wang, and H. S. Sul, "AMPK Phosphorylates Desnutrin-ATGL and Hormone-Sensitive Lipase To Regulate Lipolysis and Fatty Acid Oxidation within Adipose Tissue," vol. 36, no. 14, pp. 1961–1976, 2016.

[217] E. P. Mottillo, P. Balasubramanian, Y. Lee, C. Weng, E. E. Kershaw, and J. G. Granneman, "Coupling of lipolysis and de novo lipogenesis in brown, beige, and white adipose tissues during chronic β3-adrenergic receptor activation," *J. Lipid Res.*, vol. 55, pp. 2276–2286, 2014.

[218] S. P. Reidy and J.-M. Weber, "Accelerated substrate cycling : a new energy-wasting role for leptin in vivo," *Am. J. Physiol. - Endocrinol. Metab.*, vol. 282, pp. 312–317, 2002.

[219] J. A. Madrazo and D. P. Kelly, "The PPAR trio : Regulators of myocardial energy metabolism in health and disease," vol. 44, pp. 968–975, 2008.

[220] M. Teran-Garcia *et al.*, "Polyunsaturated fatty acid suppression of fatty acid synthase (FASN): evidence for dietary modulation of NF-Y binding to the Fasn promoter by SREBP-1c," vol. 402, pp. 591–600, 2007.

[221] B. Kalderon, N. Mayorek, E. Berry, N. Zevit, and J. Bar-Tana, "Fatty acid cycling in the fasting rat," *Am. J. Physiol. - Endocrinol. Metab.*, vol. 279, pp. 221–227, 2000.

[222] P. Flachs *et al.*, "Synergistic induction of lipid catabolism and anti-inflammatory lipids in white fat of dietary obese mice in response to calorie restriction and n-3 fatty acids," *Diabetologia*, vol. 54, pp. 2626–2638, 2011.

[223] K. L. J. Ellacott, C. B. Lawrence, N. J. Rothwell, and S. M. Luckman, "PRL-releasing peptide interacts with leptin to reduce food intake and body weight," *Endocrinology*, vol. 143, no. 2, pp. 368–374, 2002.

[224] B. Gross, M. Pawlak, P. Lefebvre, and B. Staels, "PPARs in obesity-induced T2DM, dyslipidaemia and NAFLD," *Nat. Rev. Endocrinol.*, vol. 13, no. 1, pp. 36–49, 2017.

[225] A. P. Jensen-Urstad and C. F. Semenkovich, "Fatty acid synthase and liver triglyceride metabolism: housekeeper or messenger?," *Biochim. Biophys. Acta*, vol. 1821, no. 5, pp. 747–753, 2012.

[226] M. R. Richards, J. D. Harp, D. S. Ory, and J. E. Schaffer, "Fatty acid transport protein 1 and long-chain acyl coenzyme A synthetase 1 interact in adipocytes," *J. Lipid Res.*, vol. 47, no. 3, pp. 665–672, 2006.

[227] H. Liang and W. F. Ward, "PGC-1α: A key regulator of energy metabolism," *Am. J. Physiol. - Adv. Physiol. Educ.*, vol. 30, pp. 145–151, 2006.

[228] K. Mahdaviani *et al.*, "Mfn2 deletion in brown adipose tissue protects from insulin resistance and impairs thermogenesis," *EMBO Rep.*, vol. 18, no. 7, pp. 1123–1138, 2017.

[229] J. A. Villena, "New insights into PGC-1 coactivators: Redefining their role in the regulation of mitochondrial function and beyond," *FEBS J.*, vol. 282, no. 4, pp. 647–672, 2015.